

High precision tests of QCD without scale or scheme ambiguities

The 40th anniversary of the Brodsky–Lepage–Mackenzie method

Leonardo Di Giustino^{a,b,*}, Stanley J. Brodsky^c, Philip G. Ratcliffe^{a,b}, Xing-Gang Wu^d, Sheng-Quan Wang^e

^a*Department of Science and High Technology, University of Insubria, via Valleggio 11, I-22100, Como, Italy*

^b*INFN, Sezione di Milano–Bicocca, 20126 Milano, Italy*

^c*SLAC National Accelerator Laboratory, Stanford University, Stanford, California 94039, USA*

^d*Department of Physics, Chongqing University, Chongqing 401331, P.R. China*

^e*Department of Physics, Guizhou Minzu University, Guiyang 550025, P.R. China*

Abstract

A key issue in making precise predictions in QCD is the uncertainty in setting the renormalization scale μ_r and thus determining the correct values of the QCD running coupling $\alpha_s(\mu_r)$ at each order in the perturbative expansion of a QCD observable. It has often been conventional to simply set the renormalization scale to the typical scale of the process Q and vary it in the range $\mu_r \in [Q/2, 2Q]$ in order to estimate the theoretical error. This is the practice of Conventional Scale Setting (CSS). The resulting CSS prediction will however depend on the theorist’s choice of renormalization scheme and the resulting pQCD series will diverge factorially. It will also disagree with renormalization scale setting used in QED and electroweak theory thus precluding grand unification. A solution to the renormalization scale-setting problem is offered by the Principle of Maximum Conformality (PMC), which provides a systematic way to eliminate the renormalization scale- and-scheme dependence in perturbative calculations. The PMC method has rigorous theoretical foundations, it satisfies Renormalization Group Invariance (RGI) and preserves all self-consistency conditions derived from the renormalization group. The PMC cancels the renormalon growth, reduces to the Gell-Mann–Low scheme in the $N_c \rightarrow 0$ Abelian limit and leads to scale- and scheme-invariant results. The PMC has now been successfully applied to many high-energy processes. In this article we summarize recent developments and results in solving the renormalization scale and scheme ambiguities in perturbative QCD. In particular, we present a recently developed method the PMC_∞ and its applications, comparing the results with CSS. The method preserves the property of renormalizable $\text{SU}(N)/\text{U}(1)$ gauge theories defined as *Intrinsic Conformality (iCF)*.

This property underlies the scale invariance of physical observables and leads to a remarkably efficient method to solve the conventional renormalization scale ambiguity at every order in pQCD.

This new method reflects the underlying conformal properties displayed by pQCD at NNLO, eliminates the scheme dependence of pQCD predictions and is consistent with the general properties of the PMC. A new method to identify conformal and β -terms, which can be applied either to numerical or to theoretical calculations is also shown. We present results for the thrust and C -parameter distributions in e^+e^- annihilation showing errors and comparison with the CSS. We also show results for a recent innovative comparison between the CSS and the PMC_∞ applied to the thrust distribution investigating both the QCD conformal window and the QED $N_c \rightarrow 0$ limit. In order to determine the thrust distribution along the entire renormalization group flow from the highest energies to zero energy, we consider the number of flavors near the upper boundary of the conformal window. In this flavor-number regime the theory develops a perturbative

*Corresponding author

Email addresses: leonardo.digiustino@uninsubria.it (Leonardo Di Giustino), sjbth@slac.stanford.edu (Stanley J. Brodsky), philip.ratcliffe@uninsubria.it (Philip G. Ratcliffe), wuxg@cqu.edu.cn (Xing-Gang Wu), sqwang@alu.cqu.edu.cn (Sheng-Quan Wang)

infrared interacting fixed point. These results show that PMC_∞ leads to higher precision and introduces new interesting features in the PMC. In fact, this method preserves with continuity the position of the peak, showing perfect agreement with the experimental data already at NNLO.

We also show a detailed comparison of the PMC_∞ with the other PMC approaches: the multi-scale-setting approach (PMCm) and the single-scale-setting approach (PMCs) by comparing their predictions for three important fully integrated quantities $R_{e^+e^-}$, R_τ and $\Gamma(H \rightarrow b\bar{b})$ up to the four-loop accuracy.

Keywords: QCD, Renormalization Group, Event Shape Variables, Higgs, Principle of Maximum Conformality

Contents

1	Introduction	5
2	Renormalization Scale and Scheme invariance	13
2.1	The Renormalization Group	13
2.2	The evolution of $\alpha_s(\mu)$ in perturbative QCD	15
2.2.1	One-loop result and asymptotic freedom	16
2.2.2	Two-loop solution and the perturbative conformal window	17
2.2.3	α_s at higher loops	18
2.3	Renormalization scheme dependence	20
2.4	The Extended Renormalization Group Equations	21
2.5	The running coupling constant $\alpha_s(\mu)$	23
3	The Principle of Maximum Conformality – PMC scale setting	25
3.1	The multi-scale Principle of Maximum Conformality: PMCm	29
3.2	The single-scale Principle of Maximum Conformality: PMCs	30
4	Infinite-Order Scale Setting via the Principle of Maximum Conformality: PMC$_{\infty}$	32
4.1	Intrinsic conformality (iCF)	32
4.2	Comments on the iCF and ordered scale invariance	35
4.3	The PMC $_{\infty}$	36
4.4	The iCF coefficients and scales: a new “How-To” method	37
4.5	Comment on the PMC/PMC $_{\infty}$ scales	38
5	PMC$_{\infty}$ results for thrust and the C-parameter	39
5.1	The PMC $_{\infty}$ scales at LO and NLO	40
5.2	NNLO thrust distribution results	41
5.3	NNLO C -parameter distribution results	44
5.4	The thrust distribution in the QCD conformal window and in QED	45
5.4.1	The thrust distribution according to N_f	45
5.4.2	The thrust distribution in the Abelian limit $N_c \rightarrow 0$	47
5.5	A novel method for the precise determination of the strong coupling and its behavior	48
5.5.1	Running behavior	49
5.5.2	$\alpha_s(M_Z)$ from a χ^2 fit	50
6	Comparison of the PMCm, PMCs and PMC$_{\infty}$ for fully integrated fundamental quantities	52
6.1	The pQCD predictions for $R_{e^+e^-}$, R_{τ} and $\Gamma(H \rightarrow b\bar{b})$	52
6.2	Properties using the conventional scale-setting approach	54
6.3	Properties using the PMCm approach	56
6.4	Properties using the PMCs approach	58
6.5	Properties using the PMC $_{\infty}$ approach	62

6.6 A comparison of the renormalization scale dependence of the various PMC approaches	63
7 Summary	66

1. Introduction

The renormalization scale and scheme ambiguities

The renormalization scale and scheme ambiguities are an important source of errors in many processes in perturbative QCD preventing precise theoretical predictions for both standard model (SM) and beyond standard model (BSM) physics. In principle, an infinite perturbative series is devoid of this issue, given the scheme and scale invariance of entire physical quantities [1–5]; in practice, perturbative corrections are known up to a certain order of accuracy and scale invariance is only approximated in truncated series, leading to scheme and scale ambiguities [6–18].

Although perturbative calculations for theoretical predictions are also affected by other sources of errors, e.g. the top- and Higgs-mass uncertainties and the strong-coupling $\alpha_s(M_Z)$ uncertainty, the renormalization scale and scheme ambiguities remain among of the main sources of errors. These scale and scheme ambiguities play an important role for predictions in many fundamental processes in perturbative QCD, also with respect to the other sources of uncertainties. Processes such as gluon fusion in Higgs production [19] or bottom-quark production [20], which are essential for the physics investigated at the Large Hadron Collider (LHC) and at future colliders, are all affected by these ambiguities. In the present era, high-precision predictions are crucial for both SM and BSM physics, in order to test the theory in all sectors and to enhance sensitivity to possible new physics (NP) at colliders.

At the moment two basic strategies exist to deal with this problem. On one hand, according to conventional practice or conventional scale setting (CSS), this problem cannot be avoided and is responsible for part of the theoretical errors. The simple CSS procedure starts from the scale and scheme invariance of a given observable, which translates into complete freedom for the choice of renormalization scale. According to common practice, a first evaluation of the physical observable is obtained by calculating perturbative corrections in a given scheme (commonly used are $\overline{\text{MS}}$ or $\overline{\text{MS}}$) and at an initial renormalization scale $\mu_r = \mu_r^{\text{init}}$. Thus, the renormalization scale μ_r is set to one of the typical scales of a process, Q , and errors are estimated by varying the scale over a range $[Q/2, 2Q]$.

This method is claimed to evaluate uncalculated contributions from higher-order terms and that, due to the perturbative nature of the expansion, the introduction of higher-order corrections would reduce the scheme and scale ambiguities order by order. There is no doubt that the higher the order of the loop corrections calculated, the greater is the precision of the theoretical estimates in comparison with the experimental data, but we cannot determine *a priori* the level of accuracy necessary for the CSS to achieve the desired precision. And in the majority of cases at present only the NNLO corrections are available. Moreover, the divergent nature of the asymptotic perturbative series and the presence of factorially growing terms (i.e. renormalons [21–23]) severely compromise the theoretical predictions.

However, even though this procedure may give an indication as to the level of conformality and convergence reached by the truncated expansion, it leads to a numerical evaluation of theoretical errors that is quite unsatisfactory and strongly dependent on the value of the chosen scale. Moreover, this method gives predictions with large theoretical uncertainties that are comparable with the calculated order correction; different choices of the renormalization scale may lead to very different results when higher-order corrections are included. For example, the NLO correction to $W + 3\text{jets}$ with the BlackHat code [24] can range from negligible to extremely severe, depending on the choice of the particular renormalization scale. One may argue that the proper renormalization scale for a fixed-order prediction may be judged by comparing theoretical results with experimental data, but this method would be strongly process dependent and would compromise the predictivity of the pQCD approach.

Besides the complexity of the higher-order calculations and the slow convergence of the perturbative series, there are

many critical points in the CSS method:

- In general, the proper renormalization scale value, Q , is not known, nor the correct range over which the scale and scheme parameters should be varied in order to obtain the correct error estimate. In fact, in some processes there can be more than one typical momentum scale that may be taken as the renormalization scale according to the CSS procedure; for example, in processes involving heavy quarks typical scales are either the center-of-mass energy \sqrt{s} or also the heavy-quark mass. Moreover, the idea of the typical momentum transfer as the renormalization scale only sets the order of magnitude of the scale, but does not indicate the optimal scale.
- No distinction is made among different sources of errors and their relative contributions; e.g. in addition to the errors due to scale-scheme uncertainties there are also errors from missing uncalculated higher-order terms. In such an approach theoretical uncertainties can become quite arbitrary and unreliable.
- The convergence of the perturbative series in QCD is affected by uncanceled large logarithms as well as by “renormalon” terms that diverge as $(n!\beta_i^n \alpha_s^{n+1})$ at higher orders [21, 22]; this is known as the *renormalon problem* [23]. Such renormalon terms can give sizable contributions to the theoretical estimates, as shown in e^+e^- annihilation, τ decay, deeply inelastic scattering and hard processes involving heavy quarks. These terms are responsible for important corrections at higher orders also in the perturbative region, leading to different predictions according to the different choices of scale (as shown in Ref. [24]). Large logarithms on the other hand can be resummed using the resummation technique [25–31] and results are IR renormalon free. This does not help for the renormalization scale and scheme ambiguities, which still affect theoretical predictions with or without resummed large logarithms. In fact, as recently shown in Ref. [20] for the $b\bar{b}$ -production cross-section at NNLO-order accuracy at hadron colliders, the CSS scale setting leads to theoretical uncertainties that are of the same order as the NNLO corrections $\sim 20 - 30\%$, taking as the typical momentum scale the b -quark mass $m_b \sim 4.92 \text{ GeV}$.
- In the Abelian limit $N_c \rightarrow 0$ at fixed $\alpha_{em} = C_F \alpha_s$ with $C_F = (N_c^2 - 1) / 2N_c$, a QCD case effectively approaches the analogous QED case [32, 33]. Thus, to be self-consistent, any QCD scale-setting method should also be extendable to QED and results should be in agreement with the Gell-Mann–Low (GM–L) scheme. This is an important requirement also from the perspective of a grand unified theory (GUT), where only a single global method for setting the renormalization scale may be applied and then it can be considered as a good criterion for verifying if a scale setting is correct or not. CSS leads to incorrect results when applied to QED processes. In the GM–L scheme, the renormalization scale is set with no ambiguity to the virtuality of the exchanged photon/photons, which naturally sums an infinite set of vacuum polarization contributions into the running coupling. Thus, the CSS approach of varying the scale by a factor 2 is not applicable to QED, since the scale is already optimized.
- The large amount of forthcoming high-precision experimental data, produced especially by the running at high collision energy and high luminosity of the Large Hadronic Collider (LHC), will require more accurate and refined theoretical estimates. The CSS appears to be more a “guess”; its results are afflicted by large errors and the perturbative series converges poorly with or without large-logarithm resummation or renormalon contributions. Moreover, within such a framework, it is almost impossible to distinguish between SM and BSM signals and in many cases, improved higher-order calculations are not expected to be available in the short term.

To sum up, the conventional scale-setting method assigns an arbitrary range and an arbitrary systematic error to fixed-order perturbative calculations that greatly affects the predictions of pQCD. On the other hand, various strategies

for optimization of the truncated expansion have been proposed. We point out that since its very beginning, several attempts have been performed to improve the renormalization procedure and different schemes have been introduced mainly to improve the convergence of the perturbative series. An example is the introduction of the $\overline{\text{MS}}$, as suggested in Refs.[34, 35] and later the introduction of the momentum subtraction scheme (MOM) as discussed by Celmaster and Gonsalves in Refs. [6, 36]. The MS scheme, introduced in Ref. [37], is in fact quite arbitrary and related to the particular regularization scheme used, leading to a rather higher second-order contribution in the DIS process, by reabsorbing the scheme term $\ln(4\pi - \gamma_E)$ into a redefinition of the QCD scale parameter Λ , Bardeen *et al.* noticed a significant improvement of the convergence of the perturbative series. Later, the introduction of the MOM scheme, though being gauge dependent, has been shown to also include other scheme terms into Λ , leading to a scheme which is less dependent on the regularization procedure and tending to a more "physical" scale and nearly to an "optimization procedure" [6]. A recent discussion on the gauge dependence of the MOM scheme has been given in Ref. [38]. We discuss these schemes in more detail in Sec. 2.3.

In general, an optimization or scale-setting procedure is considered reliable if it preserves important self-consistency requirements. All Renormalization Group properties, such as *uniqueness*, *reflexivity*, *symmetry* and *transitivity* should also be preserved by the scale-setting procedure in order to be generally applied [39]. A fundamental requirement is the scheme independence; other requirements can be suggested by known tested theories (such as QED), by the convergence behavior of the series in particular kinematic regions or by important phenomenological results.

The Principle of Minimal Sensitivity (PMS) is an optimization procedure proposed by Stevenson [8–11] based on the assumption that, since observables should be independent of the particular RS and scale, their optimal perturbative approximations should be stable under small RS variations. The RS-scheme parameters β_2, β_3, \dots and the scale parameter Λ (or the subtraction point μ_r) are considered “unphysical” and independent variables; their values are thus set in order to minimize the sensitivity of the estimate to their small variations. This is essentially the core of Optimized Perturbation Theory (OPT) [9], based on the PMS procedure. The convergence of the perturbative expansion is improved by requiring its independence from the choice of RS and μ . Optimization is implemented by identifying the RS-dependent parameters in the truncated series (β_i for $2 \leq i \leq n$ and Λ), with the request that the partial derivative of the perturbative expansion of the observable with respect to the RS-dependent and scale parameters vanishes. In practice, the PMS scale setting is designed to eliminate the remaining renormalization and scheme dependence in the truncated expansions of the perturbative series.

We would argue that this approach is based more on convergence rather than physical criteria. In particular, the PMS is a procedure that can be extended to higher order and it can be generally applied to calculations obtained in arbitrary initial renormalization schemes. Although this procedure leads to results that are suggested to be unique and scheme independent, it unfortunately violates important properties of the renormalization group, as shown in Ref. [40], such as reflexivity, symmetry, transitivity and also the *existence* and *uniqueness* of the optimal PMS renormalization scheme are not guaranteed since they are strictly related to the presence of maxima and minima.

Another optimization procedure, namely the Fastest Apparent Convergence (FAC) criterion was introduced by Grunberg and is based on the idea of *effective charges*. As pointed out by Grunberg [12–14], any perturbatively calculable physical quantity can be used to define an effective coupling, or “effective charge”, by entirely incorporating the radiative corrections into its definition. Effective charges can be defined from an observable starting from the assumption that the infinite series of a given quantity is scheme and scale invariant. The effective charge satisfies the same renormalization

group equations as the usual coupling. Thus, the running behavior for both the effective coupling and the usual coupling are the same if their RG equations are calculated in the same renormalization scheme. This idea has been discussed in more detail in Refs. [41, 42].

An important suggestion is that all effective couplings defined in the same scheme satisfy the same RG equations. While different schemes or effective couplings would lead to different renormalization group equations. Hence, any effective coupling can be used as a reference for the particular renormalization procedure. In general, this method can be applied to any observable calculated in any RS, also in processes with large higher-order corrections. The FAC scale setting, as has been shown in Ref. [40], preserves the RG self-consistency requirements, although the FAC method can be considered more an optimization approach rather than a proper scale-setting procedure to extend order by order. FAC results depend sensitively on the quantity to which the method is applied. In general, when the NLO correction is large, the FAC proves to be a resummation of the most important higher-order corrections and thus a RG-improved perturbation theory is achieved.

PMS and FAC are procedures commonly in use for scale setting in perturbative QCD together with CSS and an introduction to these methods can be found in Refs. [40, 43]. However, as shown in Refs. [44], these optimization methods not only have the same difficulties of CSS, but they also lead to incorrect and unphysical results in particular kinematic regions.

A solution to the renormalization scale setting problem is offered by the Principle of Maximum Conformality (PMC) [45–48]. This method is the generalization and extension of the original Brodsky-Lepage-Mackenzie (BLM) method [15] to all theories, to all orders and to all observables and it satisfies all the theoretical requirements of a reliable scale-setting procedure at once, leading to accurate and consistent results. The primary purpose of the PMC method is to solve the scale-setting ambiguity; it has been extended to all orders [49, 50] and it determines the correct running coupling and the correct momentum flow according to RGE invariance [51, 52]. This leads to results that are invariant with respect to the initial renormalization scale and in agreement with the requirement of scale invariance of observables in pQCD [40]. The approach provides a systematic method to eliminate renormalization scheme and scale ambiguities from first principles by absorbing the β terms, which govern the behavior of the running coupling via the renormalization group equation. Thus, the divergent renormalon terms cancel, improving convergence of the perturbative QCD series. Furthermore, the resulting PMC predictions do not depend on the particular scheme used, thereby preserving the principles of renormalization group invariance [39, 51]. The PMC procedure is also consistent with the standard Gell-Mann–Low method in the Abelian limit, $N_c \rightarrow 0$ [32]. Moreover, in a theory unifying all forces (electromagnetic, weak and strong interactions), such as Grand Unified Theories, one cannot trivially apply a different scale-setting or analytic procedure to different sectors of the theory. The PMC offers the possibility to apply the same method to all sectors of a theory, starting from first principles, eliminating renormalon growth, scheme dependence, scale ambiguity and satisfying the QED Gell-Mann–Low scheme in the zero-color limit $N_c \rightarrow 0$.

PMC and schemes

We remark that the fundamental task of the PMC is to solve the renormalization scale and scheme ambiguities and in order to achieve this, it makes use of the RG-equations to reabsorb the n_f -terms that are related to the UV-divergent diagrams. The procedure of the PMC works with *any* initial definition of the scheme or scale for the running coupling, $\overline{\text{MS}}$ or $\overline{\text{MS}}$ or the 't Hooft scheme are all equivalent, since the entire scheme dependence of the observable is reabsorbed

into the running coupling and into the PMC scale in the final series. In particular, the lower order terms, β_0, β_1 , of the β -function are scheme independent; thus a scheme transformation cannot lead to a prescription for determining the scale. In fact, also in the case of the 't Hooft scheme (as shown in Refs.[53, 54]) one can eliminate all scheme dependent β_i coefficients, but there is no prescription for the renormalization scale, which can be considered as the first scheme parameter. Moreover, what seems a good prescription for the running coupling is not necessarily a good prescription for the entire fixed-order calculated quantity. In fact, still considering the 't Hooft case, the entire series of $\beta_i, i \geq 2$ is removed from the definition of the coupling, but in a fixed-order calculation these β_i coefficients would have an impact on the coefficients of the series at each order of calculation and on the convergence of the series. On the other hand, the PMC gives a prescription for fixing the scale and reabsorbing all scheme-dependent terms of a cross-section into the running coupling and into the PMC scale, exposing the perturbative series to a minimization/cancellation of the effects of the scale and scheme uncertainties. An important consequence of the PMC procedure is the RS-invariance of the resulting series. We refer to RS-scheme invariance as the invariance under the extended-renormalization group and its equations (xRGE)[9, 17, 55, 56]. It can be shown that the PMC procedure may be performed either way using the same xRGE¹. The xRGE show that different scheme definitions can be related at the lowest order by a scale transformation for the case of the minimal subtraction schemes (MS and $\overline{\text{MS}}$) and the momentum space subtraction (MOM) scheme, but using the PMC, results would be scheme independent. A recent argument on the scheme dependence of the first conformal coefficient by Stevenson [57] is incorrect. The reason is that he assumes the v_1 coefficient of the scheme to be totally free with respect to the structure of the color factors and that it can be reabsorbed into the Λ parameter. There are several reasons why this certainly leads to wrong results. First, two different couplings in two different schemes at NLO can only be related by a scale transformation according to the RG group, i.e. by a shift of the type: $\beta_0 \log(\frac{\mu_1^2}{\mu_2^2})$ as shown also in Ref. [17]. In fact, given the scheme invariance of the β_0, β_1 , the only parameter that can be varied at NLO is the renormalization scale μ_r , which can have any real value or at most any value in the complex plane. Thus, the only scheme terms that can be reabsorbed into the scale (either the Λ or the renormalization scale μ_r) are those related to a shift of the scale using the standard RG group equations. This corresponds to the freedom of subtracting out any finite value together with the pole, in the renormalization procedure (e.g. MS and $\overline{\text{MS}}$). If one takes the freedom to vary the scheme according to any other relation that does not correspond to a "proper" RG equation at NLO, this consequently modifies the structure of the color factors for the coupling and thus would obtain a wrong result. If one follows this misleading assumption, one can obtain any result outside of a given initial theory and this is certainly not the aim of the xRGE, which should preserve the invariance of the final result. Moreover, if one changes the color structure for the coupling, one should be aware that, to be consistent, also the structure of the entire fixed-order calculation should be varied accordingly; though we do not agree with this procedure since a change of the color structure correspond to a change of the initial SU(N) theory (e.g. from QCD to QED Ref.[32]). Thus, any relation among couplings in different schemes, which can have perturbative validity in QCD but which cannot be considered as "proper" xRG transformations, should be considered as matching relations among quantities defined in different approximations or obtained using different approaches. Also in this case, results can be improved using the PMC and the residual dependence on the particular implicit definition of the "scheme" can be suppressed perturbatively by adding higher-order calculations. It can be shown that also in this case the results obtained are scheme-independent (e.g. see Ref. [58]). One may point out that, though the LO and the NLO conformal coefficient are scheme invariant, the higher-order conformal coefficients can be scheme dependent, we can answer that in the worst

¹We will discuss this procedure in detail in a future work soon.

case this scheme dependence for any of the PMCs procedures is highly suppressed. Another argument in Ref. [57] by Stevenson, which is based on the principle of minimum sensitivity (PMS), we hold to be incorrect. Since the PMS is based on the assumption that all the unknown higher-order terms give zero contribution to the pQCD series [9], its prediction directly breaks the standard renormalization group invariance [39, 51], its pQCD series does not have normal perturbative features [59] and can be treated as an effective prediction only when we know the series up to high enough orders and the conventional series has already shown good perturbative features [60]. On the other hand, the PMC respects all features of the renormalization group, and its prediction satisfies all the requirements of standard renormalization group invariance [39, 51, 52, 58]. Moreover, given that the PMC preserves the RG invariance, it is possible to define CSR - Commensurate Scale Relations[50] among the effective charges relating observables in different "schemes" preserving all the group properties. Applying the PMC and the CSRs, one can relate effective couplings, as also conformal coefficients, leading to scheme-independent results for the observables. We remark that in order to apply the PMC correctly, one should be able to distinguish among the nature of the different n_f -terms: whether they are related to the running of the coupling, to the running of masses or to UV-finite diagrams and in a deeper analysis also to the particular UV-divergent diagram (as discussed in Refs. [48, 61]). Once all n_f -terms have been associated with the correct diagram or parameter, conformal coefficients are RG invariant and match the coefficients of a conformal theory. Applications of the PMC to different quantities (see Ref. [62, 63]) have recently shown a direct improvement of theoretical predictions. Moreover, a deeper insight into the QCD coupling $\alpha_s(Q)$ at all scales, including $Q^2 = 0$, has been recently achieved (e.g. see Refs. [64, 65]), showing results consistent with the PMC.

PMC applications

So far, the PMC approach has been successfully applied to many high-energy processes, including Higgs boson production at the LHC [66], Higgs boson decays to $\gamma\gamma$ [67, 68], gg and $b\bar{b}$ [63, 69–73] processes, top-quark pair production at the LHC and Tevatron [47, 74–79], decay process [80, 81], semihard processes based on the BFKL approach [82–84], electron–positron annihilation to hadrons [49–51], hadronic Z^0 boson decays [85, 86], the event shapes in electron–positron annihilation [87–91], the electroweak parameter ρ [92, 93], $\Upsilon(1S)$ leptonic decay [94, 95], and charmonium production [96–98] and decay [99–102]. As shown in Ref. [103], by using the PMC, one can obtain a smooth transition for the running behavior between Bjorken sum rule effective coupling $\alpha_s^{g_1}(Q)$ in the V-scheme and the Light-Front Holographic QCD (LFHQCD) coupling, going from the perturbative to the non perturbative domain respectively. In addition, the PMC provides a possible solution to the $B \rightarrow \pi\pi$ puzzle [104] and to the $\gamma\gamma^* \rightarrow \eta_c$ puzzle [105].

In particular, with regard to the PMC application to top-quark pair hadroproduction, the resulting production cross-sections agree with precise experimental data, and the large discrepancies of the top-quark forward-backward asymmetries between SM estimations and experimental measurements are greatly reduced [47, 74–77]. Recently, an improved QCD prediction for the top-quark decay process obtained by using the PMC has also been presented in Ref.[80]. A precise top-quark mass can be extracted by the comparison of precise PMC predictions of production cross-sections with experimental data measured at LHC [78, 79]. The determined top-quark pole mass $m_t = 172.5 \pm 1.4$ GeV, from the LHC measurement at $\sqrt{s} = 13$ TeV [79] agrees with the world average cited by the Particle Data Group (PDG) [106]. More explicitly, we present a summary of the top-quark pole masses in Fig.(1.1), where our PMC result and previous determinations from collider measurements at different energies and different techniques are presented. Owing to unknown higher-order contributions, this leads to two kinds of residual scale dependence for PMC predictions. However, these two residual

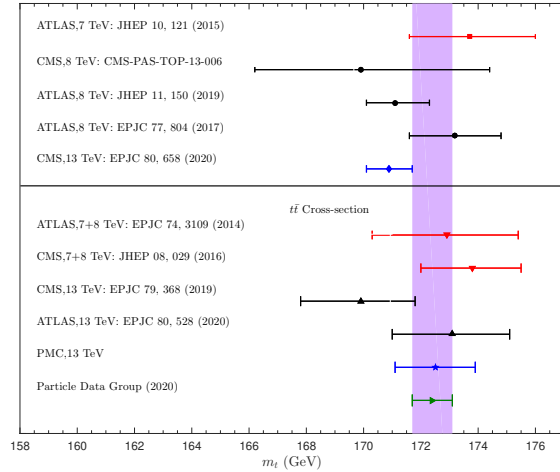


Figure 1.1: Summary of the top-quark pole masses, where the PMC result and previous determinations from collider measurements at different energies and different techniques are presented. The top-quark pole mass from the PDG [106] is also presented as the shaded band for reference.

scale dependencies are distinct from the conventional scale ambiguities, they are given by the unknown higher-order uncalculated contributions, while the scale dependence of the CSS is related more to the calculated orders. Thus, the residual scale dependence of the PMC results from the unknown higher-order terms and is an unavoidable intrinsic feature of the perturbative approach. It is to be noted that two of the three PMC ambiguities identified in Ref.[107] correspond exactly to two kinds of residual scale dependence. These two residual scale dependencies are highly suppressed; however, if the pQCD convergence of the perturbative series of either the PMC scale or the pQCD approximant is weak, such residual scale dependence could be significant. A recent discussion of the residual scale dependence of PMC predictions can also be found in the review [52].

Outline

In this review we display recent developments in solving the renormalization-scale and -scheme ambiguities based on the PMC and present some fundamental applications and results.

With respect to the previous reviews on the PMC (Refs. [40, 52]), in this review we focus on the recently developed method, namely the *Infinite-Order Scale-Setting using the Principle of Maximum Conformality* (PMC_∞), showing first some of its applications and new features, and then a comparison of this method with the CSS and the other PMC approaches, such as the multi-scale (PMCm), and the single-scale PMC (PMCs), on the Event Shape Variables and on some crucial fully integrated quantities: $R_{e^+e^-}$, R_τ and $\Gamma(H \rightarrow b\bar{b})$.

More in detail: in **Section I** we give an introduction to the renormalization scale setting problem in QCD; in **Section II** we recall fundamental equations of the renormalization group and their extended version, starting from the renormalization procedure of the strong coupling $\alpha_s(\mu)$ and its renormalization scale dependence; in **Section III** we summarize formulas and basic concepts of the PMC approach with its features and methods (PMCm, PMCs); in **Section IV** we introduce the newly developed method PMC_∞ and its new features; in **Section V** we show results for the application of the PMC_∞ to the event-shape variables: thrust and C -parameter, we show particularly new features of the PMC performing interesting limits for thrust (IR conformal and QED limit) and comparing the results under the CSS and the PMC_∞ methods; in this section we also show a novel method to determine the strong coupling and its behavior

$\alpha_s(Q)$ over a wide range of scales, from a single experiment at a single scale, using the event-shape variable results; in **Section VI** we present a detailed comparison of the CSS, PMCs, PMCm and PMC_∞ methods tested on fundamental fully integrated quantities at 4 loops: $R_{e^+e^-}$, R_τ and $\Gamma(H \rightarrow b\bar{b})$; finally, in **Section VII** we summarize and discuss the results.

2. Renormalization Scale and Scheme invariance

The focus of this section is the strong coupling constant and its renormalization-scale and -scheme dependence. We summarize fundamental basic theoretical results and updated formulas regarding the renormalization group.

2.1. The Renormalization Group

QCD is a renormalizable theory, which means that the infinite number of ultraviolet (UV) singularities that arise in loop integration may be reabsorbed into a finite number of parameters entering the Lagrangian: the masses, coupling constant and fields.

The procedure starts from the assumption that the variables entering the Lagrangian are not the effective quantities measured in experiments, but are unknown functions affected by singularities. The origin of the ultraviolet singularities is often interpreted as a manifestation that a QFT is a low-energy effective theory of a more fundamental yet unknown theory. The use of regularization UV cut-offs shields the very short-distance domain, where the perturbative approach to QFT ceases to be valid.

Once the coupling has been renormalized to a measured value and at a given energy scale, the effective coupling is no longer sensitive to the ultraviolet (UV) cut-off, nor to any unknown phenomena arising beyond this scale. Thus, the scale dependence of the coupling can be well understood formally and phenomenologically. Actually, gauge theories are affected not only by UV, but also by infrared (IR) divergencies. The cancellation of the latter is guaranteed by the Kinoshita-Lee-Nauenberg (KLN) theorem [108, 109].

Considering first the Lagrangian of a massless theory, which is free of any particular scale parameter, in order to deal with these divergences a regularization procedure is introduced. Referring to the dimensional regularization procedure [37, 110, 111], one varies the dimension of the loop integration, $D = 4 - 2\varepsilon$ and introduces a scale μ in order to restore the correct dimension of the coupling.

In order to determine the renormalized gauge coupling, we consider the quark-quark-gluon vertex and its loop corrections. UV-divergences arise from loop integration for higher-order contributions for both the external fields and the vertex. The renormalization constants of the vertices are related by Slavnov-Taylor identities, in particular:

$$Z_{\alpha_s}^{-1} = (\sqrt{Z_3 Z_2}/Z_1)^2, \quad (2.1)$$

where Z_{α_s} is the coupling renormalization constant, $Z_1(Q)$ is the vertex renormalization constant, $Z_3(Q)$ and $Z_2(Q)$ are:

$$A_{a,\mu} = Z_3^{1/2}(Q) A_{a,\mu}^R(Q) \quad \text{and} \quad \psi = Z_2^{1/2}(Q) \psi^R(Q),$$

the renormalization constants for gluon and quark fields respectively. The superscript R indicates renormalized fields. The renormalization constants in dimensional regularization are given by:

$$Z_1(Q) = 1 - \frac{\alpha_s(Q)}{4\pi} (N_c + C_F) \frac{1}{\varepsilon} \quad (2.2)$$

$$Z_2(Q) = 1 - \frac{\alpha_s(Q)}{4\pi} C_F \frac{1}{\varepsilon} \quad (2.3)$$

$$Z_3(Q) = 1 + \frac{\alpha_s(Q)}{4\pi} \left(\frac{5}{3} N_c - \frac{2}{3} N_f \right) \frac{1}{\varepsilon} \quad (2.4)$$

where ε is the regulator parameter for the UV-ultraviolet singularities. We have labelled N_f the number of flavors related

to the UV singular diagrams.² By substitution, we have that the UV divergence:

$$Z_\alpha(Q) = 1 - \frac{\alpha_s(Q)}{4\pi} \beta_0 \frac{1}{\varepsilon}, \quad (2.5)$$

with

$$\beta_0 = 11 - \frac{2N_f}{3}. \quad (2.6)$$

The singularities related to the UV poles are subtracted out by a redefinition of the coupling. In the MS scheme, the renormalized strong coupling $\alpha_s(Q)$ is related to the bare coupling $\overline{\alpha}_s$ by:

$$\overline{\alpha}_s = Q^{2\varepsilon} Z_\alpha(Q) \alpha_s(Q). \quad (2.7)$$

In the minimal subtraction scheme (MS) only the pole $1/\varepsilon$ related to the UV singularity is subtracted out. A more suitable scheme is $\overline{\text{MS}}$ [35, 112, 113], where the constant term $\ln(4\pi) - \gamma_E$ is also subtracted out. Different schemes can also be related by scale redefinition, e.g. $\mu^2 \rightarrow 4\pi\mu^2 e^{-\gamma_E}$. We remark that the renormalization procedure leads to a unique renormalization constant $Z_{\alpha_s} \equiv Z_g^2$ for the strong coupling. In fact, the other renormalization constants, such as Z_1^V , $V \in (3g, 4g, ccg, qqq)$, i.e. the renormalization constants for 3-gluon, 4-gluon, ghost-ghost-gluon, quark-quark-gluon vertex respectively, are related to it via the Slavnov–Taylor identities [114]:

$$Z_g = Z_1^{3g} (Z_3)^{-3/2}, \quad (2.8)$$

$$Z_g = \sqrt{Z_1^{4g}} (Z_3)^{-1}, \quad (2.9)$$

$$Z_g = Z_1^{ccg} (Z_3)^{-1/2} (Z_3^c)^{-1}, \quad (2.10)$$

$$Z_g = Z_1^{\psi\psi g} (Z_3)^{-1/2} (Z_2)^{-1}. \quad (2.11)$$

Thus, the renormalization procedure depends both on the particular choice of scheme and on the subtraction point μ . Hence, even though there are no dimensionful parameters in the initial bare Lagrangian, a mass scale μ is acquired during the renormalization procedure. The emergence of μ from a Lagrangian with no explicit scale is called dimensional transmutation [115]. The value of μ is arbitrary and is the momentum at which the UV divergences are subtracted out. Hence μ is called the subtraction point or renormalization scale. Thus, the definition of the renormalized coupling $\alpha_s^{\overline{\text{MS}}}(\mu)$ depends at the same time on both the chosen scheme, $\overline{\text{MS}}$ and the renormalization scale μ .

Renormalization scale invariance is recovered by introducing the Renormalization Group Equations. The scale dependence of the coupling can be determined by considering that the bare coupling $\overline{\alpha}_s$ and renormalized couplings, α_s , at different scales are related by:

$$\overline{\alpha}_s = Q^{2\varepsilon} Z_\alpha(Q) \alpha_s(Q) = \mu^{2\varepsilon} Z_\alpha(\mu) \alpha_s(\mu), \quad (2.12)$$

where ε is the regularization parameter, integrals are carried out in $4 - 2\varepsilon$ dimensions and the UV divergences are regularized to $1/\varepsilon$ poles. The Z_i are constructed as functions of $1/\varepsilon$, such that they cancel all $1/\varepsilon$ poles. From Eq. (2.12) we obtain the relation from two different couplings at two different scales:

$$\alpha_s(Q) = \mathcal{Z}_\alpha(Q, \mu) \alpha_s(\mu), \quad (2.13)$$

with $\mathcal{Z}_\alpha(Q, \mu) \equiv (\mu^{2\varepsilon}/Q^{2\varepsilon}) [Z_\alpha(Q)/Z_\alpha(\mu)]$. The \mathcal{Z}_α then clearly form a group with a composition law

$$\mathcal{Z}_\alpha(Q, \mu) = \mathcal{Z}_\alpha(Q, \mu_0) \mathcal{Z}_\alpha(\mu_0, \mu), \quad (2.14)$$

²Throughout the paper we use the following notation: n_f for the general number of active flavors, N_f to indicate the number of flavors related to the UV-divergent and N_F for the UV-finite diagrams.

a unity element $\mathcal{Z}_\alpha(Q, Q) = 1$ and an inverse: $\mathcal{Z}_\alpha(Q, \mu) = \mathcal{Z}_\alpha^{-1}(\mu, Q)$. The fundamental properties of the Renormalization Group are: *reflexivity*, *symmetry* and *transitivity*. Thus, the scale invariance of a given perturbatively calculated quantity is recovered by the invariance of the theory under the Renormalization Group Equations (RGE).

2.2. The evolution of $\alpha_s(\mu)$ in perturbative QCD

As shown in the previous section the renormalization procedure is not void of ambiguities. The subtraction of the singularities depends on the subtraction point or renormalization scale μ and on the renormalization scheme (RS). Physical observables cannot depend on the particular scheme or scale, given that the theory stems from a conformal Lagrangian. This implies that scale invariance must be recovered imposing the invariance of the renormalized theory under the renormalization group equation (RGE). In this section we discuss the dependence of the renormalized coupling $\alpha_s(Q)$ on the scale Q . As shown in QED by Gell-Mann and Low, this dependence can be described introducing the β -function given by:

$$\frac{1}{4\pi} \frac{d\alpha_s(Q)}{d\log Q^2} = \beta(\alpha_s) \quad (2.15)$$

and

$$\beta(\alpha_s) = - \left(\frac{\alpha_s}{4\pi} \right)^2 \sum_{n=0} \left(\frac{\alpha_s}{4\pi} \right)^n \beta_n. \quad (2.16)$$

Neglecting quark masses, the first two β -terms are RS independent and have been calculated in Refs. [116–120] for the $\overline{\text{MS}}$ scheme:

$$\beta_0 = \frac{11}{3} C_A - \frac{4}{3} T_R N_f, \quad (2.17)$$

$$\beta_1 = \frac{34}{3} C_A^2 - 4 \left(\frac{5}{3} C_A + C_F \right) T_R N_f \quad (2.18)$$

where $C_F = \frac{(N_c^2 - 1)}{2N_c}$, $C_A = N_c$ and $T_R = 1/2$ are the color factors for the SU(3) gauge group [121]. At higher loops β_i , $i \geq 2$ are scheme dependent; results for $\overline{\text{MS}}$ are given in Ref. [122]

$$\beta_2 = \frac{2857}{2} - \frac{5033}{18} N_f + \frac{325}{54} N_f^2, \quad (2.19)$$

in Ref. [123]

$$\begin{aligned} \beta_3 = & \left(\frac{149753}{6} + 3564\zeta_3 \right) - \left(\frac{1078361}{162} + \frac{6508}{27}\zeta_3 \right) N_f \\ & + \left(\frac{50065}{162} + \frac{6472}{81}\zeta_3 \right) N_f^2 + \frac{1093}{729} N_f^3, \end{aligned} \quad (2.20)$$

and in Ref. [124]

$$\begin{aligned} \beta_4 = & \left\{ \frac{8157455}{16} + \frac{621885}{2}\zeta_3 - \frac{88209}{2}\zeta_4 - 288090\zeta_5 \right. \\ & + N_f \left[-\frac{336460813}{1944} - \frac{4811164}{81}\zeta_3 + \frac{33935}{6}\zeta_4 + \frac{1358995}{27}\zeta_5 \right] \\ & + N_f^2 \left[\frac{25960913}{1944} + \frac{698531}{81}\zeta_3 - \frac{10526}{9}\zeta_4 - \frac{381760}{81}\zeta_5 \right] \\ & \left. + N_f^3 \left[-\frac{630559}{5832} - \frac{48722}{243}\zeta_3 + \frac{1618}{27}\zeta_4 + \frac{460}{9}\zeta_5 \right] + N_f^4 \left[\frac{1205}{2916} - \frac{152}{81}\zeta_3 \right] \right\}, \end{aligned} \quad (2.21)$$

with $\zeta_3 \simeq 1.20206$, $\zeta_4 \simeq 1.08232$ and $\zeta_5 \simeq 1.03693$, the Riemann zeta function. Given the renormalizability of QCD, new UV singularities arising at higher orders can be cancelled by redefinition of the same parameter, i.e. the strong coupling.

This procedure leads to the renormalization constant:

$$\begin{aligned}
Z_a(\mu) = & 1 - \frac{\beta_0}{\epsilon} a + \left(\frac{\beta_0^2}{\epsilon^2} - \frac{\beta_1}{2\epsilon} \right) a^2 - \left(\frac{\beta_0^3}{\epsilon^3} - \frac{7}{6} \frac{\beta_0 \beta_1}{\epsilon^2} + \frac{\beta_2}{3\epsilon} \right) a^3 \\
& + \left(\frac{\beta_0^4}{\epsilon^4} - \frac{23\beta_1 \beta_0^2}{12\epsilon^3} + \frac{5\beta_2 \beta_0}{6\epsilon^2} + \frac{3\beta_1^2}{8\epsilon^2} - \frac{\beta_3}{4\epsilon} \right) a^4 + \dots,
\end{aligned} \tag{2.22}$$

where $a = \alpha_s(\mu)/(4\pi)$ in the MS scheme. Given the arbitrariness of the subtraction procedure of also including part of the finite contributions (e.g. the constant $[\ln(4\pi) - \gamma_E]$ in $\overline{\text{MS}}$), there is an inherent ambiguity for these terms that translates into the RS dependence. In order to solve any truncated version of Eq. (2.15), this being a first order differential equation, we need an initial value of α_s at a given energy scale $\alpha_s(\mu_0)$. For this purpose, we set the initial scale $\mu_0 = M_Z$ the Z^0 mass, with the value $\alpha_s(M_Z)$ being determined phenomenologically. In QCD the number of colors N_c is set to 3, while N_f , i.e. the number of active flavors, varies with energy scale across quark thresholds.

2.2.1. One-loop result and asymptotic freedom

When all quark masses are set to zero, two physical parameters dictate the dynamics of the theory and these are the numbers of flavors N_f and colors N_c . In this section we determine the exact analytical solution to the truncated Eq. (2.15).

Considering the formula:

$$\int_{\alpha_s(\mu_0)}^{\alpha_s(\mu)} \frac{1}{4\pi} \frac{d\alpha_s}{\beta(\alpha_s)} = - \int_{\mu_0^2}^{\mu^2} \frac{dQ^2}{Q^2}, \tag{2.23}$$

and retaining only the first term:

$$\frac{Q^2}{\alpha_s^2} \frac{\partial \alpha_s}{\partial Q^2} = - \frac{1}{4\pi} \beta_0 \tag{2.24}$$

we achieve the solution for the coupling:

$$\frac{4\pi}{\alpha_s(\mu_0)} - \frac{4\pi}{\alpha_s(Q)} = \beta_0 \ln \left(\frac{\mu_0^2}{Q^2} \right). \tag{2.25}$$

This solution can be given in the explicit form:

$$\alpha_s(Q) = \frac{\alpha_s(\mu_0)}{1 + \beta_0 \frac{\alpha_s(\mu_0)}{4\pi} \ln(Q^2/\mu_0^2)}. \tag{2.26}$$

This solution relates one known (measured value) of the coupling at a given scale μ_0 with an unknown value $\alpha_s(Q)$. More conveniently, the solution can be given introducing the QCD scale parameter Λ . At β_0 order, this is defined as:

$$\Lambda^2 \equiv \mu^2 e^{-\frac{4\pi}{\beta_0 \alpha_s(\mu)}}, \tag{2.27}$$

which yields the familiar one-loop solution:

$$\alpha_s(Q) = \frac{4\pi}{\beta_0 \ln(Q^2/\Lambda^2)}.$$

Already at the one-loop level one can distinguish two regimes of the theory. For the number of flavors larger than $11N_c/2$ (i.e. the zero of the β_0 coefficient) the theory possesses an infrared noninteracting fixed point and at low energies the theory is known as non-Abelian quantum electrodynamics (non-Abelian QED). The high-energy behavior of the theory is uncertain, it depends on the number of active flavors and there is the possibility that it could develop a critical number of flavors above which the theory reaches an UV fixed point [125] and therefore becomes safe. When the number of flavors is less than $11N_c/2$, the noninteracting fixed point becomes UV in nature and then we say that the theory is *asymptotically free*.

It is straightforward to check the asymptotic limit of the coupling in the deep-UV region:

$$\lim_{s \rightarrow \infty} \alpha_s(s) = 0. \quad (2.28)$$

This result is known as *asymptotic freedom* and it is the outstanding result that has justified QCD as the most accredited candidate for the theory of strong interactions. On the other hand, we have that the perturbative coupling diverges at the scale $\Lambda \sim (200 - 300)$ MeV. This is sometimes referred to as the *Landau ghost pole* to indicate the presence of a singularity in the coupling that is actually unphysical and implies the breakdown of the perturbative regime. This itself is not an explanation for confinement, though it might indicate its presence. When the coupling becomes too large, the use of a nonperturbative approach to QCD is mandatory in order to obtain reliable results. We remark that the scale parameter Λ is RS dependent and its definition depends on the order of accuracy of the coupling $\alpha_s(Q)$. Considering that the solution α_s at order β_0 or β_1 is universal, the definition of Λ at the first two orders is usually preferred, i.e. Λ given at 1-loop by Eq. (2.27) or at 2-loops (see later) by Eq. (2.33).

2.2.2. Two-loop solution and the perturbative conformal window

In order to determine the solution for the strong coupling α_s at NNLO, it is convenient to introduce the following notation: $x(\mu) \equiv \frac{\alpha_s(\mu)}{2\pi}$, $t = \log(\mu^2/\mu_0^2)$, $B = \frac{1}{2}\beta_0$ and $C = \frac{1}{2}\frac{\beta_1}{\beta_0}$, $x^* \equiv -\frac{1}{C}$. The truncated NNLO approximation of the Eq. (2.15) leads to the differential equation:

$$\frac{dx}{dt} = -Bx^2(1 + Cx) \quad (2.29)$$

An implicit solution of Eq. (2.29) is given by the Lambert $W(z)$ function:

$$We^W = z \quad (2.30)$$

with: $W = \left(\frac{x^*}{x} - 1\right)$. The general solution for the coupling is:

$$x = \frac{x^*}{1 + W}, \quad (2.31)$$

$$z = e^{\frac{x^*}{x_0} - 1} \left(\frac{x^*}{x_0} - 1\right) \left(\frac{\mu^2}{\mu_0^2}\right)^{x^* B}. \quad (2.32)$$

Here we shall discuss the solutions to Eq. (2.29) with respect to the particular initial phenomenological value $x_0 \equiv \alpha_s(M_Z)/(2\pi) = 0.01877 \pm 0.00014$ given by the coupling determined at the Z^0 mass scale [126].

The signs of β_0, β_1 and consequently of B, x^* , depend on the values of the N_c, N_f , since the number N_c is set by the $SU(N_c)$ theory, we discuss the possible regions varying only the number of flavors N_f . We point out that different regions are defined by the signs of the β_0, β_1 , which have zeros in $\bar{N}_f^0 = \frac{11}{2}N_c$, $\bar{N}_f^1 = \frac{34N_c^3}{13N_c^2 - 3}$ respectively with $\bar{N}_f^0 > \bar{N}_f^1$. In the range $N_f < \bar{N}_f^1$ and $N_f > \bar{N}_f^0$ we have $B > 0$, $C > 0$ and the physical solution is given by the W_{-1} branch, while for $\bar{N}_f^1 < N_f < \bar{N}_f^0$ the solution for the strong coupling is given by the W_0 branch. By introducing the phenomenological value x_0 , we define a restricted range for the IR fixed point discussed by Banks and Zaks [127]. Given the value $\bar{N}_f = x^{*-1}(x_0) = 15.222 \pm 0.009$, we have that in the range $\frac{34N_c^3}{13N_c^2 - 3} < N_f < \bar{N}_f$ the β -function has both a UV and an IR fixed point, while for $N_f > \bar{N}_f$ we no longer have the asymptotically free UV behavior. The two-dimensional region in the number of flavors and colors where asymptotically free QCD develops an IR interacting fixed point is colloquially known as the *conformal window of pQCD*.

Thus, the actual physical range of a conformal window for pQCD is given by $\frac{34N_c^3}{13N_c^2 - 3} < N_f < \bar{N}_f$. The behavior of the coupling is shown in Fig. 2.1. In the IR region the strong coupling approaches the IR finite limit, x^* , in the case of

values of N_f within the conformal window (e.g. black dashed curve of Fig. 2.1), while it diverges at

$$\Lambda = \mu_0 \left(1 + \frac{|x^*|}{x_0} \right)^{\frac{1}{2B|x^*|}} e^{-\frac{1}{2Bx_0}} \quad (2.33)$$

outside the conformal window given the solution for the coupling with W_{-1} (e.g. the solid red curve of Fig. 2.1). The solution of the NNLO equation for the case $B > 0, C > 0$, i.e. $N_f < \frac{34N_c^3}{13N_c^2 - 3}$, can also be given using the standard QCD scale parameter Λ of Eq. (2.33),

$$x = \frac{x^*}{1 + W_{-1}}, \quad (2.34)$$

$$z = -\frac{1}{e} \left(\frac{\mu^2}{\Lambda^2} \right)^{x^* B}. \quad (2.35)$$

Different solutions can be achieved using different schemes, i.e. different definitions of the scale parameter Λ [128]. We stress that the presence of a Landau “ghost” pole in the strong coupling is only an effect of the breaking of the perturbative regime, including nonperturbative contributions, or using nonperturbative QCD, a finite limit is expected at any N_f [43]. Both solutions have the correct UV asymptotically free behavior. In particular, for the case $\bar{N}_f < N_f < \frac{11}{2}N_c$, we have a negative z , a negative C and a multi-valued solution, one real and the other imaginary, actually only one (the real) is acceptable given the initial conditions, but this solution is not asymptotically free. We thus restrict our analysis to the range $N_f < \bar{N}_f$, where we have the correct UV behavior. In general, IR and UV fixed points of the β -function can also be determined at different values of the number of colors N_c (different gauge group $SU(N)$) and N_f also extending this analysis to other gauge theories [129].

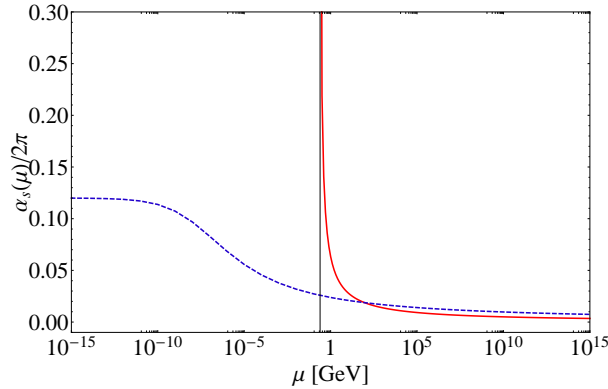


Figure 2.1: The strong running coupling $\alpha_s(\mu)$ for $N_f = 12$ (blue dashed) and for $N_f = 5$ (solid red). [90]

2.2.3. α_s at higher loops

The 3-loop truncated RG equation 2.15, written using the same normalization as Eq. (2.29) is given by

$$\beta(x) = \frac{dx}{dt} = -Bx^2 (1 + Cx + C_2x^2), \quad (2.36)$$

with $C_2 = \frac{\beta_2}{4\beta_0}$.

A straightforward integration of this equation would be hard to invert, as shown in Ref. [128], it is more convenient to extend the approach of the previous section by using the Padé Approximant Approach (PAA) [130–132]. The Padé Approximant of a given quantity calculated perturbatively in QCD up to order n , i.e. of the series:

$$S(x) = x (1 + r_1x + r_2x^2 + \dots + r_nx^n) \quad (2.37)$$

is defined as the rational function

$$x[N/M] = x \frac{1 + a_1 x + \dots + a_N x^N}{1 + b_1 x + \dots + b_M x^M}, \quad x[N/M] = S + x \mathcal{O}(x^{N+M+1}), \quad (2.38)$$

whose Taylor expansion up to order $N + M = n$ is identical to the original truncated series. The use of the PA makes the integration of Eq. (2.36) straightforward. PA's may also be used either to predict the next term of a given perturbative expansion, called a Padé Approximant prediction (PAP), or to estimate the sum of the entire series, called Padé Summation. Features of the PA are described in Ref. [133].

The Padé Approximant ($x^2[1/1]$) of the 3-loop β -function is given by

$$\beta_{\text{PA}}(x) = -Bx^2 \frac{1 + [C - (C_2/C)]x}{1 - (C_2/C)x}, \quad (2.39)$$

which leads to the solution:

$$B \ln(Q^2/\Lambda^2) = \frac{1}{x} - C \ln \left[\frac{1}{x} + C - \frac{C_2}{C} \right] \quad (2.40)$$

and finally,

$$x(Q^2) = -\frac{1}{C} \frac{1}{1 - (C_2/C^2) + W(z)}, \quad (2.41)$$

$$z = -\frac{1}{C} \exp[-1 + (C_2/C^2) - Bt/C], \quad (2.42)$$

the sign of C determines the sign of z and also the physically relevant branches of the Lambert function $W(z)$: for $C > 0, z < 0$ and the physical branch is $W_{-1}(z)$, taking real values in the range $(-\infty, -1)$, while for $C < 0, z > 0$ and the physical branch is given by the $W_0(z)$, taking real values in the range $(0, \infty)$.

We notice that the only significant difference between the 3-loop solution and the 2-loop solution (2.32) is in the solution $x(Q^2)$. This is because the difference in the definition of z can be reabsorbed into an appropriate redefinition of the scale parameter:

$$\Lambda^2 \longrightarrow \tilde{\Lambda}^2 = \Lambda^2 e^{C_2/(BC)}.$$

For orders up to β_4 , an approximate analytical solution is obtained integrating Eq. (2.15):

$$\begin{aligned} \ln \frac{\mu^2}{\Lambda^2} &= \int \frac{da}{\beta(a)} = \frac{1}{\beta_0} \left[\frac{1}{a} + b_1 \ln a + a(-b_1^2 + b_2) + a^2 \left(\frac{b_1^3}{2} - b_1 b_2 + \frac{b_3}{2} \right) \right. \\ &\quad \left. + a^3 \left(-\frac{b_1^4}{3} + b_1^2 b_2 - \frac{b_2^2}{3} - \frac{2}{3} b_1 b_3 + \frac{b_4}{3} \right) + \mathcal{O}(a^4) \right] + C \end{aligned} \quad (2.43)$$

where $a = \alpha_s(\mu)/(4\pi)$ and $b_N \equiv \beta_N/\beta_0$, ($N = 1, \dots, 4$) and performing the inversion of the last formula by iteration as shown in Ref. [134], achieving the final result of the coupling at five-loop accuracy:

$$\begin{aligned} a &= \frac{1}{\beta_0 L} - \frac{b_1 \ln L}{(\beta_0 L)^2} + \frac{1}{(\beta_0 L)^3} [b_1^2 (\ln^2 L - \ln L - 1) + b_2] \\ &\quad + \frac{1}{(\beta_0 L)^4} \left[b_1^3 \left(-\ln^3 L + \frac{5}{2} \ln^2 L + 2 \ln L - \frac{1}{2} \right) - 3b_1 b_2 \ln L + \frac{b_3}{2} \right] \\ &\quad + \frac{1}{(\beta_0 L)^5} \left[b_1^4 \left(\ln^4 L - \frac{13}{3} \ln^3 L - \frac{3}{2} \ln^2 L + 4 \ln L + \frac{7}{6} \right) + 3b_1^2 b_2 (2 \ln^2 L - \ln L - 1) \right. \\ &\quad \left. - b_1 b_3 \left(2 \ln L + \frac{1}{6} \right) + \frac{5}{3} b_2^2 + \frac{b_4}{3} \right] + \mathcal{O}\left(\frac{1}{L^6}\right). \end{aligned} \quad (2.44)$$

where $L = \ln(\mu^2/\Lambda^2)$. The same definition of the Λ scale given in Eq. (2.33) has been used for the $\overline{\text{MS}}$ scheme, which leads to setting the constant $C = (b_1/\beta_0) \ln(\beta_0)$.

Alternatively, we can relate the values of the coupling at two different scales by the 5-loop perturbative solution:

$$\begin{aligned}
a_{Q_2} = & a_{Q_1} + \beta_0 \ln\left(\frac{Q_1^2}{Q_2^2}\right) a_{Q_1}^2 + \left[\beta_0^2 \ln^2\left(\frac{Q_1^2}{Q_2^2}\right) + \beta_1 \ln\left(\frac{Q_1^2}{Q_2^2}\right) \right] a_{Q_1}^3 \\
& + \left[\beta_0^3 \ln^3\left(\frac{Q_1^2}{Q_2^2}\right) + \frac{5}{2} \beta_0 \beta_1 \ln^2\left(\frac{Q_1^2}{Q_2^2}\right) + \beta_2 \ln\left(\frac{Q_1^2}{Q_2^2}\right) \right] a_{Q_1}^4 \\
& + \left[\beta_0^4 \ln^4\left(\frac{Q_1^2}{Q_2^2}\right) + \frac{13}{3} \beta_0^2 \beta_1 \ln^3\left(\frac{Q_1^2}{Q_2^2}\right) + \frac{3}{2} \beta_1^2 \ln^2\left(\frac{Q_1^2}{Q_2^2}\right) + 3 \beta_2 \beta_0 \ln^2\left(\frac{Q_1^2}{Q_2^2}\right) + \beta_3 \ln\left(\frac{Q_1^2}{Q_2^2}\right) \right] a_{Q_1}^5 \\
& + \left[\beta_0^5 \ln^5\left(\frac{Q_1^2}{Q_2^2}\right) + \frac{77}{12} \beta_1 \beta_0^3 \ln^4\left(\frac{Q_1^2}{Q_2^2}\right) + \left(6 \beta_2 \beta_0^2 + \frac{35}{6} \beta_1^2 \beta_0 \right) \ln^3\left(\frac{Q_1^2}{Q_2^2}\right) \right. \\
& \quad \left. + \frac{7}{2} (\beta_3 \beta_0 + \beta_2 \beta_1) \ln^2\left(\frac{Q_1^2}{Q_2^2}\right) + \beta_4 \ln\left(\frac{Q_1^2}{Q_2^2}\right) \right] a_{Q_1}^6 + \dots \quad (2.45)
\end{aligned}$$

2.3. Renormalization scheme dependence

The β_i are the coefficients of the β -function arising in the loop expansion, i.e. in powers of \hbar . Although the first two coefficients β_0, β_1 are universally scheme-independent coefficients, depending only on the number of colors N_c and flavors N_f , the higher-order terms are, in contrast, scheme dependent. In particular, for the 't Hooft scheme [135] the higher β_i , $i \geq 2$ terms are set to zero, leading to the solution of Eq. (2.2.2) for the β -function valid at all orders. Moreover, in all MS-like schemes all the β_i coefficients are gauge independent, while other schemes, such as the momentum space subtraction (MOM) scheme [6, 36], depend on the particular gauge. Using the Landau gauge, the β terms for the MOM scheme are given by [136]

$$\beta_2 = 3040.48 - 625.387 N_f + 19.3833 N_f^2$$

and

$$\beta_3 = 100541 - 24423.3 N_f + 1625.4 N_f^2 - 27.493 N_f^3.$$

Results for the minimal MOM scheme and Landau gauge are given in Ref. [137]. The renormalization condition for the MOM scheme sets the virtual quark propagator to the same form as a free massless propagator. Different MOM schemes exist and the above values of β_2 and β_3 are determined with the MOM scheme defined by subtracting the 3-gluon vertex to a point with one null external momentum. This leads to a coupling that is not only RS dependent but also gauge dependent. The values of β_2 and β_3 given here are only valid in the Landau gauge. Values in the V-scheme defined by the static heavy-quark potential [138–144] can be found in Ref. [145]. They result in $\beta_2 = 4224.18 - 746.01 N_f + 20.88 N_f^2$ and $\beta_3 = 43175 - 12952 N_f + 707.0 N_f^2$ respectively. We recall that the signs of the β_i control the running of α_s . We have $\beta_0 > 0$ for $N_f \leq 16$, $\beta_1 > 0$ for $N_f \leq 8$, $\beta_2 > 0$ for $N_f \leq 5$ and β_3 is always positive. Consequently, α_s decreases at high momentum transfer, leading to the asymptotic freedom of pQCD. Note that, β_i are sometimes defined with an additional multiplying factor $1/(4\pi)^{i+1}$. Different schemes are characterized by different $\beta_i, i \geq 2$ and lead to different definitions for the effective coupling.

The Λ parameter represents the Landau ghost pole in the perturbative coupling in QCD. We recall that the Landau pole was initially identified in the context of Abelian QED. However, the presence of this pole does not affect QED. Given its value, $\Lambda \sim 10^{30-40}$ GeV, above the Planck scale [146], at which new physics is expected to occur in order to suppress the unphysical divergence. The QCD Λ parameter in contrast is at low energies, its value depends on the RS, on the order of the β -series, β_i , on the approximation of the coupling $\alpha_s(\mu)$ at orders higher than β_1 and on the number of flavors N_f . Although mass corrections due to light quarks at higher order in perturbative calculations introduce negligible terms, they actually indirectly affect α_s through N_f . In fact, the number of active quark flavors runs with the scale Q and a

quark q is considered active in loop integration if the scale $Q \geq m_q$. Thus, in general, light quarks can be considered massless regardless of whether they are active or not, while α_s varies smoothly when passing a quark threshold, rather than in discrete steps. The matching of the values of α_s below and above a quark threshold makes Λ depend on N_f . Matching requirements at leading order β_0 , imply that:

$$\alpha_s^{N_f-1}(Q=m_q) = \alpha_s^{N_f}(Q=m_q)$$

and therefore that:

$$\Lambda^{N_f} = \Lambda^{N_f-1} \left(\frac{\Lambda^{N_f-1}}{m_q} \right)^{2/(33-2N_f)}$$

The formula with β_1 , can be found in [147] and the four-loop matching in the $\overline{\text{MS}}$ RS is given in [148].

As shown in the previous section at the lowest order β_0 , the Landau singularity is a simple pole on the positive real axis of the Q^2 -plane, whereas at higher order it acquires a more complicated structure. This pole is unphysical and is located on the positive real axis of the complex Q^2 -plane. This singularity of the coupling indicates that the perturbative regime of QCD breaks down and it may also suggest that a new mechanism takes over, such as the confinement. Thus, the value of Λ is often associated with the confinement scale, or equivalently to the hadronic mass scale. An explicit relation between hadron masses and the Λ scale has been obtained in the framework of holographic QCD [149]. Landau poles on the other hand, usually do not appear in nonperturbative approaches, such as AdS/QCD.

Different schemes are related perturbatively by:

$$\alpha_s^{(2)}(Q) = \alpha_s^{(1)}(Q) \left[1 + v_1 \alpha_s^{(1)}(Q)/(4\pi) \right] + \mathcal{O}(\alpha_s^2) \quad (2.46)$$

where v_1 is the leading order difference between $\alpha_s(Q)$ in the two schemes. In the case of the V-scheme and $\overline{\text{MS}}$ scheme we have: $v_1^{\overline{\text{MS}}} = \frac{31}{9}C_A - \frac{20}{9}T_F n_l$. Thus, the relation between Λ_1 in a scheme 1 and Λ_2 in a scheme 2 is, at the one-loop order, given by:

$$\Lambda_2 = \Lambda_1 e^{\frac{v_1}{2\beta_0}}.$$

For example, the $\overline{\text{MS}}$ and V-scheme scale parameters are related by:

$$\Lambda_V = \Lambda_{\overline{\text{MS}}} e^{\frac{93-10N_f}{2(99-6N_f)}}$$

The relation is valid at each threshold, translating all values for the scale from one scheme to the other.

2.4. The Extended Renormalization Group Equations

Given that physical predictions cannot depend on the choice of the renormalization scale nor on the scheme, the same approach used for the renormalization scale based on the invariance under RGE is extended to scheme transformations. This approach leads to the Extended Renormalization Group Equations, which were introduced first by Stückelberg and Peterman [1], then discussed by Stevenson [8–11] and also improved by Lu and Brodsky [150]. A physical quantity, R , calculated at the N -th order of accuracy is expressed as a truncated expansion in terms of a coupling constant $\alpha_S(\mu)$ defined in the scheme S and at the scale μ , such as

$$R_N = r_0 \alpha_S^p(\mu) + r_1(\mu) \alpha_S^{p+1}(\mu) + \dots + r_N(\mu) \alpha_S^{p+N}(\mu). \quad (2.47)$$

At any finite order, the scale and scheme dependences of the coupling constant $\alpha_S(\mu)$ and of the coefficient functions $r_i(\mu)$ do not totally cancel, this leads to a residual dependence in the finite series and to the scale and scheme ambiguities.

In order to generalize the RGE approach, it is convenient to improve the notation by introducing the universal coupling function as the extension of an ordinary coupling constant to include the dependence on the scheme parameters $\{c_i\}$:

$$\alpha = \alpha(\mu/\Lambda, \{c_i\}). \quad (2.48)$$

where Λ is the standard two-loop $\overline{\text{MS}}$ scale parameter. The subtraction prescription is now characterized by an infinite set of continuous *scheme parameters* $\{c_i\}$ and by the renormalization scale μ . Stevenson [9] has shown that one can identify the beta-function coefficients of a given renormalization scheme with the scheme parameters. Considering that the first two coefficients of the β -function are scheme independent, each scheme is identified by its $\{\beta_i, i = 2, 3, \dots\}$ parameters.

More conveniently, let us define the rescaled coupling constant and the rescaled scale parameter as

$$a = \frac{\beta_1}{\beta_0} \frac{\alpha}{4\pi}, \quad \tau = \frac{2\beta_0^2}{\beta_1} \log(\mu/\Lambda). \quad (2.49)$$

Then, the rescaled β -function takes the canonical form:

$$\beta(a) = \frac{da}{d\tau} = -a^2 (1 + a + c_2 a^2 + c_3 a^3 + \dots) \quad (2.50)$$

with $c_n = \beta_n \beta_0^{n-1} / \beta_1^n$ for $n = 2, 3, \dots$.

The scheme and scale invariance of a given observable R , can be expressed as:

$$\begin{aligned} \frac{\delta R}{\delta \tau} &= \beta \frac{\partial R}{\partial a} + \frac{\partial R}{\partial \tau} = 0 \\ \frac{\delta R}{\delta c_n} &= \beta^{(n)} \frac{\partial R}{\partial a} + \frac{\partial R}{\partial c_n} = 0. \end{aligned} \quad (2.51)$$

The fundamental beta function that appears in Eqs. (2.51) reads:

$$\beta(a, \{c_i\}) \equiv \frac{\delta a}{\delta \tau} = -a^2 (1 + a + c_2 a^2 + c_3 a^3 + \dots) \quad (2.52)$$

and the extended or scheme-parameter beta functions are defined as:

$$\beta^{(n)}(a, \{c_i\}) \equiv \frac{\delta a}{\delta c_n}. \quad (2.53)$$

The extended beta functions can be expressed in terms of the fundamental beta function. Since the $(\tau, \{c_i\})$ are independent variables, second partial derivatives respect the commutativity relation:

$$\frac{\delta^2 a}{\delta \tau \delta c_n} = \frac{\delta^2 a}{\delta c_n \delta \tau}, \quad (2.54)$$

which implies

$$\frac{\delta \beta^{(n)}}{\delta \tau} = \frac{\delta \beta}{\delta c_n}, \quad (2.55)$$

$$\beta \beta'_{(n)} = \beta^{(n)} \beta' - a^{n+2}, \quad (2.56)$$

where $\beta'_{(n)} = \partial \beta^{(n)} / \partial a$ and $\beta' = \partial \beta / \partial a$. From here

$$\beta^{-2} \left(\frac{\beta^{(n)}}{\beta} \right)' = -a^{n+2}, \quad (2.57)$$

$$\beta^{(n)}(a, \{c_i\}) = -\beta(a, \{c_i\}) \int_0^a dx \frac{x^{n+2}}{\beta^2(x, \{c_i\})}, \quad (2.58)$$

where the lower limit of the integral has been set to satisfy the boundary condition

$$\beta^{(n)} \sim O(a^{n+1}).$$

That is, a change in the scheme parameter c_n can only affect terms of order a^{n+1} or higher in the evolution of the universal coupling function.

The extended renormalization group equations Eqs. (2.51) can be written in the form:

$$\begin{aligned}\frac{\partial R}{\partial \tau} &= -\beta \frac{\partial R}{\partial a} \\ \frac{\partial R}{\partial c_n} &= -\beta_{(n)} \frac{\partial R}{\partial a}.\end{aligned}\tag{2.59}$$

Thus, provided we know the extended beta functions, we can determine any variation of the expansion coefficients of R under scale-scheme transformations. In particular, we can evolve a given perturbative series into another, determining the expansion coefficients of the latter and vice versa. Thus, different schemes and scales can be related according to the extended renormalization group equations and the fundamental requirement of “renormalization scale and scheme invariance” is recovered via the extended renormalization group invariance of perturbative QCD. Unfortunately, these relations and in general all perturbative calculations are known only up to a certain level of accuracy and the truncated formulas are responsible for an important source of uncertainties: the *scheme* and *scale ambiguities*.

2.5. The running coupling constant $\alpha_s(\mu)$

The strong coupling α_s , is a fundamental parameter of the SM theory and determines the strength of the interactions among quarks and gluons in quantum chromodynamics (QCD).

In order to understand hadronic interactions, it is necessary to determine the magnitude of the coupling and its behavior over a wide range of values, from low- to high-energy scales. Long and short distances are related to low and high energies respectively. In the high-energy region the strong coupling has an *asymptotic behavior* and QCD becomes perturbative, while in the region of low energies, e.g. at the proton-mass scale, the dynamics of QCD is affected by processes such as quark confinement, soft radiation and hadronization. In the first case experimental results can be matched with theoretical calculations and a precise determination of α_s depends on both experimental accuracy and theoretical errors. In the latter case experimental results are difficult to achieve and theoretical predictions are affected by the confinement and hadronization mechanisms, which are rather model dependent. Various processes also involve a precise knowledge of the coupling in both the high and low momentum transfer regions and in some cases calculations must be improved with electroweak (EW) corrections. Thus, the determination of the QCD coupling over a wide range of energy scales is a crucial task in order to achieve results and to test QCD to the highest precision. Theoretical uncertainties in the value of $\alpha_s(Q)$ contribute to the total theoretical uncertainty in the physics investigated at the Large Hadron Collider (LHC), such as the Higgs sector, e.g. Higgs production via gluon fusion [19]. The behavior of the perturbative coupling at low-momentum transfer is also fundamental for the scale of the proton mass, in order to understand hadronic structure, quark confinement and hadronization processes. IR effects, such as soft radiation and renormalon factorial growth, spoil the perturbative nature of QCD in the low-energy domain. Higher-twist effects can also play an important role. Processes involving the production of heavy quarks near threshold require knowledge of the QCD coupling at very low momentum scales. Even reactions at high energies may involve the integration of the behavior of the strong coupling over a large domain of momentum scales, including IR regions. Precision tests of the coupling are crucial also for other aspects of QCD that are still under continuous investigation, such as the hadron masses and their internal structure. In fact, the strong interaction is responsible for the mass of hadrons in the zero-mass limit of the u , d quarks.

The origin and phenomenology of the behavior of $\alpha_s(\mu)$ at small distances, where asymptotic freedom appears, is well

understood and explained in many textbooks on Quantum Field Theory and Particle Physics. Numerous reviews exist; see e.g. Refs. [151, 152]. However, standard explanations often create an apparent puzzle. Other questions remain even in this well understood regime: a significant issue is how to identify the scale Q that controls a given hadronic process, especially if it depends on many physical scales.

3. The Principle of Maximum Conformality – PMC scale setting

The Principle of Maximum Conformality (PMC) [45–47, 49, 50] is the principle underlying BLM and it generalizes the BLM method to all possible applications and to all orders.

BLM scale setting is greatly inspired by QED. The standard Gell-Mann–Low scheme determines the correct renormalization scale identifying the scale with the virtuality of the exchanged photon [2]. For example, in electron–muon elastic scattering, the renormalization scale is given by the virtuality of the photon exchanged, i.e. the spacelike momentum transfer squared $\mu_r^2 = q^2 = t$. Thus,

$$\alpha(t) = \frac{\alpha(t_0)}{1 - \Pi(t, t_0)}, \quad (3.1)$$

where

$$\Pi(t, t_0) = \frac{\Pi(t) - \Pi(t_0)}{1 - \Pi(t_0)}$$

is the vacuum polarization (VP) function. From Eq. (3.1) it follows that the renormalization scale $\mu_R^2 = t$ can be determined by the β_0 -term at the lowest order. This scale is sufficient to sum all the vacuum polarization contributions into the dressed photon propagator, both proper and improper to all orders. Starting from a first evaluation of the physical observable that is obtained by calculating perturbative corrections in a given scheme (commonly used are MS or $\overline{\text{MS}}$) and at an initial renormalization scale $\mu_r = \mu_r^{\text{init}}$, one obtains the truncated expansion:

$$\rho_n = C_0 \alpha_s^p(\mu_r) + \sum_{i=1}^n C_i(\mu_r) \alpha_s^{p+i}(\mu_r), \quad (p \geq 0), \quad (3.2)$$

where C_0 is the tree-level term, while C_1, C_2, \dots, C_n are the one-loop, two-loop and n -loop corrections respectively and p is the power of the coupling at tree-level. In order to improve the pQCD estimate of the observable, after the initial renormalization a change of scale using the RGE is performed according to the BLM scale setting.

Following the GM–L scheme in QED, the BLM scales can be determined at LO in perturbation theory by writing explicit contributions coming from the different N_f terms of the NLO coefficient in a physical observable as [15]:

$$\begin{aligned} \rho &= C_0 \alpha_{s, \overline{\text{MS}}}^p(\mu_r) \left[1 + (AN_f + B) \frac{\alpha_{s, \overline{\text{MS}}}(\mu_r)}{\pi} \right] \\ &= C_0 \alpha_{s, \overline{\text{MS}}}^p(\mu_r) \left[1 + \left(-\frac{3}{2}A\beta_0 + \frac{33}{2}A + B \right) \frac{\alpha_{s, \overline{\text{MS}}}(\mu_r)}{\pi} \right], \end{aligned} \quad (3.3)$$

where $\mu_r = \mu_r^{\text{init}}$ stands for an initial renormalization scale, which practically can be taken as the typical momentum transfer of the process. The N_f term is due to the quark vacuum polarization. Calculations are in the $\overline{\text{MS}}$ -scheme.

At the NLO level, all N_f terms should be resummed into the coupling. Using the NLO α_s -running formula:

$$\alpha_{s, \overline{\text{MS}}}(\mu_r^*) = \frac{\alpha_{s, \overline{\text{MS}}}(\mu_r)}{1 + \frac{\beta_0}{4\pi} \alpha_{s, \overline{\text{MS}}}(\mu_r) \ln\left(\frac{\mu_r^*}{\mu_r}\right)}, \quad (3.4)$$

we obtain

$$\rho = C_0 \alpha_{s, \overline{\text{MS}}}^p(\mu_r^*) \left[1 + C_1^* \frac{\alpha_{s, \overline{\text{MS}}}(\mu_r^*)}{\pi} \right], \quad (3.5)$$

where

$$\mu_r^* = \mu_r \exp\left(\frac{3A}{p}\right)$$

is the BLM scale and

$$C_1^* = \frac{33}{2}A + B$$

is the *conformal* coefficient, i.e. the NLO coefficient not depending on the RS and scale μ . Both the effective BLM scale μ_r^* and the coefficient C_1^* are N_f independent and conformal at LO. By including the term $33A/2$ into the scale we eliminate the β_0 term of the NLO coefficient C_1 , which is responsible for the running of the coupling constant, and the observable in the final results can be written in its *maximal conformal form*, Eq. (3.5).

The BLM method can be extended to higher orders in a systematic way by including the n_f terms arising at higher order into the BLM scales consistently. In order to extend the BLM beyond the NLO, the following points are considered essential:

1. All n_f -terms associated with the β -function (i.e. N_f terms) and then with the renormalization of the coupling constant, must be absorbed into the effective coupling, while those n_f -terms that have no relation with UV-divergent diagrams (i.e. N_F -terms) should be identified and considered as part of the conformal coefficients. After BLM scale setting, the perturbative series for the physical observable becomes a conformal series, all nonconformal terms should be absorbed into the effective coupling in a consistent manner.
2. New N_f -terms (corresponding to new β_0 coefficients) arise at each perturbative order, thus a new BLM scale that sums these terms consistently into the running coupling, should be introduced at each calculated perturbative order. In fact, there is no reason to use a unified effective scale for the entire perturbative series as shown in Refs. [153, 154].
3. The BLM scales themselves should be a RG-improved perturbative series [46]. The length of the perturbative series for each BLM scale depends on how many new N_f -terms (or β_i -terms) we have from the higher-order calculation and to what perturbative order we have performed.

Actually, the last point is not mandatory and needs clarification. In order to apply the BLM/PMC using perturbative scales, the argument of the coupling in the expansion of the BLM/PMC scale should be the physical scale of the process Q , that may be either the center-of-mass energy \sqrt{s} or even another variable, such as \sqrt{t} , \sqrt{u} , M_H, \dots , depending on the process. Setting the initial scale to the physical scale would greatly simplify the BLM/PMC procedure, preserving the original scale invariance of the observable and eliminating the initial scale dependence from the BLM/PMC scales. In case the BLM/PMC scales are not perturbatively calculated, as will be shown in Section 4.1, the initial scale can be treated as an arbitrary parameter.

In agreement with these indications, it is possible to achieve a scale setting method extendible iteratively to all orders, which leads to the correct coefficients $\mathcal{C}_i(\mu_{BLM}^*)$ for the final “maximally conformal” series:

$$\rho_n = \mathcal{C}_0 \alpha_s^p(\mu_{BLM}^*) + \mathcal{C}_1(\mu_{BLM}^{**}) \alpha_s^{p+1}(\mu_{BLM}^{**}) + \mathcal{C}_2(\mu_{BLM}^{***}) \alpha_s^{p+2}(\mu_{BLM}^{***}) + \dots \quad (3.6)$$

where the BLM scales $\mu_{BLM}^*, \mu_{BLM}^{**}, \dots$ are set by a recursive use of the RG equations in order to cancel all the N_f terms from the series. We remark that since the coefficients $\mathcal{C}_i(\mu_{BLM}^*)$ have been obtained cancelling all β terms related to running of the coupling they actually are free of any scale and scheme dependence left. In other words, the $\mathcal{C}_i(\mu_{BLM}^*) \equiv \tilde{\mathcal{C}}_i$, where the $\tilde{\mathcal{C}}_i$ are conformal coefficients not depending on the renormalization scale. Hence, the BLM approach leads to an maximally conformal observable, i.e. where all the renormalization scale and scheme dependence has been confined to the effective coupling and to its renormalization scale $\alpha_s(\mu_{BLM})$.

Fundamental features of the BLM method:

- A) BLM scales at LO, are set simply by identifying the coefficient A of the N_f term.
- B) Since all n_f -terms related to the running of the coupling are reabsorbed, scheme differences do not affect the results and the perturbative expansions in $\alpha_s(\mu_r^*)$ in two different schemes, e.g. $\overline{\text{MS}}$ and $\overline{\overline{\text{MS}}}$, are identical. We notice that

n_f -terms related to the UV finite diagrams, may arise at every order in perturbation theory. These terms might be related either to the particular kinematics of the initial state or even to finite loop diagrams arising at higher orders, thus in both cases are insensitive to the UV cutoff or to the RS and cannot be considered as β -terms. We label these terms as N_F -terms and they do not give contributions to the BLM scales.

- C) Using BLM scale setting, the perturbative expansion does not change across quark threshold, given that all vacuum-polarization effects due to a new quark are automatically absorbed into the effective coupling. This implies that in a process with fixed kinematic variables (e.g. a total cross-section), we can use a naive LO/NLO $\alpha_s(\mu_r^{\text{BLM}})$ -running, with the number of active flavor N_f fixed to the value determined by the BLM scale, to perform the calculation [155].
- D) The BLM method preserves all the RG properties of *existence* and *uniqueness*, *reflexivity*, *symmetry* and *transitivity*. As shown in Refs. [156–159], the RG invariance of the BLM leads to scheme-independent transformations that relate couplings in different schemes. These are known as *commensurate scale relations* (CSRs) and it has been shown that, even though the expansion coefficients under different renormalization schemes can be different, after a proper scale setting, one can determine a relation between the effective couplings leading to an invariant result for the calculated quantity. Using this approach it is also possible to extend conformal properties to renormalizable gauge theories, such as the generalized Crewther relation [160–163].
- E) The BLM approach reduces to the GM–L scheme for QED in the Abelian limit $N_c \rightarrow 0$ [32]; the results are in perfect agreement.
- F) The elimination of the N_f term related to the β_0 coefficient from the perturbative series eliminates the renormalon terms $n!\beta_0^n \alpha_s^{n+1}$ over the entire range of the accessible physical energies and not only in the low-energy domain. The convergence of the resulting series is then greatly improved.

Several extended versions of the BLM approach beyond the NLO have been proposed in the literature, such as the dressed-skeleton expansion, the large- β_0 expansion, the BLM expansion with an overall renormalization scale and the sequential BLM (seBLM), an extension to the sequential BLM (xBLM) in Refs. [153, 159, 163–168]. These different extensions of the BLM are mostly partial or *ad hoc* improvements of the first LO-BLM [15] in some cases up to NNLO, in other cases using a rather effective approach, i.e. by introducing an overall effective BLM scale for the entire perturbative expansion. Results obtained with these approaches also did not respect the basic points (1–3). Most importantly, these methods lead to results that are still dependent on the initial renormalization scale. The fundamental feature of the BLM is to obtain results free of scale ambiguities and thus independent of the choice of initial renormalization scale. The first aim of the BLM scale is to eliminate the renormalization scale and scheme uncertainties; thus any extension of the BLM not respecting this basic requirement does not represent a real improvement of the standard conventional scale setting CSS method.

The reasons for the different extensions of the BLM method to higher orders were mainly two: firstly, it was not clear how to generalize this approach to all possible quantities, which translates into the question: what is the principle underlying the BLM method? And secondly, what is the correct procedure to identify and reabsorb the N_f -terms unambiguously order-by-order? A practical reason that renders the extension to higher orders not straightforward is the presence of finite UV corrections given by the three- and four-gluon vertices of the additional N_F -terms that are unrelated to the running of α_s .

In its first formulation in Ref. [45] it was suggested to use a unique PMC scale at LO to reabsorb all β contributions

related to different skeleton-graph scales by properly weighting the two contributions, such as that of the t -channel and s -channel. This approach was more oriented towards a single PMC scale that reabsorbs all β terms related to the running coupling. A multi-scale approach was later developed considering different scales arising at each order of accuracy including different β coefficients according to the perturbative expansion. We remark that the PMC method preserves all the properties (A–F) of the BLM procedure and it extends these properties to all orders, eliminating the renormalization scale and scheme ambiguities. The PMC also generalizes this approach to all gauge theories. Firstly, this is crucial in order to apply the same method to all SM sectors. Secondly, in the perspective of a *grand unified theory* (GUT), only one scale-setting method may be applied for consistency, and this method must agree with the GM–L scheme and with the QED results.

In order to apply the PMC, is convenient to follow the flowchart shown in Fig. 3.1 and to write the observable of Eq. (3.2) with the explicit contributions of the n_f terms in the coefficients calculated at each order of accuracy:

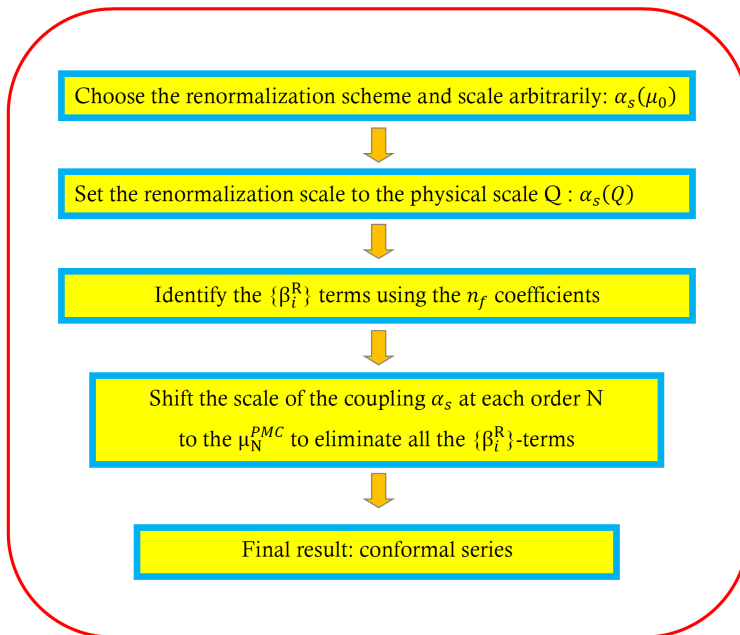


Figure 3.1: Flowchart for the PMC procedure.

$$\rho(Q) = \sum_{i=1}^n \left(\sum_{j=0}^{i-1} c_{i,j}(\mu_r, Q) n_f^j \right) a_s^{p+i-1}(\mu_r), \quad (3.7)$$

where Q represents the kinematic scale or the physical scale of the measured observable and p is the power of α_s associated with the tree-level terms. In general, this procedure is always possible either for analytic or numerical (e.g. Monte Carlo) calculations, given that both strategies keep track of terms related to different color factors. The core of the PMC method, as was for BLM, is that all N_f terms related to the β -function arising in a perturbative calculation must be summed, by proper definition of the renormalization scale μ_{PMC} , into the effective coupling α_s by recursive use of the RGE. Essentially the difference between the two procedures is that while in BLM the scales are set iteratively order-by-order to remove all n_f terms, in the PMC the n_f terms are written first as β terms and then reabsorbed into the effective coupling. The two procedures are related by the *correspondence principle* [46].

3.1. The multi-scale Principle of Maximum Conformality: PMCm

The PMCm method is based on a multi-scale application of the PMC. In this section we show how to implement this method to any order of accuracy. First, as shown in the flowchart in Fig. 3.1, for the pQCD approximant (3.7), it is convenient to transform the $\{n_f\}$ series at each order into the $\{\beta_i\}$ series. The QCD degeneracy relations [169] ensure the realizability of such a transformation. For example, Eq. (3.7) may be rewritten as [49, 50]

$$\begin{aligned} \rho(Q) &= r_{1,0} a_s(\mu_r) + \left(r_{2,0} + \beta_0 r_{2,1} \right) a_s^2(\mu_r) \\ &+ \left(r_{3,0} + \beta_1 r_{2,1} + 2\beta_0 r_{3,1} + \beta_0^2 r_{3,2} \right) a_s^3(\mu_r) \\ &+ \left(r_{4,0} + \beta_2 r_{2,1} + 2\beta_1 r_{3,1} + \frac{5}{2} \beta_1 \beta_0 r_{3,2} + 3\beta_0 r_{4,1} + 3\beta_0^2 r_{4,2} + \beta_0^3 r_{4,3} \right) a_s^4(\mu_r) + \dots, \end{aligned} \quad (3.8)$$

where $r_{i,j}$ can be derived from $c_{i,j}$, $r_{i,0}$ are conformal coefficients and $r_{i,j}$ ($j \neq 0$) are nonconformal. For definiteness and without loss of generality, we have set $p = 1$ and $n = 4$ to illustrate the PMC procedures. Different types of $\{\beta_i\}$ -terms can be absorbed into α_s in an order-by-order manner by using the RGE, which leads to distinct PMC scales at each order:

$$\begin{aligned} a_s^k(Q_k) &\leftarrow a_s^k(\mu_r) \left\{ 1 + k\beta_0 \frac{r_{k+1,1}}{r_{k,0}} a_s(\mu_r) \right. \\ &+ k \left(\beta_1 \frac{r_{k+1,1}}{r_{k,0}} + \frac{k+1}{2} \beta_0^2 \frac{r_{k+2,2}}{r_{k,0}} \right) a_s^2(\mu_r) \\ &\left. + k \left(\beta_2 \frac{r_{k+1,1}}{r_{k,0}} + \frac{2k+3}{2} \beta_0 \beta_1 \frac{r_{k+2,2}}{r_{k,0}} + \frac{(k+1)(k+2)}{3!} \beta_0^3 \frac{r_{k+3,3}}{r_{k,0}} \right) a_s^3(\mu_r) + \dots \right\}. \end{aligned} \quad (3.9)$$

The coefficients $r_{i,j}$ are generally functions of μ_r , which can be redefined as

$$r_{i,j} = \sum_{k=0}^j C_j^k \hat{r}_{i-k,j-k} \ln^k(\mu_r^2/Q^2), \quad (3.10)$$

where the reduced coefficients $\hat{r}_{i,j} = r_{i,j}|_{\mu_r=Q}$ (specifically, we have $\hat{r}_{i,0} = r_{i,0}$) and the combinatorial coefficients $C_j^k = j!/(k!(j-k)!)$. As discussed in the previous section, we set the renormalization scale μ_r to the physical scale of the process Q :

$$\begin{aligned} \ln \frac{Q^2}{Q_1^2} &= \frac{\hat{r}_{2,1}}{\hat{r}_{1,0}} + \beta_0 \left(\frac{\hat{r}_{1,0} \hat{r}_{3,2} - \hat{r}_{2,1}^2}{\hat{r}_{1,0}^2} \right) a_s(Q) \\ &+ \left[\beta_1 \left(\frac{3\hat{r}_{3,2}}{2\hat{r}_{1,0}} - \frac{3\hat{r}_{2,1}^2}{2\hat{r}_{1,0}^2} \right) + \beta_0^2 \left(\frac{\hat{r}_{4,3}}{\hat{r}_{1,0}} - \frac{2\hat{r}_{3,2}\hat{r}_{2,1}}{\hat{r}_{1,0}^2} + \frac{\hat{r}_{2,1}^3}{\hat{r}_{1,0}^3} \right) \right] a_s^2(Q) + \dots, \end{aligned} \quad (3.11)$$

$$\ln \frac{Q^2}{Q_2^2} = \frac{\hat{r}_{3,1}}{\hat{r}_{2,0}} + 3\beta_0 \frac{\hat{r}_{2,0}\hat{r}_{4,2} - \hat{r}_{3,1}^2}{2\hat{r}_{2,0}^2} a_s(Q) + \dots, \quad (3.12)$$

$$\ln \frac{Q^2}{Q_3^2} = \frac{\hat{r}_{4,1}}{\hat{r}_{3,0}} + \dots. \quad (3.13)$$

Note that the PMC scales are of a perturbative nature, which is also a sort of resummation and we need to know more loop terms to achieve more accurate predictions. The PMC resums all the known same type of $\{\beta_i\}$ -terms to form precise PMC scales for each order. Thus, the precision of the PMC scale for the high-order terms decreases at higher and higher orders due to the less known $\{\beta_i\}$ -terms in those higher-order terms. For example, Q_1 is determined up to next-to-next-to-leading-logarithm (N²LL) accuracy, Q_2 is determined up to NLL accuracy and Q_3 is determined at LL accuracy. Thus, the PMC scales at higher orders are of less accuracy due to more of the perturbative terms being unknown. This perturbative property of the PMC scale causes the *first kind of residual scale dependence*.

After fixing the magnitude of $a_s(Q_k)$, we achieve a conformal series

$$\rho(Q) = \sum_{i=1}^4 \hat{r}_{i,0} a_s^i(Q_i) + \dots \quad (3.14)$$

The PMC scale for the highest-order term, e.g. Q_4 for the present case, is unfixed, since there is no $\{\beta_i\}$ -term to determine its magnitude. This renders the last perturbative term unfixed and causes the *second kind of residual scale dependence*. Usually, the PMCm suggests setting Q_4 as the last determined scale Q_3 , which ensures the scheme independence of the prediction due to commensurate scale relations among the predictions under different renormalization schemes [159, 170]. The pQCD series (3.14) is renormalization scheme and scale independent and becomes more convergent due to the elimination of the β terms including those related to the renormalon divergence. Thus, a more accurate pQCD prediction can be achieved by applying the PMCm. Two residual scale dependences are due to perturbative nature of either the pQCD approximant or the PMC scale, which is in principal different from the conventional arbitrary scale dependence. In practice, we have found that these two residual scale dependences are quite small even at low orders. This is due to a generally faster pQCD convergence after applying the PMCm. Some examples can be found in Ref. [171].

3.2. The single-scale Principle of Maximum Conformality: PMCs

In some cases, the perturbative series might have a weak convergence and the PMC scales might retain a comparatively larger residual scale dependence. To overcome this, a single-scale approach has been proposed, namely the PMCs, in order to suppress the residual scale dependence by directly fixing a single effective α_s . Following the standard procedures of PMCs [172], the pQCD approximant (3.8) changes to the following conformal series,

$$\rho(Q) = \sum_{i=1}^4 \hat{r}_{i,0} a_s^i(Q_*) + \dots \quad (3.15)$$

As in the previous section, we have set $p = 1$ and $n = 4$ for illustrating the procedure. The PMC scale Q_* can be determined by requiring all the nonconformal terms to vanish, which can be fixed up to N²LL accuracy for $p = 1$ and $n = 4$, i.e. $\ln Q_*^2/Q^2$ can be expanded as a power series over $a_s(Q)$,

$$\ln \frac{Q_*^2}{Q^2} = T_0 + T_1 a_s(Q) + T_2 a_s^2(Q) + \dots, \quad (3.16)$$

where the coefficients T_i ($i = 0, 1, 2$) are

$$T_0 = -\frac{\hat{r}_{2,1}}{\hat{r}_{1,0}}, \quad (3.17)$$

$$T_1 = \frac{\beta_0(\hat{r}_{2,1}^2 - \hat{r}_{1,0}\hat{r}_{3,2})}{\hat{r}_{1,0}^2} + \frac{2(\hat{r}_{2,0}\hat{r}_{2,1} - \hat{r}_{1,0}\hat{r}_{3,1})}{\hat{r}_{1,0}^2},$$

and

$$T_2 = \frac{3\beta_1(\hat{r}_{2,1}^2 - \hat{r}_{1,0}\hat{r}_{3,2})}{2\hat{r}_{1,0}^2}$$

$$+ \frac{4(\hat{r}_{1,0}\hat{r}_{2,0}\hat{r}_{3,1} - \hat{r}_{2,0}^2\hat{r}_{2,1}) + 3(\hat{r}_{1,0}\hat{r}_{2,1}\hat{r}_{3,0} - \hat{r}_{1,0}^2\hat{r}_{4,1})}{\hat{r}_{1,0}^3}$$

$$+ \frac{\beta_0(4\hat{r}_{2,1}\hat{r}_{3,1}\hat{r}_{1,0} - 3\hat{r}_{4,2}\hat{r}_{1,0}^2 + 2\hat{r}_{2,0}\hat{r}_{3,2}\hat{r}_{1,0} - 3\hat{r}_{2,0}\hat{r}_{2,1}^2)}{\hat{r}_{1,0}^3}$$

$$+ \frac{\beta_0^2(2\hat{r}_{1,0}\hat{r}_{3,2}\hat{r}_{2,1} - \hat{r}_{2,1}^3 - \hat{r}_{1,0}^2\hat{r}_{4,3})}{\hat{r}_{1,0}^3}. \quad (3.18)$$

Eq. (3.16) shows that the PMC scale Q_* is also a power series over α_s , which resums all the known $\{\beta_i\}$ -terms and is explicitly independent of μ_r at any fixed order, but depends only on the physical scale Q . It represents the correct momentum flow of the process and determines an overall effective α_s value. Together with the μ_r -independent conformal coefficients, the resultant PMC pQCD series is scheme and scale independent [58]. By using a single PMC scale determined with the highest accuracy from the known pQCD series, both the *first* and the *second kind of residual scale dependence* are suppressed.

4. Infinite-Order Scale Setting via the Principle of Maximum Conformality:

PMC_∞

In this section we introduce a parametrization of the observables that stems directly from the analysis of the perturbative QCD corrections and which reveals interesting properties, such as scale invariance, independently of the process or of the kinematics. We point out that this parametrization can be an intrinsic general property of gauge theories and we define this property *intrinsic conformality* (iCF³). We also show how this property directly indicates the correct renormalization scale μ_r at each order of calculation and we define this new method PMC_∞: *Infinite-Order Scale Setting using the Principle of Maximum Conformality*. We apply the iCF property and the PMC_∞ to the case of the thrust and C -parameter distributions in $e^+e^- \rightarrow 3\text{jets}$ and we display the results.

4.1. Intrinsic conformality (iCF)

In order to introduce intrinsic conformality (iCF), we consider the case of a normalized IR-safe single-variable distribution and write the explicit sum of pQCD contributions calculated up to NNLO at the initial renormalization scale μ_0 :

$$\frac{1}{\sigma_0} \frac{O d\sigma(\mu_0)}{dO} = \left\{ \frac{\alpha_s(\mu_0)}{2\pi} \frac{O dA_O(\mu_0)}{dO} + \left(\frac{\alpha_s(\mu_0)}{2\pi} \right)^2 \frac{O dB_O(\mu_0)}{dO} + \left(\frac{\alpha_s(\mu_0)}{2\pi} \right)^3 \frac{O dC_O(\mu_0)}{dO} + \mathcal{O}(\alpha_s^4) \right\}, \quad (4.1)$$

where the σ_0 is a tree-level hadronic cross-section, A_O, B_O, C_O are respectively the LO, NLO and NNLO coefficients, O is the selected unintegrated variable. For the sake of simplicity, we shall refer to the perturbatively calculated differential coefficients as *implicit coefficients* and drop the derivative symbol, i.e.

$$\begin{aligned} A_O(\mu_0) &\equiv \frac{O dA_O(\mu_0)}{dO}, & B_O(\mu_0) &\equiv \frac{O dB_O(\mu_0)}{dO}, \\ C_O(\mu_0) &\equiv \frac{O dC_O(\mu_0)}{dO}. \end{aligned} \quad (4.2)$$

We define here the *intrinsic conformality* as the property of a renormalizable SU(N)/U(1) gauge theory, such as QCD, which yields a particular structure of the perturbative corrections that can be made explicit by representing the perturbative coefficients using the following parametrization:⁴

$$\begin{aligned} A_O(\mu_0) &= A_{Conf}, \\ B_O(\mu_0) &= B_{Conf} + \frac{1}{2} \beta_0 \ln \left(\frac{\mu_0^2}{\mu_1^2} \right) A_{Conf}, \\ C_O(\mu_0) &= C_{Conf} + \beta_0 \ln \left(\frac{\mu_0^2}{\mu_1^2} \right) B_{Conf} + \frac{1}{4} \left[\beta_1 + \beta_0^2 \ln \left(\frac{\mu_0^2}{\mu_1^2} \right) \right] \ln \left(\frac{\mu_0^2}{\mu_1^2} \right) A_{Conf}, \end{aligned} \quad (4.3)$$

where the $A_{Conf}, B_{Conf}, C_{Conf}$ are the scale-invariant *Conformal Coefficients* (i.e. the coefficients of each perturbative order not depending on the scale μ_0), while we define the μ_N as *Intrinsic Conformal Scales* and β_0, β_1 are the first two coefficients of the β -function. We recall that the implicit coefficients are defined at the scale μ_0 and that they change

³Here the conformality must be understood as RG invariance only.

⁴We are neglecting here other running parameters, such as the mass terms.

according to the standard RG equations under a change of the renormalization scale according to:

$$\begin{aligned}
A_O(\mu_r) &= A_O(\mu_0), \\
B_O(\mu_r) &= B_O(\mu_0) + \frac{1}{2}\beta_0 \ln\left(\frac{\mu_r^2}{\mu_0^2}\right) A_O(\mu_0), \\
C_O(\mu_r) &= C_O(\mu_0) + \beta_0 \ln\left(\frac{\mu_r^2}{\mu_0^2}\right) B_O(\mu_0) + \frac{1}{4}\left[\beta_1 + \beta_0^2 \ln\left(\frac{\mu_r^2}{\mu_0^2}\right)\right] \ln\left(\frac{\mu_r^2}{\mu_0^2}\right) A_O(\mu_0).
\end{aligned} \tag{4.4}$$

It can be shown that the form of Eq. (4.3) is scale invariant and it is preserved under a change of the renormalization scale from μ_0 to μ_r by standard RG equations Eq. (4.4), i.e.:

$$\begin{aligned}
A_O(\mu_r) &= A_{Conf}, \\
B_O(\mu_r) &= B_{Conf} + \frac{1}{2}\beta_0 \ln\left(\frac{\mu_r^2}{\mu_I^2}\right) A_{Conf}, \\
C_O(\mu_r) &= C_{Conf} + \beta_0 \ln\left(\frac{\mu_r^2}{\mu_{II}^2}\right) B_{Conf} + \frac{1}{4}\left[\beta_1 + \beta_0^2 \ln\left(\frac{\mu_r^2}{\mu_I^2}\right)\right] \ln\left(\frac{\mu_r^2}{\mu_I^2}\right) A_{Conf}.
\end{aligned} \tag{4.5}$$

We note that the form of Eq. (4.3) is invariant and that the initial scale dependence is exactly removed by μ_r . Extending this parametrization to all orders we achieve a scale-invariant quantity: *the iCF parametrization is a sufficient condition in order to obtain a scale-invariant observable.*

In order to show this property we collect together the terms identified by the same *conformal coefficient*, we call each set a *conformal subset* and extend the property to order n :

$$\begin{aligned}
\sigma_I &= \left\{ \left(\frac{\alpha_s(\mu_0)}{2\pi}\right) + \frac{1}{2}\beta_0 \ln\left(\frac{\mu_0^2}{\mu_I^2}\right) \left(\frac{\alpha_s(\mu_0)}{2\pi}\right)^2 \right. \\
&\quad \left. + \frac{1}{4}\left[\beta_1 + \beta_0^2 \ln\left(\frac{\mu_0^2}{\mu_I^2}\right)\right] \ln\left(\frac{\mu_0^2}{\mu_I^2}\right) \left(\frac{\alpha_s(\mu_0)}{2\pi}\right)^3 + \dots \right\} A_{Conf} \\
\sigma_{II} &= \left\{ \left(\frac{\alpha_s(\mu_0)}{2\pi}\right)^2 + \beta_0 \ln\left(\frac{\mu_0^2}{\mu_{II}^2}\right) \left(\frac{\alpha_s(\mu_0)}{2\pi}\right)^3 + \dots \right\} B_{Conf} \\
\sigma_{III} &= \left\{ \left(\frac{\alpha_s(\mu_0)}{2\pi}\right)^3 + \dots \right\} C_{Conf}, \\
&\vdots \\
\sigma_n &= \left\{ \left(\frac{\alpha_s(\mu_0)}{2\pi}\right)^n \right\} \mathcal{L}_{nConf}.
\end{aligned} \tag{4.6}$$

In each subset we have only one intrinsic scale and only one conformal coefficient and the subsets are disjoint; thus, no mixing terms among the scales or the coefficients are introduced in this parametrization. Moreover, the structure of the subsets remains invariant under a global change of the renormalization scale, as shown from Eq. (4.5). The structure of each conformal set $\sigma_I, \sigma_{II}, \sigma_{III}, \dots$ and consequently the iCF are preserved, also if we fix a different renormalization scale for each conformal subset, i.e.

$$\left(\mu^2 \frac{\partial}{\partial \mu^2} + \beta(\alpha_s) \frac{\partial}{\partial \alpha_s}\right) \sigma_n = 0. \tag{4.7}$$

We define here this property of Eq. 4.6 of separating an observable into the union of ordered scale-invariant disjoint subsets $\sigma_I, \sigma_{II}, \sigma_{III}, \dots$ an *ordered scale invariance*.

In order to extend the iCF to all orders, we perform the $n \rightarrow \infty$ limit using the following strategy: we first perform a partial limit $J/n \rightarrow \infty$ including the higher-order corrections relative only to those $\beta_0, \beta_1, \beta_2, \dots, \beta_{n-2}$ terms that have

been determined already at order n for each subset and we then perform the complementary \bar{n} limit, which consists in including all the remaining higher-order terms. For the J/n limit we have:

$$\begin{aligned}
\lim_{J/n \rightarrow \infty} \sigma_{\text{I}} &\rightarrow \left(\frac{\alpha_s(\mu_{\text{I}})|_{n-2}}{2\pi} \right) A_{\text{Conf}} \\
\lim_{J/n \rightarrow \infty} \sigma_{\text{II}} &\rightarrow \left(\frac{\alpha_s(\mu_{\text{II}})|_{n-3}}{2\pi} \right)^2 B_{\text{Conf}} \\
\lim_{J/n \rightarrow \infty} \sigma_{\text{III}} &\rightarrow \left(\frac{\alpha_s(\mu_{\text{III}})|_{n-4}}{2\pi} \right)^3 C_{\text{Conf}} \\
&\vdots \\
\lim_{J/n \rightarrow \infty} \sigma_n &\equiv \left(\frac{\alpha_s(\mu_0)}{2\pi} \right)^n \mathcal{L}_{n\text{Conf}}, \tag{4.8}
\end{aligned}$$

where $\alpha_s(\mu_{\text{I}})|_{n-2}$ is the coupling calculated up to β_{n-2} at the intrinsic scale μ_{I} . Given the particular ordering of the powers of the coupling, in each conformal subset we have the coefficients of the $\beta_0, \dots, \beta_{n-k-1}$ terms, where k is the order of the conformal subset and the n is the order of the highest subset with no β terms. We note that the limit of each conformal subset is finite and scale invariant up to σ_{n-1} . The remaining scale dependence is confined to the coupling of the n^{th} term. Any combination of the $\sigma_{\text{I}}, \dots, \sigma_{n-1}$ subsets is finite and scale invariant. We can now extend the iCF to all orders performing the \bar{n} limit. In this limit we include all the remaining higher-order corrections. For the calculated conformal subsets this leads to defining the coupling at the same scales but including all the missing β terms. Thus, each conformal subset remains scale invariant. We point out that we are not making any assumption on the convergence of the series for this limit. We thus have:

$$\begin{aligned}
\lim_{\bar{n} \rightarrow \infty} \sigma_{\text{I}} &\rightarrow \left(\frac{\alpha_s(\mu_{\text{I}})}{2\pi} \right) A_{\text{Conf}} \\
\lim_{\bar{n} \rightarrow \infty} \sigma_{\text{II}} &\rightarrow \left(\frac{\alpha_s(\mu_{\text{II}})}{2\pi} \right)^2 B_{\text{Conf}} \\
\lim_{\bar{n} \rightarrow \infty} \sigma_{\text{III}} &\rightarrow \left(\frac{\alpha_s(\mu_{\text{III}})}{2\pi} \right)^3 C_{\text{Conf}} \\
&\vdots \\
\lim_{\bar{n} \rightarrow \infty} \sigma_n &\equiv \lim_{n \rightarrow \infty} \left(\frac{\alpha_s(\mu_0)}{2\pi} \right)^n \mathcal{L}_{n\text{Conf}} \rightarrow \text{Conformal Limit}, \tag{4.9}
\end{aligned}$$

where here now $\alpha_s(\mu_{\text{I}})$ is the complete coupling determined at the same scale μ_{I} . Equation (4.9) shows that the entire renormalization scale dependence has been completely removed. In fact, neither the intrinsic scales μ_{N} nor the conformal coefficients $A_{\text{Conf}}, B_{\text{Conf}}, C_{\text{Conf}}, \dots, \mathcal{L}_{n\text{Conf}}, \dots$ depend on the particular choice of the initial scale. The only term with a residual μ_0 dependence is the n -th term, but this dependence cancels in the limit $n \rightarrow \infty$. The scale dependence is totally confined to the coupling $\alpha_s(\mu_0)$ and its behavior does not depend on the particular choice of any scale μ_0 in the perturbative region, i.e. $\lim_{n \rightarrow \infty} \alpha_s(\mu_0)^n \sim a^n$ with $a < 1$. Hence, the limit of $\lim_{n \rightarrow \infty} \sigma_n$ depends only on the properties of the theory and not on the scale of the coupling in the perturbative regime. The proof given here shows that the iCF is *sufficient* to have a scale-invariant observable and it does not depend on the particular convergence of the series.

In order to show the *necessary* condition, we separate the two cases of a convergent series and an asymptotic expansion. For the first case the *necessary* condition stems directly from the uniqueness of the iCF form, since given a finite limit and the scale invariance, any other parametrization can be reduced to the iCF by means of appropriate transformations in agreement with the RG equations. For the second case, we have that an asymptotic expansion though not convergent,

can be truncated at a certain order n , which is the case of Eq. (4.6). Given the particular structure of the iCF we can perform the first partial limit J/n and we would achieve a finite and scale-invariant prediction, $\sigma_{N-1} = \sum_{i=1}^{n-1} \sigma_i$, for a truncated asymptotic expansion, as shown in Eq. (4.8). Given the truncation of the series in the region of maximum of convergence the n -th term would be reduced to the lowest value and so the scale dependence of the observable would reach its minimum. Given the finite and scale-invariant limit σ_{N-1} we conclude that the iCF is unique and thus *necessary* for an *ordered* scale-invariant truncated asymptotic expansion up to the n -th order.

We point out that in general the iCF form is the most general and irreducible parametrization that leads to scale invariance; other parametrizations are forbidden, since if we were to introduce more scales⁵ into the logarithms of one subset, we would spoil the invariance under the RG transformation and we could not achieve Eq. (4.5), while on the other hand no scale dependence can be introduced into the intrinsic scales since it would remain in the observable already in the first partial limit J/n and it could not be eliminated. The conformal coefficients are conformal at each order by definition; thus, they do not depend on the renormalization scale and they do not have a perturbative expansion. Hence *the iCF is a necessary and sufficient condition for scale invariance.*

4.2. Comments on the iCF and ordered scale invariance

The iCF parametrization can stem either from an inner property of the theory, the iCF, or from direct parametrization of the scale-invariant observable. In both cases the iCF parametrization makes the scale dependence of the observable explicit and it exactly preserves the scale invariance. The iCF parametrization is invariant with respect to the choice of initial scale μ_0 , this implies that the same calculation performed choosing different arbitrary initial scales, μ_0, μ'_0 leads to the same result in the limit J/n , a limit that is scale and scheme independent. The iCF is also strongly motivated by the renormalizability of QCD and by the uniqueness of the β -function in a given scheme; i.e. two different β_i, β'_i do not occur in a perturbative calculation at any order in one RS and the UV divergencies are cancelled by redefinition of the same parameters at lowest and higher orders. We remark that the conservation of the iCF form in one observable is strongly related to the validity of the RG transformations; we thus expect the iCF to be well preserved in the deep Euclidean region.

Once we have defined an observable in the iCF-form, we have not only the scale invariance of the entire observable, but also the *ordered scale invariance* (i.e. the scale invariance of each subset σ_n or σ_{N-1}). The latter property is crucial in order to obtain scale-invariant observables independently from the particular kinematic region and independently from the starting order of the observable or the order of the truncation of the series. Since in general, a theory is blind with respect to the particular observable/process that we might investigate, the theory should preserve the *ordered* scale invariance in order to always define scale-invariant observables. Hence if the iCF is an inner property of the theory, it leads to implicit coefficients that are neither independent nor conformal. This is made explicit in Eq. (4.3), but it is hidden in the perturbative calculations in the case of the implicit coefficients. For instance, the presence of the iCF clearly reveals itself when a particular kinematic region is approached and the A_O becomes null. This would cause a breaking of the scale invariance since a residual initial scale dependence would remain in the observable in the higher-order coefficients. The presence of the iCF solves this issue by leading to the correct redefinition of all the coefficients at each order preserving the

⁵Here we refer to the form of Eq. (4.3). In principle, it is possible to write other parametrizations preserving the scale invariance, but these can be reduced to the iCF in agreement with the RG equations.

correct scale invariance exactly. Thus, in the case of a scale-invariant observable O , defined according to the implicit form (Eq. (4.1)), by the coefficients $\{A_O, B_O, C_O, \dots, O_O, \dots\}$, it cannot simply undergo the change $\rightarrow \{0, B_O, C_O, \dots, O_O, \dots\}$, since this would break the scale invariance. In order to preserve the scale invariance, we must redefine the coefficients $\{\tilde{A}_O = 0, \tilde{B}_O, \tilde{C}_O, \dots, \tilde{O}_O, \dots\}$ cancelling out all the initial scale dependence originating from the LO coefficient A_O at all orders. This is equivalent to subtracting out an entire invariant conformal subset σ_I related to the coefficient A_{Conf} from the scale-invariant observable O . This mechanism is clear in the case of the explicit form of the iCF, Eq. (4.3), where, if $A_{Conf} = 0$, then the entire conformal subset is null and the scale invariance is preserved.

We stress that the conformal coefficients may acquire all possible values without breaking scale invariance, they contain the essential information on the physics of the process, while all the correlation factors can be reabsorbed into the renormalization scales as shown by the PMC method [46, 47, 49, 50]. Hence, if a theory has the property of *ordered scale invariance*, it exactly preserves the scale invariance of observables independently of the process, the kinematics and the starting order of the observable. We stress that if a theory has intrinsic conformality, all renormalized quantities, such as cross sections, can be parametrized with the iCF-form. This property should be preserved by the renormalization scheme or by the definition of IR safe quantities and it should also be preserved in observables defined in effective theories. The iCF shows that point (3) of the BLM/PMC approach (Section 3) can be improved by eliminating the perturbative expansion of the BLM/PMC scales, leading to a scale- and scheme-invariant result. We remark though that the perturbative corrections in the BLM or PMCm scales are suppressed in the perturbative region.

4.3. The PMC_∞

We introduce here a new method for eliminating the scale-setting ambiguity in single variable scale-invariant distributions, which we call PMC_∞ . This method is based on the original PMC principle and agrees with all the different PMC formulations for the PMC scales at lowest order. The core of the PMC_∞ is essentially the same for all BLM-PMC prescriptions, i.e. the effective running-coupling value and hence its renormalization scale at each order is determined by the β_0 -term of the next-higher order, or equivalently by the *intrinsic conformal scale* μ_N . The PMC_∞ preserves the iCF and thus the scale and scheme invariance, absorbing an infinite set of β -terms to all orders.

This method differs from the other PMC prescriptions since, due to the presence of the intrinsic conformality, no perturbative correction in α_s needs to be introduced at higher orders in the PMC scales. Given that all the β -terms of a single conformal subset are included in the renormalization scale already with the definition at lowest order, no initial scale or scheme dependences are left due to the unknown β -terms in each subset. The PMC_∞ scale of each subset can be unambiguously determined by β_0 -term of each order, we stress that all logarithms of each subset have the same argument and all the differences arising at higher orders have to be included only in the conformal coefficients. Reabsorbing all the β -terms into the scale also eliminates the $n!\beta_0^n\alpha_s^n$ terms (related to renormalons [23]); thus, the precision is improved and the perturbative QCD predictions can be extended to a wider range of values. The initial scale dependence is totally confined in the unknown PMC_∞ scale of the last order of accuracy (i.e. up to NNLO case in the $\alpha_s(\mu_0)^3$). Thus, if we fix the renormalization scale independently to the proper intrinsic scale for each subset μ_N , we end up with a perturbative

sum of totally conformal contributions up to the order of accuracy:

$$\frac{1}{\sigma_0} \frac{Od\sigma(\mu_I, \mu_{II}, \mu_{III})}{dO} = \left\{ \frac{\alpha_s(\mu_I)}{2\pi} \frac{OdA_{Conf}}{dO} + \left(\frac{\alpha_s(\mu_{II})}{2\pi} \right)^2 \frac{OdB_{Conf}}{dO} + \left(\frac{\alpha_s(\mu_{III})}{2\pi} \right)^3 \frac{OdC_{Conf}}{dO} \right\} + \mathcal{O}(\alpha_s^4). \quad (4.10)$$

At this order, the last scale is set to the physical scale Q , i.e. $\mu_{III} = \mu_0 = Q$.

4.4. The iCF coefficients and scales: a new ‘‘How-To’’ method

We describe here how all the coefficients of Eq. (4.3) can be identified from either a numerical or analytical perturbative calculation. This method applies in general to any perturbative calculation once results for the different color factors are kept separate; however, we refer to the particular case of the NNLO thrust distribution results calculated in Refs. [173, 174] for the purpose. Since the leading order is already (A_{Conf}) void of β -terms, we start with NLO coefficients. A general numerical/analytical calculation keeps tracks of all the color factors and the respective coefficients:

$$B_O(N_f) = C_F \left[C_A B_O^{N_c} + C_F B_O^{C_F} + T_F N_f B_O^{N_f} \right] \quad (4.11)$$

where $C_F = \frac{(N_c^2 - 1)}{2N_c}$, $C_A = N_c$ and $T_F = 1/2$. The dependence on N_f is made explicit here for sake of clarity. We can determine the conformal coefficient B_{Conf} of the NLO order straightforwardly, by fixing the number of flavors N_f in order to kill the β_0 term:

$$B_{Conf} = B_O \left(N_f \equiv \frac{33}{2} \right),$$

$$B_{\beta_0} \equiv \log \frac{\mu_0^2}{\mu_1^2} = 2 \frac{B_O - B_{Conf}}{\beta_0 A_{Conf}}. \quad (4.12)$$

We would achieve the same results in the usual PMC way; i.e. by identifying the N_f coefficient with the β_0 term and then determining the conformal coefficient. Both methods are consistent and results for the intrinsic scales and the coefficients are in perfect agreement. At NNLO a general coefficient is composed of the contribution of six different color factors:

$$C_O(N_f) = \frac{C_F}{4} \left\{ N_c^2 C_O^{N_c^2} + C_O^{N_c^0} + \frac{1}{N_c^2} C_O^{\frac{1}{N_c^2}} + N_f N_c \cdot C_O^{N_f N_c} + \frac{N_f}{N_c} C_O^{N_f/N_c} + N_f^2 C_O^{N_f^2} \right\}. \quad (4.13)$$

In order to identify all the terms of Eq. (4.3), we notice first that the coefficients of the terms β_0^2 and β_1 are already given by the NLO coefficient B_{β_0} ; we thus need to determine only the β_0 and the conformal C_{Conf} terms. In order to determine the latter coefficients, we use the same procedure used for the NLO; i.e. we set the number of flavors $N_f \equiv 33/2$ in order to remove all the β_0 terms. We then have

$$C_{Conf} = C_O \left(N_f \equiv \frac{33}{2} \right) - \frac{1}{4} \bar{\beta}_1 B_{\beta_0} A_{Conf},$$

$$C_{\beta_0} \equiv \log \left(\frac{\mu_0^2}{\mu_{II}^2} \right) = \frac{1}{\beta_0 B_{Conf}} \left(C_O - C_{Conf} - \frac{1}{4} \beta_0^2 B_{\beta_0}^2 A_{Conf} - \frac{1}{4} \beta_1 B_{\beta_0} A_{Conf} \right), \quad (4.14)$$

with $\bar{\beta}_1 \equiv \beta_1(N_f = 33/2) = -107$. Up to accuracy $\mathcal{O}(\alpha_s^5)$, we have:

$$D_{Conf} = D_O \left(N_f \equiv \frac{33}{2} \right) - \frac{1}{8} \bar{\beta}_2 B_{\beta_0} A_{Conf} - \frac{1}{2} \bar{\beta}_1 C_{\beta_0} B_{Conf},$$

$$D_{\beta_0} \equiv \log \left(\frac{\mu_0^2}{\mu_{III}^2} \right) = \frac{2}{3\beta_0 C_{Conf}} \left[D_O - D_{Conf} - \frac{1}{8} \left(\beta_0^3 B_{\beta_0}^3 + \frac{5}{2} \beta_0 \beta_1 B_{\beta_0}^2 + \beta_2 B_{\beta_0} \right) A_{Conf} - \frac{1}{4} (3\beta_0^2 C_{\beta_0}^2 + 2\beta_1 C_{\beta_0}) B_{Conf} \right], \quad (4.15)$$

with $\overline{\beta}_2 \equiv \beta_2(N_f = 33/2)$.

This procedure may be extended to all orders and one may decide whether to cancel β_0 , β_1 or β_2 by fixing the appropriate number of flavors. The results can be compared to exactly determine all the coefficients. We point out that extending the intrinsic conformality to all orders, we can at this stage predict the coefficients of all the color factors of the higher orders related to the β -terms, except those related to the higher-order conformal coefficients and β_0 -terms (e.g. at $N^4\text{LO}$, E_{Conf} and E_{β_0}).

4.5. Comment on the PMC/PMC $_{\infty}$ scales

PMC scales stem directly from the renormalization of the UV-divergent diagrams. As pointed out in Sec. 2.1, the finite part of the divergent integrals contribute to the β -terms. In fact, these coefficients derive from the UV-divergent diagrams connected with the running of the coupling constant and not from UV-finite diagrams. UV-finite N_F terms may arise but would not contribute to the β -terms. These terms can be easily identified by the kinematic constraint at lowest order or by checking deviations of the n_f coefficients from the iCF form. In fact, only the N_f terms coming from UV-divergent diagrams, depending dynamically on the virtuality of the underlying quark and gluon subprocesses have to be considered as β -terms and they would determine the intrinsic conformal scales. In general, each μ_N is an independent function of the physical scale of the process \sqrt{s} (or $\sqrt{t}, \sqrt{u}, \dots$), of the selected variable O and it varies with the number of colors N_c mainly due to the ggg and $gggg$ vertices. The latter terms arise at higher orders only in a non-Abelian theory, but they are not expected to spoil the iCF-form. We stress that iCF applies to scale-invariant single-variable differential distributions, in case one is interested in the renormalization of a particular diagram, e.g. the ggg vertex, contributions from different β -terms should be singled out in order to identify the respective intrinsic conformal scale consistently with the renormalization of the non-Abelian ggg vertex, as shown in [175].

In the renormalization procedure of gauge theories, one first identifies the UV singularities of a scattering amplitude, which appear as poles using dimensional regularization. The UV-divergent contributions are absorbed into renormalization constants Z_i adopting a particular scheme (e.g. the \overline{MS} scheme). This cancels the UV divergences and at the same time defines the finite part of the loop integral.

The finite parts, such as the finite β_i and γ_i contributions, are associated with the renormalization of the running coupling and running mass, respectively. The β_i terms can then be summed into the running coupling using the standard renormalization group equations; this is basically the core of the BLM-PMC scale-setting procedure that is analogous to the Gell-Mann–Low scheme in QED. This procedure eliminates the scale ambiguity and reabsorbs the scheme dependence at once into the effective running coupling up to the computed order. In addition, the factorial renormalon divergence is eliminated. One thus can use the same renormalization procedure for QED, QCD and EW in a grand unified theory,

Given the renormalizability of QCD, once the coupling is renormalized all the vertices are finite, but this does not cancel the contributions of the finite parts of the integrals, i.e. the β_n terms, which define the PMC scale for each vertex ($3g, 4g, ccg, qqg$).

5. PMC_∞ results for thrust and the C -parameter

The thrust distribution and event-shape variables are fundamental tools for probing the geometrical structure of a given process at colliders. Being observables that are exclusive enough with respect to the final state, they allow for a deeper geometrical analysis of the process and are also particularly suited for measurement of the strong coupling α_s [176].

Given the high-precision data collected at LEP and SLAC [177–181], refined calculations are crucial in order to extract information to the highest possible precision. Although extensive studies on these observables have been produced during the last few decades, including higher-order corrections from next-to-leading order (NLO) calculations [182–187] to the next-to-next-to-leading order (NNLO) [173, 174, 188–190] and including resummation of the large logarithms [30, 31], the theoretical predictions are still affected by significant theoretical uncertainties that are related to large renormalization scale ambiguities. In the particular case of the three-jet event-shape distributions the conventional practice of CSS leads to results that do not match the experimental data and the extracted values of α_s deviate from the world average [126].

The thrust (T) and C -parameter (C) are defined by

$$T = \max_{\vec{n}} \left(\frac{\sum_i |\vec{p}_i \cdot \vec{n}|}{\sum_i |\vec{p}_i|} \right), \quad (5.1)$$

$$C = \frac{3}{2} \frac{\sum_{i,j} |\vec{p}_i| |\vec{p}_j| \sin^2 \theta_{ij}}{(\sum_i |\vec{p}_i|)^2}, \quad (5.2)$$

where the sum runs over all particles in the hadronic final state and \vec{p}_i denotes the three-momentum of particle i . The unit vector \vec{n} is varied to maximize thrust T ; the corresponding \vec{n} is called the thrust axis and denoted by \vec{n}_T . The variable $(1 - T)$ is often used, which for the LO of 3-jet production is restricted to the range $(0 < 1 - T < 1/3)$. We have a back-to-back or a spherically symmetric event at $T = 1$ and at $T = 2/3$ respectively. For the C -parameter, θ_{ij} is the angle between \vec{p}_i and \vec{p}_j . At LO for 3-jet production the C -parameter is restricted by kinematics to the range $0 \leq C \leq 0.75$.

In general, a normalized IR-safe single-variable observable, such as the thrust distribution for $e^+e^- \rightarrow 3$ jets [191, 192], is the sum of pQCD contributions calculated up to NNLO at the initial renormalization scale $\mu_0 = \sqrt{s} = M_Z$:

$$\frac{1}{\sigma_{tot}} \frac{O d\sigma(\mu_0)}{dO} = \left\{ x_0 \cdot \frac{O d\bar{A}_O(\mu_0)}{dO} + x_0^2 \cdot \frac{O d\bar{B}_O(\mu_0)}{dO} + x_0^3 \cdot \frac{O d\bar{C}_O(\mu_0)}{dO} + \mathcal{O}(\alpha_s^4) \right\}, \quad (5.3)$$

where $x(\mu) \equiv \alpha_s(\mu)/(2\pi)$, O is the selected event-shape variable, σ the cross-section of the process,

$$\sigma_{tot} = \sigma_0 \left(1 + x_0 A_{tot} + x_0^2 B_{tot} + \mathcal{O}(\alpha_s^3) \right)$$

is the total hadronic cross-section and $\bar{A}_O, \bar{B}_O, \bar{C}_O$ are respectively the normalized LO, NLO and NNLO coefficients:

$$\begin{aligned} \bar{A}_O &= A_O \\ \bar{B}_O &= B_O - A_{tot} A_O \\ \bar{C}_O &= C_O - A_{tot} B_O - (B_{tot} - A_{tot}^2) A_O, \end{aligned} \quad (5.4)$$

where A_O, B_O, C_O are the coefficients normalized to the tree-level cross-section σ_0 calculated by Monte Carlo (see e.g. the EERAD and Event2 codes [173, 174, 188–190]) and A_{tot}, B_{tot} are

$$\begin{aligned} A_{tot} &= \frac{3}{2} C_F; \\ B_{tot} &= \frac{C_F}{4} N_c + \frac{3}{4} C_F \frac{\beta_0}{2} (11 - 8\zeta(3)) - \frac{3}{8} C_F^2, \end{aligned} \quad (5.5)$$

where ζ is the Riemann zeta function.

In general, according to CSS the renormalization scale is set to $\mu_0 = \sqrt{s} = M_Z$ and theoretical uncertainties are evaluated using standard criteria. In this case, we have used the definition of the parameter δ given in Ref. [189]; we define the average error for the event-shape variable distributions as:

$$\bar{\delta} = \frac{1}{N} \sum_i^N \frac{\max_{\mu}(\sigma_i(\mu)) - \min_{\mu}(\sigma_i(\mu))}{2\sigma_i(\mu=M_Z)}, \quad (5.6)$$

where i is the index of the bin and N is the total number of bins, the renormalization scale is varied in the range $\mu \in [M_Z/2, 2M_Z]$.

5.1. The PMC_{∞} scales at LO and NLO

According to the PMC_{∞} prescription, we fix the renormalization scale to μ_N at each order absorbing all the β terms into the coupling. We notice a small mismatch between the zeroes of the conformal coefficient B_{Conf} and those of the remaining β_0 term in the numerator (the formula is shown in Eq. (4.14)). Due to our limited knowledge of the strong coupling at low energies, in order to avoid singularities in the NLO scale μ_{II} , we introduce a regularization that leads to a finite scale $\tilde{\mu}_{\text{II}}$ over the entire range of values of the variable $(1 - T)$. These singularities might be due either to the presence of UV finite N_F terms or to the logarithmic behavior of the conformal coefficients when low values of the variable $1 - T$ are approached. Large logarithms arise from the IR-divergence cancellation procedure and they can be resummed in order to restore a predictive perturbative regime [25–27, 30, 31]. We point out that IR cancellation should not spoil the iCF property. Whether this is an actual deviation from the iCF-form must be investigated further. However, since the discrepancies between the coefficients are rather small, we introduce a regularization method based on redefinition of the norm of the coefficient B_{Conf} in order to cancel out these singularities in the μ_{II} scale. This regularization is consistent with the PMC principle and up to the accuracy of the calculation it does not introduce any bias effect in the results or any ambiguity in the NLO- PMC_{∞} scale. All differences introduced by the regularization would enter at N^3LO accuracy and they may be reabsorbed later in the higher-order PMC_{∞} scales. For the PMC_{∞} scales, μ_N we thus obtain

$$\begin{aligned} \mu_{\text{I}} &= \sqrt{s} \cdot e^{f_{sc} - \frac{1}{2}B_{\beta_0}} & (1 - T) < 0.33, & (5.7) \\ \tilde{\mu}_{\text{II}} &= \begin{cases} \sqrt{s} \cdot e^{f_{sc} - \frac{1}{2}C_{\beta_0}} \cdot \frac{B_{\text{Conf}}}{B_{\text{Conf}} + \eta \cdot A_{\text{tot}} A_{\text{Conf}}} & (1 - T) < 0.33, \\ \sqrt{s} \cdot e^{f_{sc} - \frac{1}{2}C_{\beta_0}} & (1 - T) > 0.33, \end{cases} & (5.8) \end{aligned}$$

where $\sqrt{s} = M_Z$ and the third scale is set to $\mu_{\text{III}} = \mu_0 = \sqrt{s}$. The renormalization scheme factor for the QCD results is set to $f_{sc} \equiv 0$. This scheme factor also reabsorbs the scheme difference into the renormalization scale and is related to the particular choice of the scale parameter Λ as discussed in Section 2.3. The coefficients B_{β_0}, C_{β_0} are the coefficients related to the β_0 -terms of the NL and NNL perturbative order of the thrust distribution respectively. They are determined from the calculated A_O, B_O, C_O coefficients.

The η parameter is a regularization term to cancel the singularities of the NLO scale, μ_{II} , in the range $(1 - T) < 0.33$, depending on non-matching zeroes between numerator and denominator in C_{β_0} . In general, this term is not mandatory for applying the PMC_{∞} , it is necessary only in case one is interested in applying the method over the entire range covered by thrust, or any other observable. Its value has been determined as $\eta = 3.51$ for the thrust distribution and it introduces no bias effects up to the accuracy of the calculations and the related errors are totally negligible up to this stage.

We point out that in the region $(1 - T) > 0.33$ we have a clear example of intrinsic conformality-iCF where the kinematic constraints set the $A_{\text{Conf}} = 0$. According to Eq. (4.5) setting the $A_{\text{Conf}} = 0$ the entire conformal subset σ_{I}

becomes null. In this case all the β terms at NLO and NNLO disappear except the β_0 -term at NNLO, which determines the μ_{II} scale. The surviving n_f terms at NLO or the n_f^2 at NNLO are related to the finite N_F -term at NLO and to the mixed $N_f \cdot N_F$ term arising from $B_O \cdot \beta_0$ at NNLO. Using the parametrization with explicit n_f terms, we have for $(1 - T) > 0.33$:

$$\begin{aligned} A_O &= 0, \\ B_O &= B_0 + B_1 \cdot N_F, \\ C_O &= C_0 + C_1 \cdot n_f + C_2 \cdot N_f \cdot N_F. \end{aligned} \tag{5.9}$$

we can determine $\tilde{\mu}_{\text{II}}$ for the region $(1 - T) > 0.33$ as shown in Eq. (5.8):

$$C_{\beta_0} = \left(\frac{C_1}{\frac{11}{3}C_A B_1 - \frac{2}{3}B_0} \right) \tag{5.10}$$

by identifying the β_0 -term at NNLO. The LO and NLO PMC_∞ scales are shown in Fig. 5.1. We notice that the two

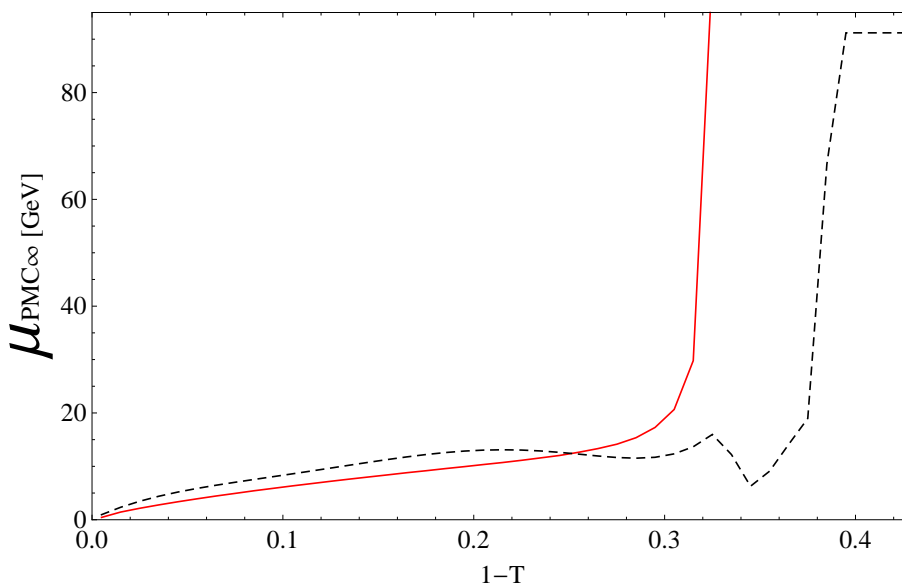


Figure 5.1: The LO- PMC_∞ (solid red) and the NLO- PMC_∞ (dashed black) scales for thrust. [89]

PMC_∞ scales have similar behaviors in the range $(1 - T) < 0.33$ and that the LO- PMC_∞ scale agrees with the PMC scale used in Ref. [87]. Small numerical fluctuations are visible in the NLO- PMC_∞ scale as unphysical "kinks", due to the Monte-Carlo simulation results of Ref.[174]. In the range $(1 - T) < 0.33$, where they are more evident, an interpolation has been performed. However, for the case of thrust, these have a negligible effect on the final distribution and do not depend on the method used for setting the scale, e.g. the PMC_∞ , but on the method used for performing the calculations (i.e. the Monte-Carlo [174]).

The PMC_∞ method totally eliminates both the ambiguity in the choice of the renormalization scale and the scheme dependence to all orders in QCD.

5.2. NNLO thrust distribution results

We use here the results of Ref. [173, 174] and for the running coupling $\alpha_s(Q)$ we use the RunDec program [193]. In order to normalize the thrust distribution consistently, we expand the denominator in $\alpha_0 \equiv \alpha_s(\mu_0)$ while the numerator has

the couplings renormalized at different PMC_∞ scales $\alpha_I \equiv \alpha_s(\mu_I)$ and $\alpha_{II} \equiv \alpha_s(\tilde{\mu}_{II})$. We point out here that the proper normalization would be given by the integration of the total cross-section after renormalization with the PMC_∞ scales, nonetheless since the PMC_∞ prescription only involves absorption of higher-order terms into the scales, the difference would be within the accuracy of the calculations, i.e. $\sim \mathcal{O}(\alpha_s^4(\mu_0))$. Equation (5.3) becomes:

$$\frac{1}{\sigma_{tot}} \frac{d\sigma(\mu_I, \tilde{\mu}_{II}, \mu_0)}{dO} = \{\bar{\sigma}_I + \bar{\sigma}_{II} + \bar{\sigma}_{III} + \mathcal{O}(\alpha_s^4)\}, \quad (5.11)$$

where the $\bar{\sigma}_N$ are normalized subsets that are given by:

$$\begin{aligned} \bar{\sigma}_I &= A_{Conf} \cdot x_I \\ \bar{\sigma}_{II} &= (B_{Conf} + \eta A_{tot} A_{Conf}) \cdot x_{II}^2 - \eta A_{tot} A_{Conf} \cdot x_0^2 - A_{tot} A_{Conf} \cdot x_0 x_I \\ \bar{\sigma}_{III} &= (C_{Conf} - A_{tot} B_{Conf} - (B_{tot} - A_{tot}^2) A_{Conf}) \cdot x_0^3, \end{aligned} \quad (5.12)$$

$A_{Conf}, B_{Conf}, C_{Conf}$ are the scale-invariant conformal coefficients (i.e. the coefficients of each perturbative order not depending on the scale μ_r) while x_I, x_{II}, x_0 are the couplings determined at the $\mu_I, \tilde{\mu}_{II}, \mu_0$ scales respectively.

Normalized subsets for the region $(1-T) > 0.33$ can be achieved simply by setting $A_{Conf} \equiv 0$ in the Eq. (5.12). Within the numerical precision of these calculations there is no evidence of the presence of spurious terms, such as any further UV-finite N_F term up to NNLO [194], besides the kinematic term at lowest order in the multi-jet region. These terms, if there are any, must remain rather small over the entire range of the thrust variable in comparison with the β term or even be compatible with numerical fluctuations. Moreover, we notice a small rather constant difference between the iCF-predicted and the calculated coefficient for the N_f^2 color factor of Ref. [173], which might be due to an n_f^2 UV-finite coefficient or possibly to statistics. This small difference must be included in the conformal coefficient but it has a completely negligible impact on the total thrust distribution. In Fig. 5.2 we show the thrust distribution at NLO and at

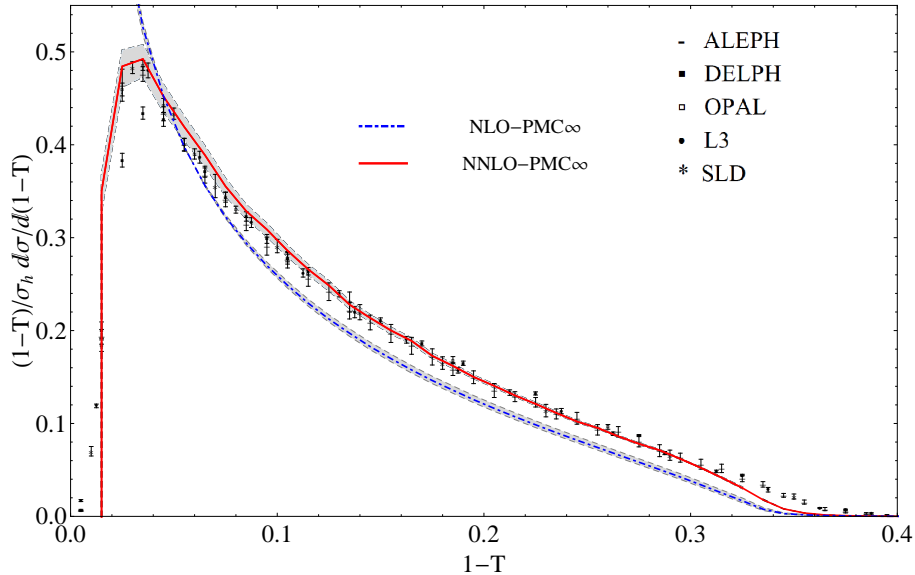


Figure 5.2: The thrust distribution under the PMC_∞ at NLO (dot-dashed blue) and at NNLO (solid red) [89]. The experimental data points are taken from the ALEPH, DELPHI, OPAL, L3, SLD experiments [177–181]. The shaded area shows theoretical errors for the PMC_∞ predictions at NLO and at NNLO.

NNLO with the use of the PMC_∞ method. Theoretical errors for the thrust distribution at NLO and at NNLO are also shown (the shaded area). Conformal quantities are not affected by a change of renormalization scale. Thus, the errors

shown give an evaluation of the level of conformality achieved up to the order of accuracy and they have been calculated using standard criteria, i.e. varying the remaining initial scale value in the range $\sqrt{s}/2 \leq \mu_0 \leq 2\sqrt{s}$.

We recall that the distributions are calculated by a Monte-Carlo simulation, considering 50 equidistant bins in the range $0 < 1 - T < 0.5$, thus the peak in the NNLO-PMC $_{\infty}$ distribution appears more as a broken-straight line also due to the linear interpolation used in the figure to join the points.

Using the same definition of the parameter $\bar{\delta}$ given in Eq. (5.6), we have in the interval $0 < (1 - T) < 0.33$ an average error of $\bar{\delta} \simeq 3.54\%$ and 1.77% for the thrust at NLO and at NNLO respectively. A greater improvement has been obtained over the entire range of reliable results for thrust distribution, i.e. $0 < (1 - T) < 0.42$, from $\bar{\delta} \simeq 7.36\%$ to 1.95% from NLO to the NNLO accuracy with the PMC $_{\infty}$.

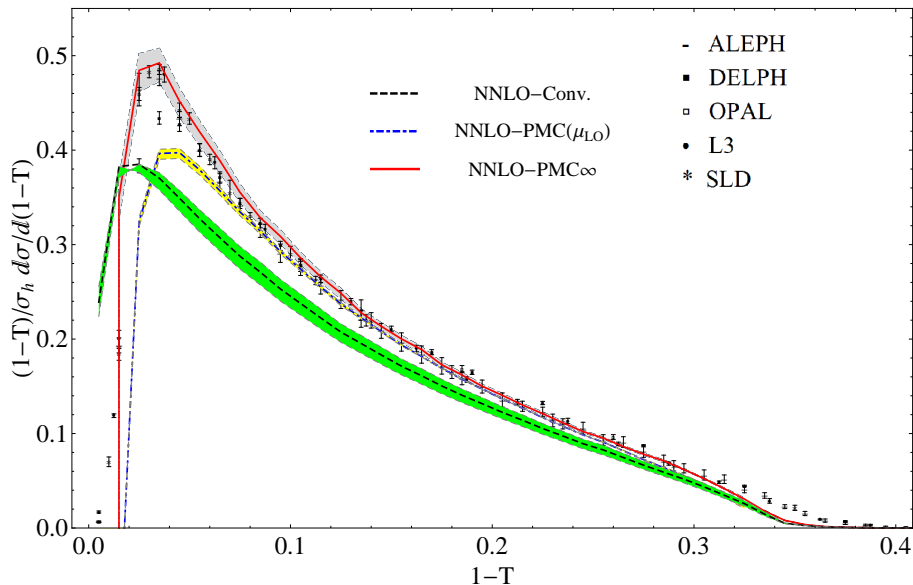


Figure 5.3: The thrust distribution at NNLO under the Conventional (dashed black), the PMC(μ_{LO}) (dot-dashed blue) and the PMC $_{\infty}$ (solid red) [89]. The experimental data points are taken from the ALEPH, DELPHI, OPAL, L3, SLD experiments [177–181]. The shaded areas show theoretical error predictions at NNLO, which have been calculated varying the remaining initial scale value in the range $\sqrt{s}/2 \leq \mu_0 \leq 2\sqrt{s}$.

In Fig. 5.3 a direct comparison of the PMC $_{\infty}$ with the CSS results (obtained in [173] and [189, 190]) is shown. In addition, we show the results of the first PMC approach used in [87], which we indicate as PMC(μ_{LO}) extended to NNLO accuracy. In this approach the last unknown PMC scale μ_{NLO} of the NLO was set to the last known PMC scale μ_{LO} of the LO, while the NNLO scale $\mu_{NNLO} \equiv \mu_0$ was left unset and varied in the range $\sqrt{s}/2 \leq \mu_0 \leq 2\sqrt{s}$.

Average errors calculated in different regions of the spectrum are reported in Table 5.1. The PMC(μ_{LO}) cannot be defined in the range $0.33 < 1 - T < 0.42$ since $A_{\text{Conf}} = 0$; thus the third and fifth row in Table 5.1 are blank. In fact, this further analysis was performed in order to show that the procedure of setting the last unknown scale to the last known one leads to stable and precise results and is consistent with the proper PMC method over a wide range of accessible values of the $(1 - T)$ variable.

From the comparison with the CSS, we notice that the PMC $_{\infty}$ prescription significantly improves the theoretical predictions. Moreover, results are in remarkable agreement with the experimental data over a wider range of values ($0.015 \leq 1 - T \leq 0.33$) and they show an improvement of the PMC(μ_{LO}) results when the two-jet and multi-jet regions are approached, i.e. the region of the peak and the region $(1 - T) > 0.33$ respectively. The use of the PMC $_{\infty}$ approach in perturbative QCD thrust calculations restores the correct behavior of the thrust distribution in the region

$\bar{\delta}[\%]$	Conv.	PMC(μ_{LO})	PMC $_{\infty}$
$0.10 < (1 - T) < 0.33$	6.03	1.41	1.31
$0.21 < (1 - T) < 0.33$	6.97	2.19	0.98
$0.33 < (1 - T) < 0.42$	8.46	—	2.61
$0.00 < (1 - T) < 0.33$	5.34	1.33	1.77
$0.00 < (1 - T) < 0.42$	6.00	—	1.95

Table 5.1: The average error $\bar{\delta}$ for the NNLO thrust distribution under Conventional, PMC(μ_{LO}) and PMC $_{\infty}$ scale settings calculated in different ranges of values of the $(1 - T)$ variable.

$(1 - T) > 0.33$ and this is a clear effect of the iCF property. Comparison with experimental data has been improved over the entire spectrum and the introduction of the N³LO correction would improve this comparison especially in the multi-jet $(1 - T) > 0.33$ region. In the PMC $_{\infty}$ method theoretical errors are given by the unknown intrinsic conformal scale of the last order of accuracy. We expect this scale not to be significantly different from that of the previous orders. In this particular case, as shown in Eq. (5.12), we also have a dependence on the initial scale $\alpha_s(\mu_0)$ left due to the normalization and to the regularization terms. These errors represent 12.5% and 1.5% respectively of the full theoretical errors in the range $0 < (1 - T) < 0.42$ and they could be improved by means of a correct normalization.

5.3. NNLO C -parameter distribution results

The same analysis applies straightforwardly to the C -parameter distribution including the regularizing η parameter, which has been set to the same value 3.51. The same scales of Eq. (5.7) and Eq. (5.8) apply to the C -parameter distribution in the region $0 < C < 0.75$ and in the region $0.75 < C < 1$. In fact, due to kinematic constraints that set the $A_{Conf} = 0$, we also have the same iCF effect for the C -parameter.

Results for the C -parameter scales are shown in Fig. 5.4. We notice the effect of the iCF intrinsic conformality on the LO-PMC $_{\infty}$ scale, which terminates at the kinematic boundary $C = 0.75$. In fact, at this boundary $A_{Conf} = 0$ and thus sets the whole conformal subset $\sigma_1 = 0$. The NLO-PMC $_{\infty}$ scale has two distinct domains separated by the kinematic constraint $C = 0.75$. In the range $0 < C < 0.75$, the NLO-PMC $_{\infty}$ scale has the same physical behavior as the LO-PMC $_{\infty}$ scale, in the range $0.75 < C < 0.97$ is almost constant, due to a similar behavior of the numerator and denominator in Eq.5.10 and at $C = 0.97$ it goes through a saturation effect given by the C_1 coefficient in Eq.5.10, which becomes null. Results for the C -parameter distributions are shown in Fig. 5.5.

Theoretical errors have been calculated, as in the previous case, using standard criteria and results indicate an average error over the entire spectrum $0 < C < 1$ of the C -parameter distribution at NLO and at NNLO of $\bar{\delta} \simeq 7.26\%$ and 2.43% respectively. A comparison of average errors according to the different methods is displayed in Table 5.2. Results show

$\bar{\delta} [\%]$	Conv.	PMC(μ_{LO})	PMC $_{\infty}$
$0.00 < (C) < 0.75$	4.77	0.85	2.43
$0.75 < (C) < 1.00$	11.51	3.68	2.42
$0.00 < (C) < 1.00$	6.47	1.55	2.43

Table 5.2: The average error $\bar{\delta}$ for the NNLO C -parameter distribution under Conventional, PMC(μ_{LO}) and PMC $_{\infty}$ scale settings calculated in different ranges of values of the (C) variable.

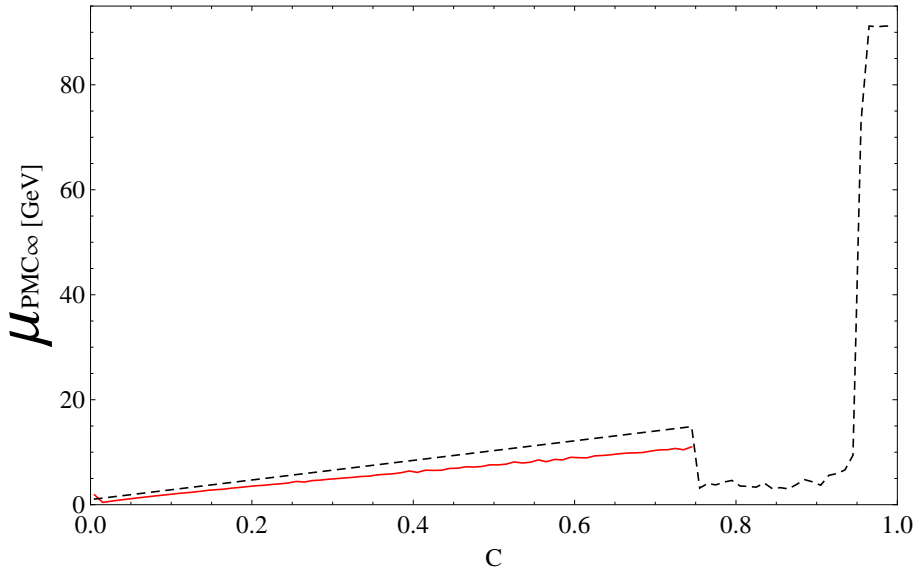


Figure 5.4: The LO- PMC_∞ (solid red) and the NLO- PMC_∞ (dashed black) scales for the C -parameter [89].

that the PMC_∞ improves the NNLO QCD predictions for the C -parameter distribution over the entire spectrum.

A comparison of the distributions calculated with the CSS, the $\text{PMC}(\mu_{\text{LO}})$ [88] and the PMC_∞ is shown in Fig. 5.6. The results for the PMC_∞ display remarkable agreement with the experimental data away from the regions $C < 0.05$ and $C \simeq 0.75$. The errors due to the normalization and to the regularization terms (Eq. (5.12)) are respectively 8.8% and 0.7% of the full theoretical errors.

The perturbative calculations could be further improved using a correct normalization and also by introducing the resummation of the large-logarithm technique in order to extend the perturbative regime and to eliminate the unphysical spike at $C = 0.75$, which is due to enhanced logarithmic terms at the kinematic boundary.

5.4. The thrust distribution in the QCD conformal window and in QED

For the first time, we employ the perturbative regime of the quantum chromodynamics (pQCD) infrared conformal window as a laboratory to investigate in a controllable manner (near) conformal properties of physically relevant quantities, such as the thrust distribution in electron–positron annihilation processes [90]. The conformal window of pQCD has a long and noble history conveniently summarized and generalized to arbitrary representations in Ref. [195]. Several lattice gauge theory applications and results have been summarized in a recent report on the subject in Ref. [196].

5.4.1. The thrust distribution according to N_f

It would be highly desirable to compare the PMC and CSS methods along the entire renormalization group flow from the highest energies down to zero energy. This is precluded in standard QCD with a number of active flavors less than six because the theory becomes strongly coupled at low energies. We therefore employ the perturbative regime of the conformal window (Sec. 2.2.2) which allows us to arrive at arbitrary low energies and obtain the corresponding results for the SU(3) case at the cost of increasing the number of active flavors. Here we are able to deduce the full solution at NNLO in the strong coupling. In this section we shall consider the region of flavors and colors near the upper bound of the conformal window, i.e. $N_f \sim 11/2N_c$, where the IR fixed point can be reliably accessed in perturbation theory and we compare the two renormalization scale setting methods, the CSS and the PMC_∞ .

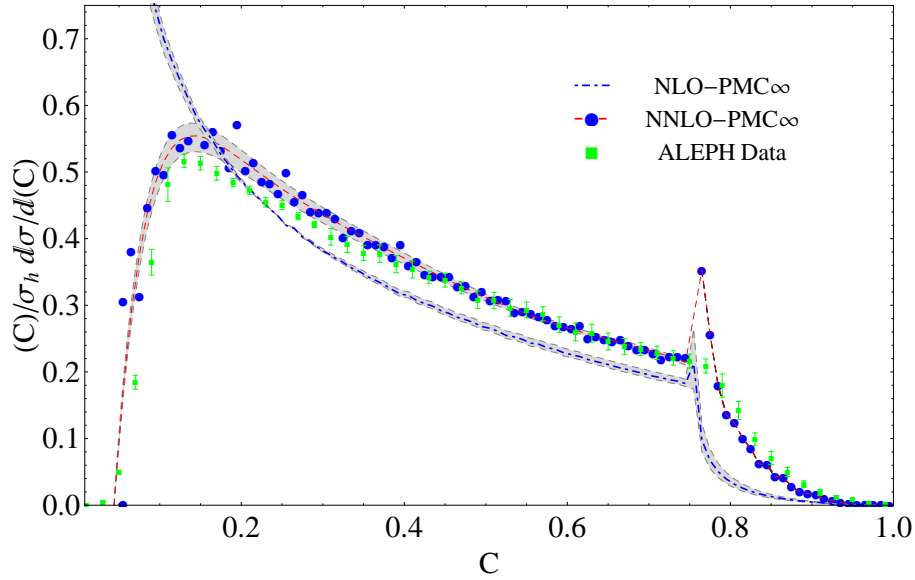


Figure 5.5: The C -parameter distribution under the PMC_∞ at NLO (dot-dashed blue) and at NNLO (dashed red) [89]. The blue points indicate the NNLO- PMC_∞ thrust distribution obtained with $\mu_{\text{II}} = \mu_0 = M_Z$. The experimental data points (green) are taken from the ALEPH experiment [177]. The dashed lines of the NNLO distribution show fits of the theoretical calculations with interpolating functions for the values of the remaining initial scale $\mu_0 = 2M_Z$ and $M_Z/2$. The shaded area shows theoretical errors for the PMC_∞ predictions at NLO and at NNLO calculated varying the remaining initial scale value in the range $\sqrt{s}/2 \leq \mu_0 \leq 2\sqrt{s}$.

Results for the thrust distribution calculated using the NNLO solution for the coupling $\alpha_s(\mu)$, at different values of the number of flavors, N_f , is shown in Fig. 5.7. A direct comparison between PMC_∞ (solid line) and CSS (dashed line) is shown at different values of the number of flavors. We notice that, despite the phase transition (i.e. the transition from an infrared finite coupling to an infrared divergent coupling), the curves given by the PMC_∞ at different N_f , preserve with continuity the same characteristics of the conformal distribution setting N_f outside the conformal window of pQCD.

Technically, this is explained by the fact that the PMC_∞ reabsorbs all the N_f terms into the running coupling and the PMC_∞ scales are both above 2 GeV in almost the entire range of the distribution; in particular, for values in the range $0.015 < 1 - T < 0.42$, and thus the PMC_∞ thrust distribution is affected by the change of behavior of the coupling only in the first two bins at $1 - T \sim 0$. However, this region is a multi-scale region and is not only affected by nonperturbative effects, but also by the presence of large-logarithms deriving from incomplete IR cancellation. On the other hand, the CSS distribution is more sensitive to the decreasing of N_f .

In fact, the position of the thrust distribution peak is well preserved varying N_f in and outside the conformal window using the PMC_∞ , while there is a constant shift towards lower values using the CSS. These trends are shown in Fig. 5.8. We notice that in the central range, $2 < N_f < 15$, the position of the peak is exactly preserved using the PMC_∞ and overlaps with the position of the peak shown by the experimental data. According to our analysis for the case PMC_∞ , in the range $N_f < 2$, the number of bins is insufficient to resolve the peak, although the behavior of the curve is consistent with the presence of a peak in the same position, while for $N_f \rightarrow 0$, the peak is no longer visible. Theoretical uncertainties on the position of the peak have been calculated using standard criteria, i.e. by varying the remaining initial scale value in the range $M_Z/2 \leq \mu_0 \leq 2M_Z$ and considering the lowest uncertainty given by the half the spacing between two adjacent bins.

Using the definition given in Eq. (5.6), we have determined the average error, $\bar{\delta}$, calculated in the interval $0.005 < (1 - T) < 0.4$ of thrust and results for CSS and PMC_∞ are shown in Fig. 5.9. We notice that the PMC_∞ in the

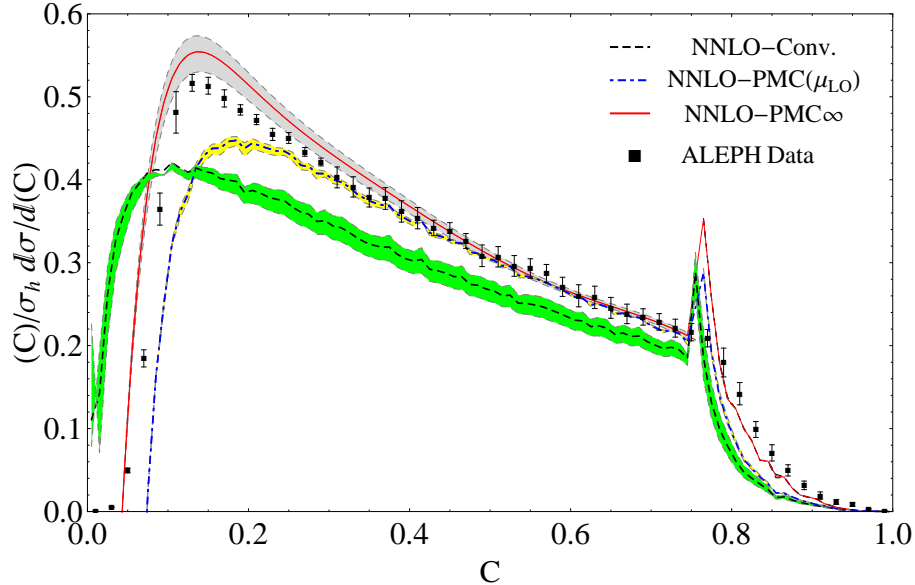


Figure 5.6: The NNLO C -parameter distribution under CSS (dashed black), the $\text{PMC}(\mu_{L0})$ (dot-dashed blue) and the PMC_∞ (solid red) [89]. The experimental data points (Black) are taken from the ALEPH experiment [177]. The shaded area shows theoretical error predictions at NNLO calculated varying the remaining initial scale value in the range $\sqrt{s}/2 \leq \mu_0 \leq 2\sqrt{s}$.

perturbative and IR conformal window, i.e. $12 < N_f < \bar{N}_f$, which is the region where $\alpha_s(\mu) < 1$ in the entire range of the renormalization scale values, from 0 up to ∞ , the average error given by PMC_∞ tends to zero ($\sim 0.23 - 0.26\%$) while the error given by the CSS tends to remain constant ($0.85 - 0.89\%$). Comparison of the two methods shows that, outside the conformal window, $N_f < \frac{34N_c^3}{13N_c^2 - 3}$, the PMC_∞ leads to higher precision.

From our analysis in section 2.2.2, it follows that the IR fixed point at $N_f = \frac{11}{2}N_c$ is not phenomenologically accessible, assuming a measured value of the coupling at a certain scale, since in the region $\bar{N}_f < N_f < \frac{11}{2}N_c$, the coupling would no longer have the UV asymptotically free behavior. Thus, in order to have a phenomenological application of the Banks-Zaks variable, (i.e. $\Delta_f = 33/2 - N_f \simeq \epsilon$, as shown in Refs.[197, 198]), one should be able to reach any small value of the coupling above the Planck scale in QCD, since the IR fixed point is interacting. Moreover, a conformal result is just characterized by the absence of running of the coupling and not necessarily by a null value. A straight conformal solution of Eqs. 2.31 and 2.32, is given by: $z = 0$, $W = 0$ with $x(\mu) = x^* = x_0$ for any scale $0 < \mu < \infty$. Our application of the Banks-Zaks results shows that the conformal limit of the thrust distribution is less sensitive to the method adopted to set the renormalization scale, CSS or PMC_∞ , once the same phenomenological value of the coupling has been determined at a certain scale. We suggest that a more suitable variable for the expansion would be given by $\tilde{\Delta} = \bar{N}_f - N_f \simeq \epsilon$, where \bar{N}_f is the maximum allowed value of N_f to be asymptotically free, introduced by the phenomenological value of the coupling at an initial scale μ_0 .

5.4.2. The thrust distribution in the Abelian limit $N_c \rightarrow 0$

We consider now the thrust distribution in U(1) Abelian QED, which rather than being infrared interacting is infrared free. We obtain the QED thrust distribution performing the $N_c \rightarrow 0$ limit of the QCD thrust at NNLO according to [32, 145]. In the zero number of colors limit the gauge group color factors are fixed by $N_A = 1$, $C_F = 1$, $T_R = 1$, $C_A = 0$, $N_c = 0$, $N_f = N_l$, where N_l is the number of active leptons, while the β -terms and the coupling rescale as β_n/C_F^{n+1} and $\alpha_s \cdot C_F$ respectively. In particular, $\beta_0 = -\frac{4}{3}N_l$ and $\beta_1 = -4N_l$ using the normalization of Eq. (2.15). According to this

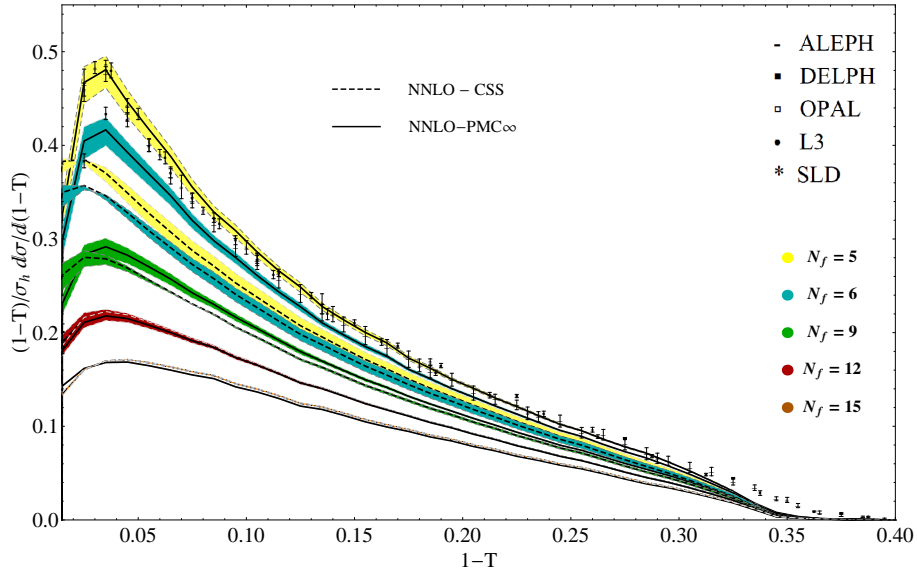


Figure 5.7: Thrust distributions for different values of N_f , using the PMC_∞ (solid line) and the CSS (dashed line) [90]. Shaded colored areas show error bars for each curve respectively. The experimental data points are taken from the ALEPH, DELPHI, OPAL, L3, SLD experiments [177–181].

rescaling of the color factors, we have determined the QED thrust and the QED PMC_∞ scales. For the QED coupling, we have used the analytic formula for the effective fine structure constant in the $\overline{\text{MS}}$ scheme:

$$\alpha(Q) = \frac{\alpha}{\left(1 - \Re e \Pi^{\overline{\text{MS}}}(Q^2)\right)}, \quad (5.13)$$

with $\alpha^{-1} \equiv \alpha(0)^{-1} = 137.036$ and the vacuum polarization function (Π) calculated perturbatively to two loops, including contributions from leptons, quarks and the W boson. The QED PMC_∞ scales have the same form of Eqs. (5.7) and (5.8) with the factor for the $\overline{\text{MS}}$ scheme set to $f_{sc} \equiv 5/6$ and the η regularization parameter introduced to cancel singularities in the NLO PMC_∞ scale μ_{II} in the $N_c \rightarrow 0$ limit tends to the same QCD value, $\eta = 3.51$. A direct comparison between QED and QCD PMC_∞ scales is shown in Fig. 5.10.

We note that in the QED limit the PMC_∞ scales have analogous dynamical behavior to those calculated in QCD; differences arise mainly owing to the $\overline{\text{MS}}$ scheme factor reabsorption, the effects of the N_c number of colors at NLO are very small. Thus, we notice that perfect consistency is shown from QCD to QED using the PMC_∞ method. The normalized QED thrust distribution is shown in Fig. 5.11. We note that the curve is peaked at the origin, $T = 1$, which suggests that the three-jet event in QED occurs with a rather back-to-back symmetry. Results for the CSS and the PMC_∞ methods in QED are $O(\alpha)$ and show very small differences, given the good convergence of the theory.

5.5. A novel method for the precise determination of the strong coupling and its behavior

In this section we present a novel method for precisely determining the running QCD coupling constant $\alpha_s(Q)$ over a wide range of Q from event-shape variables for electron–positron annihilation measured at a single center-of-mass energy \sqrt{s} , based on PMC scale setting. In particular, we display the results obtained in Refs. [87, 88] using the approach of a single PMC scale at LO and NLO, i.e. the $\text{PMC}(\mu_{\text{LO}})$ of the previous section.

The precise determination of the strong coupling $\alpha_s(Q)$ is one of the crucial tests of QCD. The dependence of $\alpha_s(Q)$ on the renormalization scale Q obtained from many different physical processes shows consistency with QCD predictions

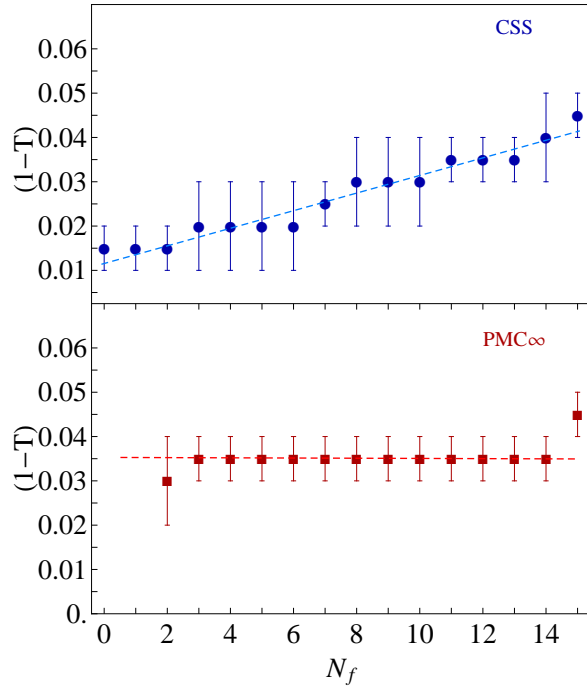


Figure 5.8: Comparison of the position of the peak for the thrust distribution using the CSS and the PMC_∞ vs the number of flavors, N_f . Dashed lines indicate the particular trend in each graph [90].

and asymptotic freedom. The Particle Data Group (PDG) currently gives the world average: $\alpha_s(M_Z) = 0.1179 \pm 0.0009$ [126] in the $\overline{\text{MS}}$ renormalization scheme.

Particularly suitable to the determination of the strong coupling is the process $e^+e^- \rightarrow 3\text{jets}$ since its leading order is $\mathcal{O}(\alpha_s)$ [176]. Currently, theoretical calculations for event shapes are based on CSS. By using conventional scale setting, only one value of α_s at the scale \sqrt{s} can be extracted and the main source of the uncertainty is given by the choice of the renormalization scale. Several values for the strong coupling have been extracted from several processes, e.g. $\alpha_s(M_Z) = 0.1224 \pm 0.0035$ [199] is obtained by using perturbative corrections and resummation of the large logarithms in the NNLO+NLL accuracy predictions. Other evaluations improving the resummation calculations up to N^3LL give a result of $\alpha_s(M_Z) = 0.1135 \pm 0.0011$ [31] from thrust and $\alpha_s(M_Z) = 0.1123 \pm 0.0015$ [200] from the C -parameter. Nonperturbative corrections for hadronization effects have also been included in Ref. [201], but as pointed out in Ref. [202], the systematics of the theoretical uncertainties introduced by hadronization effects are not well understood.

In this section we show that by using the PMC, it is possible to eliminate the renormalization scale ambiguities and obtain consistent results for the strong coupling using the precise experimental data of event-shape variable distributions. We notice that improved event-shape distributions have been obtained in Refs. [44, 194, 203] using BLM and soft and collinear effective theory (SCET).

5.5.1. Running behavior

Given that the PMC scale ($\text{PMC}(\mu_{LO})$) is not a single-valued but rather a monotonically increasing function of \sqrt{s} and of the selected observable, (as shown in Figs. 5.1 and 5.4), it is possible to determine the strong coupling at different scales from one single experiment at one single center-of-mass energy. The dependence of the scale on the observable reflects the dynamics of the underlying gluon and quark subprocess. This dynamics also varies the number of active flavors N_f .

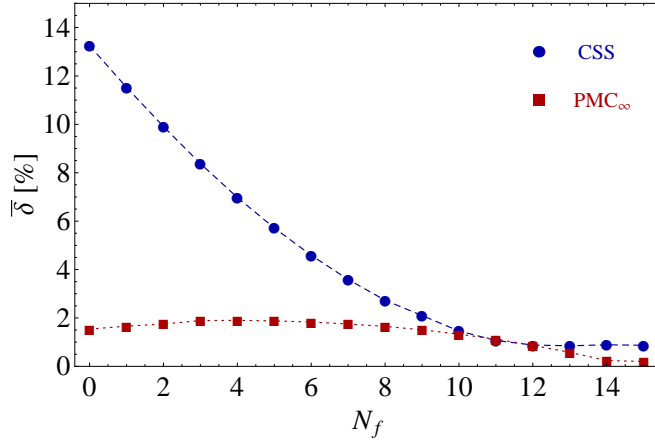


Figure 5.9: Comparison of the average theoretical error, $\bar{\delta}$, calculated using standard criteria in the range: $0.005 < (1 - T) < 0.4$, using the CSS and the PMC_{∞} for the thrust distribution vs. the number of flavors, N_f [90].

Considering that PMC scales for QCD and QED show the same behavior and that their relation at LO is only given by a RS redefinition term, $Q_{\text{QCD}}^2/Q_{\text{QED}}^2 = e^{-5/3}$, this approach may also be extended to QED.

We extract α_s at different scales bin-by-bin from the comparison of PMC predictions for $(1 - T)$ and C differential distributions with measurements at $\sqrt{s} = M_Z$. The extracted α_s values from the C -parameter distribution are shown in Fig. 5.12. We note that the α_s values extracted in the scale range of $3 \text{ GeV} < Q < 11 \text{ GeV}$ are in excellent agreement with those evaluated from the world average $\alpha_s(M_Z)$ [126]. Given that the PMC scale setting eliminates the scale uncertainties, the corresponding extracted α_s values are not plagued by ambiguities in the choice of μ_r . The extracted α_s values from the thrust observable using PMC are shown in Fig. 5.13. There is good agreement also in this case in the range $3.5 \text{ GeV} < \mu_r < 16 \text{ GeV}$ (corresponding to the range $0.05 < (1 - T) < 0.29$). These extracted values of α_s are also in good agreement with the world average value of the PDG [126]. Thus, PMC scale setting provides a remarkable way to verify the running of $\alpha_s(Q)$ from event shapes measured at a single energy of \sqrt{s} . Analogously in QED, the running of the QED coupling $\alpha(Q)$ can be measured at a single energy of \sqrt{s} (see e.g. [204]).

The differential distributions of event shapes are afflicted with large logarithms especially in the two-jet region. Thus, the comparison of QCD predictions with experimental data and thus the extracted α_s values are restricted to the region where the theory is able to describe the data well. Choosing a different area of distributions leads to the different values of α_s .

5.5.2. $\alpha_s(M_Z)$ from a χ^2 fit

In order to obtain a reliable α_s at the scale of the Z^0 mass, we determine $\alpha_s(M_Z)$ from the fit of the PMC predictions to measurements. In particular, we perform the fit by minimizing the χ^2 respect to the $\alpha_s(M_Z)$ parameter. The variable χ^2 is defined as:

$$\chi^2 = \sum_i \left(\frac{\langle y \rangle_i^{\text{expt}} - \langle y \rangle_i^{\text{th}}}{\sigma_i} \right)^2,$$

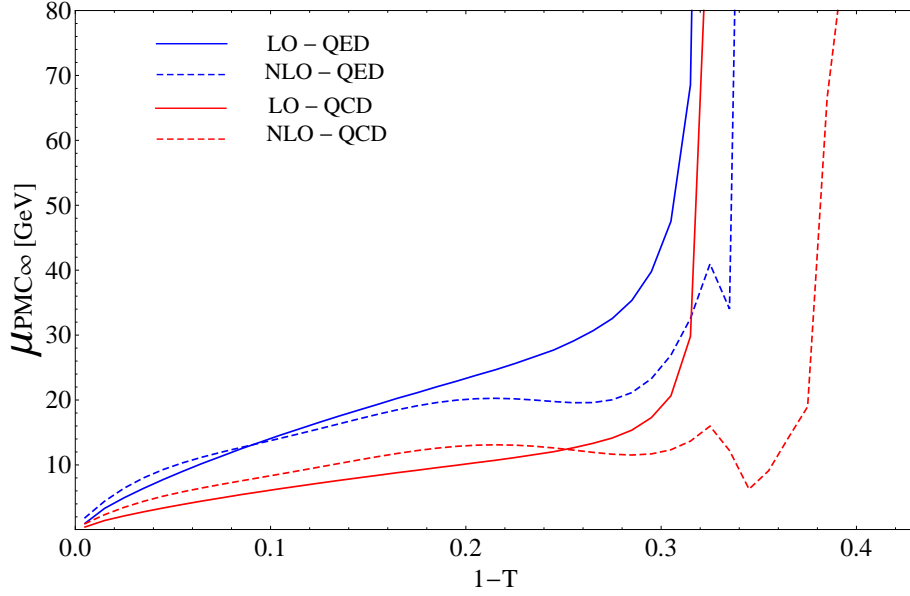


Figure 5.10: PMC_∞ scales for the thrust distribution: LO-QCD scale (solid red); LO-QED scale (solid blue); NLO-QCD scale (dashed red); NLO-QED scale (dashed blue) [90].

where $\langle y \rangle_i^{\text{expt}}$ is the value of the experimental data, σ_i is the corresponding experimental uncertainty and $\langle y \rangle_i^{\text{th}}$ is the theoretical prediction. The fit for thrust and the C -parameter leads to the following results:

$$\begin{aligned} \alpha_s(M_Z) &= 0.1185 \pm 0.0011(\text{expt}) \pm 0.0005(\text{th}) \\ &= 0.1185 \pm 0.0012, \end{aligned} \quad (5.14)$$

with $\chi^2/\text{d.o.f.} = 27.3/20$ for the thrust mean value and

$$\begin{aligned} \alpha_s(M_Z) &= 0.1193_{-0.0010}^{+0.0009}(\text{expt})_{-0.0016}^{+0.0019}(\text{th}) \\ &= 0.1193_{-0.0019}^{+0.0021}, \end{aligned} \quad (5.15)$$

with $\chi^2/\text{d.o.f.} = 43.9/20$ for the C -parameter mean value, where the first error is the experimental uncertainty and the second the theoretical uncertainty. Both results are consistent with the world average $\alpha_s(M_Z) = 0.1179 \pm 0.0009$ [126].

The precision of the extracted α_s has been greatly improved by using the PMC: the dominant μ_r scale uncertainties are eliminated and the convergence of pQCD series is greatly improved. In particular, a strikingly much faster pQCD convergence is obtained for the mean thrust value [87], theoretical uncertainties are even smaller than the experimental uncertainties. We remark that these results for $\alpha_s(M_Z)$ are among the most precise determinations of the strong coupling at the Z^0 mass from event-shape variables.

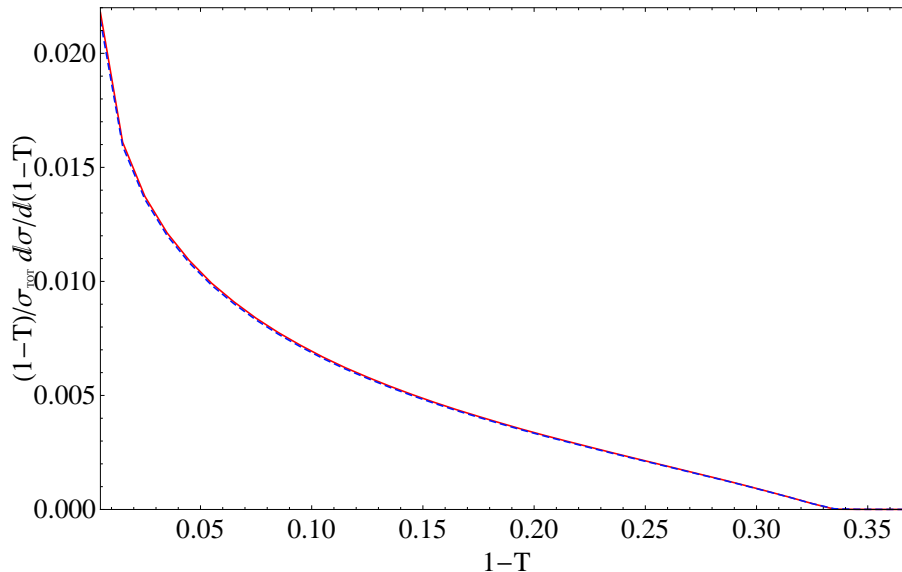


Figure 5.11: Thrust distributions in the QED limit at NNLO using the PMC_∞ (solid red) and the CSS (dashed blue) [90].

6. Comparison of the PMCM, PMCs and PMC_∞ for fully integrated fundamental quantities

In this section, we show predictions for three important quantities: $R_{e^+e^-}$, R_τ and $\Gamma(H \rightarrow b\bar{b})$, which have been calculated up to four-loop QCD corrections using alternative PMC scale-setting procedures. Numerical results for the conventional, PMCM, PMCs and PMC_∞ approaches will be presented. For self-consistency, the same loop α_s -running behavior will be adopted for calculating the same loop perturbative series. The QCD asymptotic scale (Λ_{QCD}) is then fixed by using $\alpha_s(M_Z) = 0.1179$ [126] and for a four-loop prediction, we obtain $\Lambda_{\text{QCD}}^{n_f=4} = 291.7 \text{ MeV}$ and $\Lambda_{\text{QCD}}^{n_f=5} = 207.2 \text{ MeV}$ in a conventional $\overline{\text{MS}}$ renormalization scheme.

6.1. The pQCD predictions for $R_{e^+e^-}$, R_τ and $\Gamma(H \rightarrow b\bar{b})$

The annihilation of electrons and positrons into hadrons provides one of the most important platforms for determining the running behavior of the QCD coupling. The R ratio is defined as

$$\begin{aligned} R_{e^+e^-}(Q) &= \frac{\sigma(e^+e^- \rightarrow \text{hadrons})}{\sigma(e^+e^- \rightarrow \mu^+\mu^-)} \\ &= 3 \sum_q e_q^2 [1 + R(Q)], \end{aligned} \quad (6.1)$$

where $Q = \sqrt{s}$, corresponding to the electron-positron collision energy in the center-of-mass frame. The pQCD series for $R(Q)$, up to $(n+1)$ -loop QCD corrections, is

$$R_n(Q) = \sum_{i=0}^n \mathcal{C}_i(Q, \mu_r) \alpha_s^{i+1}(\mu_r).$$

The perturbative coefficients $\mathcal{C}_i(Q, \mu_r)$ in the $\overline{\text{MS}}$ scheme up to four-loop level have been calculated in Refs. [162, 205–207]. As a reference point, at $\sqrt{s} = 31.6 \text{ GeV}$, we have $\frac{3}{11} R_{e^+e^-}^{\text{expt}} = 1.0527 \pm 0.0050$ [208].

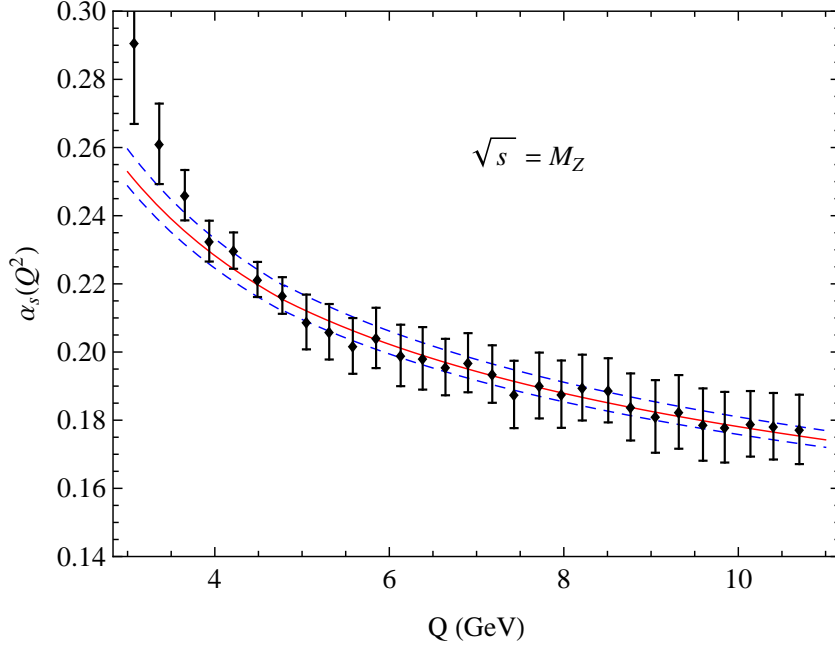


Figure 5.12: The coupling constant $\alpha_s(Q)$ extracted by comparing PMC predictions with the ALEPH data [177] at a single energy of $\sqrt{s} = M_Z$ from the C -parameter distributions in the $\overline{\text{MS}}$ scheme (from Ref. [88]). The error bars are the squared averages of the experimental and theoretical errors. The three lines are the world average evaluated from $\alpha_s(M_Z) = 0.1179 \pm 0.009$ [126].

Another useful ratio is R_τ for τ -lepton decays into hadrons, defined as

$$\begin{aligned} R_\tau(M_\tau) &= \frac{\Gamma(\tau \rightarrow \nu_\tau + \text{hadrons})}{\Gamma(\tau \rightarrow \nu_\tau + \bar{\nu}_l + l)} \\ &= 3|V_{ud}|^2 S_{\text{EW}} \left[1 + \hat{R}(M_\tau) + \delta'_{\text{EW}} + \delta_2 + \delta_{\text{NP}} \right], \end{aligned} \quad (6.2)$$

where $V_{ud} = 0.97373 \pm 0.00031$ [126] is the relevant Cabibbo–Kobayashi–Maskawa matrix element, $S_{\text{EW}} = 1.0198 \pm 0.0006$ and $\delta'_{\text{EW}} = 0.001$ for the electroweak corrections, $\delta_2 = (-4.4 \pm 2.0) \times 10^{-4}$ for light-quark mass effects⁶, $\delta_{\text{NP}} = (-4.8 \pm 1.7) \times 10^{-3}$ for the nonperturbative effects and $M_\tau = 1.777 \text{ GeV}$ [205, 210, 211]. The pQCD series for $\hat{R}(M_\tau)$ up to $(n+1)$ -loop QCD corrections is

$$\hat{R}_n(M_\tau) = \sum_{i=0}^n \hat{C}_i(M_\tau, \mu_r) a_s^{i+1}(\mu_r),$$

where the perturbative coefficients $\hat{C}_i(M_\tau, \mu_r)$ up to four-loop QCD corrections can be derived by using the relation between $R_\tau(M_\tau)$ and $R_{e^+e^-}(\sqrt{s})$ [212].

The decay width for Higgs boson decay into a bottom and anti-bottom pair, $H \rightarrow b\bar{b}$, can be written as

$$\Gamma(H \rightarrow b\bar{b}) = \frac{3G_F M_H m_b^2(M_H)}{4\sqrt{2}\pi} [1 + \tilde{R}(M_H)], \quad (6.3)$$

where the Fermi constant $G_F = 1.16638 \times 10^{-5} \text{ GeV}^{-2}$, the Higgs mass $M_H = 125.1 \text{ GeV}$ and the b -quark $\overline{\text{MS}}$ running mass is $m_b(M_H) = 2.78 \text{ GeV}$ [69]. The pQCD series for $\tilde{R}(M_H)$ up to $(n+1)$ -loop QCD corrections is

$$\tilde{R}_n(M_H) = \sum_{i=0}^n \tilde{C}_i(M_H, \mu_r) a_s^{i+1}(\mu_r).$$

The perturbative coefficients $\tilde{C}_i(M_H, \mu_r)$ up to four-loop QCD corrections have been calculated in Ref. [213]. In the following, we give the properties for the pQCD series of $R_n(Q=31.6 \text{ GeV})$, $\hat{R}_n(M_\tau)$ and $\tilde{R}_n(M_H)$ using each scale-setting

⁶An improved determination of the m_s and $|V_{\text{us}}|$ from the τ -decay has been recently shown in Ref. [209].

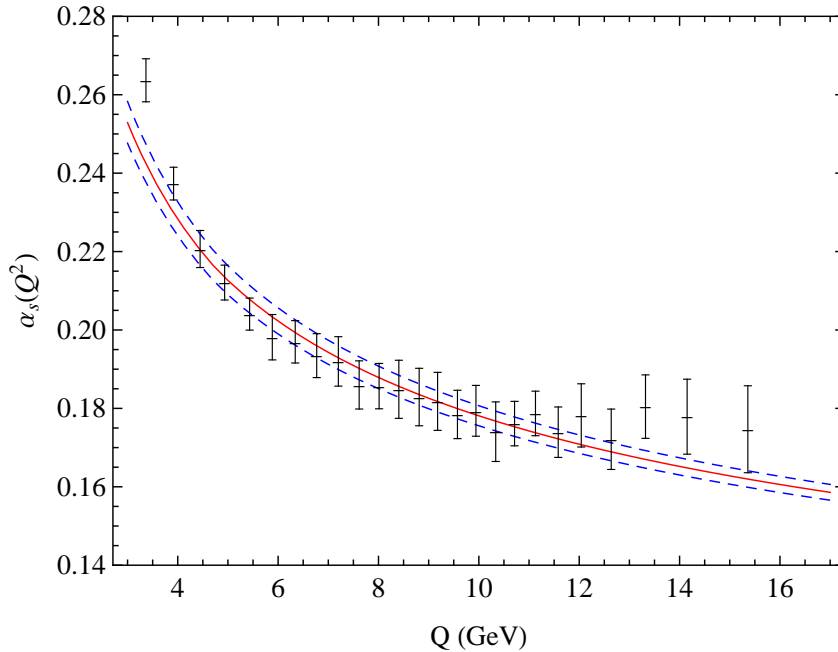


Figure 5.13: The extracted α_s from the comparison of PMC predictions with ALEPH data at $\sqrt{s} = M_Z$ (from Ref. [87]). The error bars are from the experimental data. The three lines are the world average evaluated from $\alpha_s(M_Z) = 0.1179 \pm 0.0009$ [126].

approach. As for the leading-order ratios with $n = 0$, we have no information to set the renormalization scale for all the scale-setting approaches; and for convenience, we directly set it to be Q , M_τ , or M_H , respectively, which gives $R_0 = 0.04428$, $\hat{R}_0 = 0.0891$ and $\tilde{R}_0 = 0.2034$. We point out that all four-loop calculations for these observables derive from analytic properties (of the Adler function) rather than from a direct multi-loop calculation of the perturbative series.

6.2. Properties using the conventional scale-setting approach

	$\mathcal{C}_1(\mu_r)$	$\mathcal{C}_2(\mu_r)$	$\mathcal{C}_3(\mu_r)$	$\mathcal{C}_4(\mu_r)$
$R(Q)$	4	$22.55^{+42.51}_{-42.51}$	$-819.50^{+1145.54}_{-266.26}$	$-20591^{+31244.8}_{-7812.4}$
$\hat{R}(M_\tau)$	4	$83.24^{+49.91}_{-41.39}$	$1687.42^{+3054.60}_{-1588.77}$	$32532.1^{+139210.0}_{-37674.5}$
$\tilde{R}(M_H)$	22.6667	$466.347^{+240.907}_{-240.907}$	$2672.49^{+13688.40}_{-8567.51}$	$-211391^{+358424}_{-27651.9}$

Table 6.1: The scale-dependent coefficients $\mathcal{C}_i(\mu_r)$ of the conventional series for $R_n(Q=31.6 \text{ GeV})$, $\hat{R}_n(M_\tau)$ and $\tilde{R}_n(M_H)$, respectively. The central values are for $\mu_r = Q$, M_τ , or M_H , respectively. The errors are evaluated by taking $\mu_r \in [Q/2, 2Q]$ for $R_n(Q=31.6 \text{ GeV})$, $\mu_r \in [1 \text{ GeV}, 2M_\tau]$ for $\hat{R}_n(M_\tau)$ and $\mu_r \in [M_H/2, 2M_H]$ for $\tilde{R}_n(M_H)$, respectively.

We present the perturbative coefficients $\mathcal{C}_i(\mu_r)$ in Table 6.1, where the errors are evaluated by taking $\mu_r \in [Q/2, 2Q]$ for $R(Q=31.6 \text{ GeV})$, $\mu_r \in [1 \text{ GeV}, 2M_\tau]$ for $\hat{R}(M_\tau)$ and $\mu_r \in [M_H/2, 2M_H]$ for $\tilde{R}(M_H)$, respectively. Table 6.1 shows that those coefficients are highly scale dependent.

We present the results of $R_n(Q=31.6 \text{ GeV})$, $\hat{R}_n(M_\tau)$ and $\tilde{R}_n(M_H)$ up to four-loop QCD corrections using the conventional scale-setting approach in Table 6.2, where the errors are evaluated by taking $\mu_r \in [Q/2, 2Q]$ for $R_3(Q=31.6 \text{ GeV})$, $\mu_r \in [1 \text{ GeV}, 2M_\tau]$ for $\hat{R}_3(M_\tau)$ and $\mu_r \in [M_H/2, 2M_H]$ for $\tilde{R}_3(M_H)$, respectively. For self-consistency, we adopt the $(n+1)$ th-loop α_s -running behavior in deriving $(n+1)$ th-loop prediction for $R_n(Q=31.6 \text{ GeV})$, $\hat{R}_n(M_\tau)$ and $\tilde{R}_n(M_H)$. We

	$n = 1$	$n = 2$	$n = 3$	κ_1	κ_2	κ_3
$R_n _{\text{Conv.}}$	$0.04753^{+0.00044}_{-0.00138}$	$0.04638^{+0.00012}_{-0.00070}$	$0.04608^{+0.00015}_{-0.00009}$	$7.3^{+2.9\%}_{-9.2\%}$	$2.4^{+0.7\%}_{-1.4\%}$	$0.6^{+0.0\%}_{-0.1\%}$
$\hat{R}_n _{\text{Conv.}}$	$0.1522^{+0.0482}_{-0.0295}$	$0.1826^{+0.0360}_{-0.0268}$	$0.1980^{+0.0170}_{-0.0194}$	$70.8^{+2.6\%}_{+2.3\%}$	$20.0^{+10.9\%}_{+7.0\%}$	$8.4^{+6.8\%}_{+6.2\%}$
$\tilde{R}_n _{\text{Conv.}}$	$0.2404^{+0.0074}_{-0.0075}$	$0.2423^{+0.0002}_{-0.0007}$	$0.2409^{+0.0015}_{-0.0007}$	$18.2^{+8.0\%}_{+6.7\%}$	$0.8^{+1.3\%}_{+2.9\%}$	$0.6^{+0.6\%}_{+0.0\%}$

Table 6.2: Results for $R_n(Q=31.6\text{ GeV})$, $\hat{R}_n(M_\tau)$, $\tilde{R}_n(M_H)$ up to four-loop QCD corrections using the conventional scale-setting approach. The central values are obtained by setting μ_r as Q , M_τ , or M_H , respectively. The errors are evaluated by taking $\mu_r \in [Q/2, 2Q]$ for $R_n(Q=31.6\text{ GeV})$, $\mu_r \in [1\text{ GeV}, 2M_\tau]$ for $\hat{R}_n(M_\tau)$ and $\mu_r \in [M_H/2, 2M_H]$ for $\tilde{R}_n(M_H)$.

define the ratio

$$\kappa_n = \left| \frac{\mathcal{R}_n - \mathcal{R}_{n-1}}{\mathcal{R}_{n-1}} \right|,$$

where \mathcal{R} stands for R , \hat{R} and \tilde{R} , respectively. It shows how the ‘‘known’’ prediction \mathcal{R}_{n-1} is affected by the one-order-higher terms. Table 6.2 shows that generally we have $\kappa_1 > \kappa_2 > \kappa_3$ for all those quantities, consistently with the perturbative nature of the series and indicates that one can obtain more precise predictions by including more loop terms. To show the perturbative nature more explicitly, we present the magnitudes of each loop term for the four-loop approximants $R_3(Q = 31.6\text{ GeV})$, $\hat{R}_3(M_\tau)$ and $\tilde{R}_3(M_H)$ in Table 6.3, which displays the relative importance among the LO, NLO, N²LO and N³LO terms, which for those approximants are

$$1 : +0.063^{+0.099}_{-0.100} : -0.026^{+0.034}_{-0.016} : -0.007^{+0.001}_{+0.009}, \quad (6.4)$$

$$1 : +0.531^{+0.108}_{+0.101} : +0.275^{+0.205}_{+0.152} : +0.135^{+0.186}_{+0.159}, \quad (6.5)$$

$$1 : +0.184^{+0.071}_{-0.085} : +0.009^{+0.039}_{-0.035} : -0.007^{+0.010}_{-0.002}, \quad (6.6)$$

where the central values are for $\mu_r = Q$, $\mu_r = M_\tau$ and $\mu_r = M_H$; and the errors are for $\mu_r \in [Q/2, 2Q]$, $\mu_r \in [1\text{ GeV}, 2M_\tau]$ and $\mu_r \in [M_H/2, 2M_H]$, respectively. Consistently with Table 6.2, the scale dependence for each loop term is large, but due to the cancellation of scale dependence among different orders, the net scale dependence is small, e.g. $\left(\begin{smallmatrix} +0.3\% \\ -0.2\% \end{smallmatrix}\right)$, $\left(\begin{smallmatrix} +8.6\% \\ -9.8\% \end{smallmatrix}\right)$ and $\left(\begin{smallmatrix} +0.6\% \\ -0.3\% \end{smallmatrix}\right)$ for $R_3(Q=31.6\text{ GeV})$, $\hat{R}_3(M_\tau)$ and $\tilde{R}_3(M_H)$, respectively. Note that due to the usual renormalon divergence and a larger α_s value at a smaller scale M_τ , i.e. $\alpha_s(M_\tau) \sim 0.33$, the net scale dependence of the four-loop prediction $\hat{R}_3(M_\tau)$ is still sizable.

	LO	NLO	N ² LO	N ³ LO	Total
$R_3 _{\text{Conv.}}$	$0.04473^{+0.00499}_{+0.00512}$	$0.00282^{+0.00360}_{-0.00468}$	$-0.00115^{+0.00147}_{-0.00095}$	$-0.00032^{+0.00007}_{+0.00042}$	$0.04608^{+0.00015}_{-0.00009}$
$\hat{R}_3 _{\text{Conv.}}$	$0.1020^{+0.0471}_{-0.0261}$	$0.0542^{+0.0089}_{-0.0062}$	$0.0280^{+0.0176}_{+0.0044}$	$0.0138^{+0.0214}_{+0.0085}$	$0.1980^{+0.0170}_{-0.0194}$
$\tilde{R}_3 _{\text{Conv.}}$	$0.2030^{+0.0175}_{+0.0226}$	$0.0374^{+0.0100}_{-0.0151}$	$0.0019^{+0.0070}_{-0.0077}$	$-0.0014^{+0.0020}_{-0.0005}$	$0.2409^{+0.0015}_{-0.0007}$

Table 6.3: The value of each loop term (LO, NLO, N²LO and N³LO) for the four-loop QCD predictions $R_3(Q=31.6\text{ GeV})$, $\hat{R}_3(M_\tau)$ and $\tilde{R}_3(M_H)$ using the conventional scale-setting approach. The errors are evaluated by taking $\mu_r \in [Q/2, 2Q]$ for $R_3(Q=31.6\text{ GeV})$, $\mu_r \in [1\text{ GeV}, 2M_\tau]$ for $\hat{R}_3(M_\tau)$ and $\mu_r \in [M_H/2, 2M_H]$ for $\tilde{R}_3(M_H)$.

In the pQCD calculation, it is helpful to give a reliable prediction of the uncalculated higher-order terms. The Padé approximant approach (PAA) [130–132], shown in Eq. (2.38), provides an effective method to estimate the $(n+1)$ th-order coefficient from a given n -th-order series.⁷ In practice, it has been found that the PAA becomes more effective when more

⁷Another method, which uses the scale-invariant conformal series together with the Bayesian model [214–216] to provide probabilistic

loop terms are known. For a pQCD approximant, $\rho(Q) = c_1 a_s + c_2 a_s^2 + c_3 a_s^3 + c_4 a_s^4 + \dots$, the predicted N³LO and the N⁴LO terms are

$$\rho_{[1/1]}^{\text{N}^3\text{LO}} = \frac{c_3^2}{c_2} a_s^4, \quad (6.7)$$

$$\rho_{[0/2]}^{\text{N}^3\text{LO}} = \frac{2c_1 c_2 c_3 - c_2^3}{c_1^2} a_s^4, \quad (6.8)$$

$$\rho_{[1/2]}^{\text{N}^4\text{LO}} = \frac{2c_2 c_3 c_4 - c_3^3 - c_1 c_2^2}{c_2^2 - c_1 c_3} a_s^5, \quad (6.9)$$

$$\rho_{[2/1]}^{\text{N}^4\text{LO}} = \frac{c_4^2}{c_3} a_s^5, \quad (6.10)$$

$$\rho_{[0/3]}^{\text{N}^4\text{LO}} = \frac{c_2^4 - 3c_1 c_2^2 c_3 + 2c_1^2 c_2 c_4 + c_1^2 c_3^2}{c_1^3} a_s^5. \quad (6.11)$$

Table 6.4 displays the preferable diagonal-type PAA predictions [133] of the N³LO and N⁴LO terms of $R_3(Q=31.6 \text{ GeV})$,

	N ³ LO	N ⁴ LO
$R_3 _{\text{Conv.}}$	[1/1]: $0.00047_{-0.00284}^{+0.00000}$	[1/2]: $-0.00002_{-0.00010}^{+0.00011}$
	—	[2/1]: $-0.00009_{-0.00000}^{+0.00028}$
$\hat{R}_3 _{\text{Conv.}}$	[1/1]: $0.0145_{-0.0128}^{+0.0074}$	[1/2]: $+0.0061_{-0.0142}^{+0.0093}$
	—	[2/1]: $+0.0068_{-0.0011}^{+0.0085}$
$\tilde{R}_3 _{\text{Conv.}}$	[1/1]: $0.0001_{-0.0000}^{+0.0016}$	[1/2]: $-0.0006_{-0.0000}^{+0.0005}$
	—	[2/1]: $+0.0010_{-0.0016}^{+0.0000}$

Table 6.4: The preferable diagonal-type PAA predictions of the N³LO and N⁴LO terms of $R_3(Q=31.6 \text{ GeV})$, $\hat{R}_3(M_\tau)$ and $\tilde{R}_3(M_H)$ using the conventional scale-setting approach. The uncertainties correspond to taking $\mu_r \in [Q/2, 2Q]$, $\mu_r \in [1 \text{ GeV}, 2M_\tau]$ and $\mu_r \in [M_H/2, 2M_H]$, respectively.

$\hat{R}_3(M_\tau)$ and $\tilde{R}_3(M_H)$ using the conventional scale-setting approach. Owing to the large scale dependence of each loop term, the PAA predictions show large scale dependence. The two allowable diagonal-type PAA predictions for N⁴LO terms are consistent with each order within errors. Comparing Table 6.4 with Table 6.3, we note that the values of the predicted N³LO terms agree with their exact values within errors. Thus, by employing a perturbative series with enough higher-order terms, the PAA prediction can be made reliable.

6.3. Properties using the PMCm approach

Following the standard PMCm procedures, the nonconformal $\{\beta_i\}$ -terms are eliminated by using the RGE recursively, determining the effective α_s at each perturbative order and resulting in the renormalon-free and scheme-independent conformal series (3.14). We present the conformal coefficients $\hat{r}_{i,0}$ in Table 6.5. The PMC scales are of a perturbative nature, which leads to the *first kind of residual scale dependence* for PMCm predictions. If the pQCD approximants are known up to four-loop QCD corrections, three PMC scales (Q_1 , Q_2 and Q_3) can be determined up to N²LL, NLL and LL order, which are $\{41.19, 36.85, 168.68\} \text{ GeV}$ for $R_n(Q=31.6 \text{ GeV})$, $\{1.26, 0.98, 0.36\} \text{ GeV}$ for $\hat{R}_n(M_\tau)$ and $\{62.03, 40.76, 52.76\} \text{ GeV}$ for $\tilde{R}_n(M_H)$, accordingly. There is no $\{\beta_i\}$ -term to set the scale Q_4 , the PMCm prediction has the *second kind of residual scale dependence*. As mentioned in Sec. 3.1, there is the *second kind of residual scale dependence* for

estimates of the unknown higher-orders terms has been proposed [217]

	$\hat{r}_{1,0}$	$\hat{r}_{2,0}$	$\hat{r}_{3,0}$	$\hat{r}_{4,0}$
$R(Q)$	4	29.44	-64.25	-2812.74
$\hat{R}(M_\tau)$	4	34.33	219.89	1741.15
$\tilde{R}(M_H)$	22.6667	216.356	-8708.09	-110597

Table 6.5: Conformal coefficients $\hat{r}_{i,0}$ for $R_n(Q=31.6 \text{ GeV})$, $\hat{R}_n(M_\tau)$ and $\tilde{R}_n(M_H)$, respectively.

PMCm series and, for convenience, we set $Q_4 = Q_3$ as the default choice of Q_4 . A discussion of the magnitude of the *second kind of residual scale dependence* by taking some other typical choices of Q_4 will be presented at the end of this subsection. For the scales $\gg \Lambda_{\text{QCD}}$, we adopt the usual approximate four-loop analytic solution of the RGE to derive the value of α_s . Due to the sizable difference between the approximate analytic solution and the exact numerical solution of the RGE at scales below a few GeV [52, 126], we adopt the exact numerical solution of the RGE to evaluate $R_\tau(M_\tau)$ at 1.26 GeV and 0.98 GeV. For the scales close to Λ_{QCD} , various low-energy models have been suggested in the literature; a detailed comparison of various low-energy models can be found in Ref. [99]. For definiteness, we shall adopt the Massive Perturbation Theory (MPT) model [218] to evaluate $R_\tau(M_\tau)$ at $Q_3 = 0.36 \text{ GeV}$, which gives $\alpha_s^{\xi=10^{\pm 2}}(0.36) = 0.559^{+0.042}_{-0.032}$, where ξ is the parameter in the MPT model.

	$n = 1$	$n = 2$	$n = 3$	κ_1	κ_2	κ_3
$R_n _{\text{PMCm}}$	0.04735	0.04640	0.04610	6.9%	2.0%	0.6%
$\hat{R}_n _{\text{PMCm}}$	0.2133	0.1991	0.2087	139.4%	6.7%	4.8%
$\tilde{R}_n _{\text{PMCm}}$	0.2481	0.2402	0.2400	22.0%	3.2%	0.1%

Table 6.6: Results for $R_n(Q=31.6 \text{ GeV})$, $\hat{R}_n(M_\tau)$, $\tilde{R}_n(M_H)$ up to four-loop QCD corrections using the PMCm scale-setting approach. The renormalization scale is set as Q , M_τ and M_H , respectively.

We present the results of $R_n(Q=31.6 \text{ GeV})$, $\hat{R}_n(M_\tau)$ and $\tilde{R}_n(M_H)$ up to four-loop QCD corrections using the PMCm scale-setting approach in Table 6.6. Table 6.6 shows that the PMCm predictions generally have behavior close to the central predictions under conventional scale-setting procedures, especially when more loop terms are known. This is due to the fact that when the renormalization scale of the conventional series is set as the one to eliminate the large logarithms, the divergent renormalon terms may also be simultaneously removed, since the $\{\beta_i\}$ -terms are always accompanied by the logarithm terms.

	LO	NLO	N ² LO	N ³ LO	Total
$R_3 _{\text{PMCm}}$	$0.04267^{+0.00003}_{-0.00001}$	$0.00349^{+0.00003}_{-0.00004}$	-0.00004	-0.00002	$0.04610^{+0.00006}_{-0.00005}$
$\hat{R}_3 _{\text{PMCm}}$	$0.1272^{+0.0062}_{-0.0090}$	$0.0553^{+0.0147}_{-0.0178}$	0.0194	0.0068	$0.2087^{+0.0209}_{-0.0268}$
$\tilde{R}_3 _{\text{PMCm}}$	0.2258	$0.0247^{+0.0001}_{-0.0001}$	-0.0093	-0.0012	$0.2400^{+0.0001}_{-0.0001}$

Table 6.7: The value of each loop term (LO, NLO, N²LO and N³LO) for the four-loop QCD predictions $R_3(Q=31.6 \text{ GeV})$, $\hat{R}_3(M_\tau)$ and $\tilde{R}_3(M_H)$ using the PMCm scale-setting approach. The uncertainties correspond to taking $\mu_r \in [Q/2, 2Q]$ for $R_3(Q=31.6 \text{ GeV})$, $\mu_r \in [1 \text{ GeV}, 2M_\tau]$ for $\hat{R}_3(M_\tau)$ and $\mu_r \in [M_H/2, 2M_H]$ for $\tilde{R}_3(M_H)$.

We present the value of each loop term for the four-loop predictions $R_3(Q=31.6 \text{ GeV})$, $\hat{R}_3(M_\tau)$ and $\tilde{R}_3(M_H)$ using the

PMCm scale-setting approach in Table 6.7.⁸ The relative importance among the LO terms, the NLO terms, the N²LO terms and the N³LO terms for those approximants are

$$1 : +0.0818 : -0.0009 : -0.0005 \quad (\mu_r=Q), \quad (6.12)$$

$$1 : +0.4347 : +0.1525 : +0.0535 \quad (\mu_r=M_\tau), \quad (6.13)$$

$$1 : +0.1094 : -0.0412 : -0.0053 \quad (\mu_r=M_H). \quad (6.14)$$

Table 6.7 shows that there are residual scale dependences of $R_3(Q=31.6 \text{ GeV})$ and $\tilde{R}_3(M_H)$ for the LO and NLO terms that are quite small (e.g. the errors are only about $\pm 0.1\%$ of the LO terms and $\pm 0.04\%$ of the NLO terms, respectively), which are smaller than the corresponding ones under the conventional scale-setting approach. However, the residual scale dependence of $\hat{R}_3(M_\tau)$ is sizable – approximately $\pm 10\%$ – and is comparable to the conventional scale dependence. Here the large residual scale dependence of $\hat{R}_3(M_\tau)$ is reasonable, caused by the poor pQCD convergence for the PMC scales at higher orders and the uncertainties of the α_s -running behavior in the low-energy region.

	$Q_4 = 2Q_3$	$Q_4 = \frac{1}{2}Q_3$	$Q_4 = Q_1$	$Q_4 = Q_2$	$Q_4 = (Q_1 + Q_2 + Q_3)/3$
$R_3 _{\text{PMCm}}$	0.04611	0.04610	0.04608	0.04608	0.04610
$\hat{R}_3 _{\text{PMCm}}$	$0.2054^{+0.0054}_{-0.0036}$	$0.2105^{+0.0088}_{-0.0053}$	$0.2033^{+0.0049}_{-0.0032}$	$0.2041^{+0.0050}_{-0.0033}$	$0.2046^{+0.0051}_{-0.0034}$
$\tilde{R}_3 _{\text{PMCm}}$	0.2404	0.2392	0.2401	0.2398	0.2400

Table 6.8: The four-loop pQCD predictions of $R_3(Q=31.6 \text{ GeV})$, $\hat{R}_3(M_\tau)$ and $\tilde{R}_3(M_H)$ under some other choices of the undetermined Q_4 as an estimate of the *second kind of residual scale dependence* under the PMCm scale-setting approach. The uncertainty for $\hat{R}_3(M_\tau)$ is obtained by changing the MPT-model parameter $\xi = 10 \pm 2$.

As a final remark, we discuss the possible magnitudes of the *second kind of residual scale dependence* under the PMCm scale-setting approach by taking some other typical choices of Q_4 , e.g. $2Q_3$, $Q_3/2$, Q_1 , Q_2 and $(Q_1 + Q_2 + Q_3)/3$, which also ensures the scheme independence of the PMCm series. Table 6.8 shows that the *second kind of residual scale dependence* of R_3 , \hat{R}_3 and \tilde{R}_3 are $(\begin{smallmatrix} +0.00001 \\ -0.00002 \end{smallmatrix})$, $(\begin{smallmatrix} +0.0018 \\ -0.0054 \end{smallmatrix})$ and $(\begin{smallmatrix} +0.0004 \\ -0.0008 \end{smallmatrix})$, respectively. It shows that those choices will change the magnitudes of R_3 , \hat{R}_3 and \tilde{R}_3 at the default choice of $Q_4 = Q_3$ by about $\pm 0.04\%$, $\pm 2.6\%$ and $\pm 0.3\%$, respectively. For $\hat{R}_3(M_\tau)$, another uncertainty caused by the MPT model parameter $\xi = 10 \pm 2$ is $\hat{R}_3|_{\text{PMCm}} = 0.2087^{+0.0072}_{-0.0046}$ in the choice of $Q_4 = Q_3$. We also give the numerical results under some other choices of the undetermined Q_4 in Table 6.8. It shows that the MPT model parameter $\xi = 10 \pm 2$ will lead to $\sim 3\%$ uncertainties. These uncertainties caused by the small scale Q_3 and undetermined scale Q_4 indicate that we still need a more appropriate scale-setting approach to suppress the theoretical uncertainties.

6.4. Properties using the PMCs approach

The PMCs approach provides a method to suppress the residual scale dependence. Applying the standard PMCs scale-setting procedures, we obtain an overall effective α_s and, accordingly, an overall effective scale (Q_*) for $R_n(Q=31.6 \text{ GeV})$, $\hat{R}_n(M_\tau)$ and $\tilde{R}_n(M_H)$, respectively. If they are known up to two-loop, three-loop and four-loop levels, the PMC scale Q_*

⁸By using the RGE recursively, one can obtain correct α_s value and achieve good matching of α_s to its coefficients at the same perturbative order. However, such treatment is a sort of $\{\beta_i\}$ -resummation and the resultant PMC series is no longer the usual fixed-order series. Thus, the function of Table 6.7 is to show its own perturbative behavior.

can be determined up to LL, NLL and N²LL accuracies, respectively. That is, for $n = 1, 2, 3$, we have

$$Q_*|_{e^+e^-} = \{35.36, 39.49, 40.12\} \text{ GeV}, \quad (6.15)$$

$$Q_*|_{\tau} = \{0.90, 1.06, 1.07\} \text{ GeV}, \quad (6.16)$$

$$Q_*|_{H \rightarrow b\bar{b}} = \{60.94, 56.51, 58.80\} \text{ GeV}. \quad (6.17)$$

Their magnitudes become more precise as one includes more loop terms and the difference between the two nearby values becomes smaller and smaller when more loop terms are included, e.g. the N²LL scales only shift by about 2% – 4% to the NLL ones. Since these PMCs scales are numerically sizable, one avoids confronting the possibly small scale problem at certain perturbative orders of the multi-scale-setting approaches, such as PMCm, PMC_∞.

	$n = 1$	$n = 2$	$n = 3$	κ_1	κ_2	κ_3
$R_n _{\text{PMCs}}$	0.04735	0.04629	0.04613	6.9%	2.2%	0.3%
$\hat{R}_n _{\text{PMCs}}$	0.2136	0.1997	0.2064	139.7%	6.5%	3.4%
$\tilde{R}_n _{\text{PMCs}}$	0.2481	0.2424	0.2398	22.0%	2.3%	1.1%

Table 6.9: Results for $R_n(Q=31.6 \text{ GeV})$, $\hat{R}_n(M_\tau)$, $\tilde{R}_n(M_H)$ up to four-loop QCD corrections using the PMCs scale-setting approach, which are independent of any choice of renormalization scale.

	LO	NLO	N ² LO	N ³ LO	Total
$R_3 _{\text{PMCs}}$	0.04287	0.00338	-0.00008	-0.00004	0.04613
$\hat{R}_3 _{\text{PMCs}}$	0.1465	0.0460	0.0108	0.0031	0.2064
$\tilde{R}_3 _{\text{PMCs}}$	0.2278	0.0219	-0.0088	-0.0011	0.2398

Table 6.10: The value of each loop term (LO, NLO, N²LO or N³LO) for the four-loop predictions $R_3(Q=31.6 \text{ GeV})$, $\hat{R}_3(M_\tau)$, $\tilde{R}_3(M_H)$ using the PMCs scale-setting approach.

We present the results of $R_n(Q=31.6 \text{ GeV})$, $\hat{R}_n(M_\tau)$ and $\tilde{R}_n(M_H)$ up to four-loop QCD corrections using the PMCs scale-setting approach in Table 6.9. We also present the value of each loop term for the four-loop approximants $R_3(Q=31.6 \text{ GeV})$, $\hat{R}_3(M_\tau)$ and $\tilde{R}_3(M_H)$ using the PMCs scale-setting approach in Table 6.10. The relative importance among the LO terms, the NLO terms, the N²LO terms and the N³LO terms for those approximants are

$$1 : +0.0788 : -0.0019 : -0.0009, \quad (6.18)$$

$$1 : +0.3140 : +0.0737 : +0.0212, \quad (6.19)$$

$$1 : +0.0961 : -0.0386 : -0.0048. \quad (6.20)$$

These are comparable to the convergent behavior of the PMCm series and are more convergent than conventional predictions. Moreover, the sizable residual scale dependence of $\hat{R}_3(M_\tau)$ appearing in Table 6.7 has been eliminated by using the PMCs procedure. Thus, the PMCs approach, which requires a much simpler analysis, can be adopted as a reliable substitute for the basic PMCm approach to setting the renormalization scales for high-energy processes, with small residual scale dependence. As a conservative estimate of the *first kind of residual scale dependence*, we take the magnitude of its last known term as the unknown N³LL term, e.g. $\pm(|S_2 a_s^2(Q_*)|)$ for $R_3(Q=31.6 \text{ GeV})$, $\hat{R}_3(M_\tau)$ and $\tilde{R}_3(M_H)$. We

then obtain

$$R_3(Q=31.6 \text{ GeV}) = 0.04613 \pm 0.00014, \quad (6.21)$$

$$\hat{R}_3(M_\tau) = 0.2064_{-0.0024}^{+0.0026}, \quad (6.22)$$

$$\tilde{R}_3(M_H) = 0.2398_{-0.0016}^{+0.0014}, \quad (6.23)$$

which show that the *first kind of residual scale dependence* is about $\pm 0.3\%$, $\pm 1.3\%$ and $\pm 0.7\%$.⁹ More explicitly, we show the conservative estimate of the *first kind of residual scale dependence* under the PMCs in Figs. 6.1, (6.2) and (6.3), respectively.

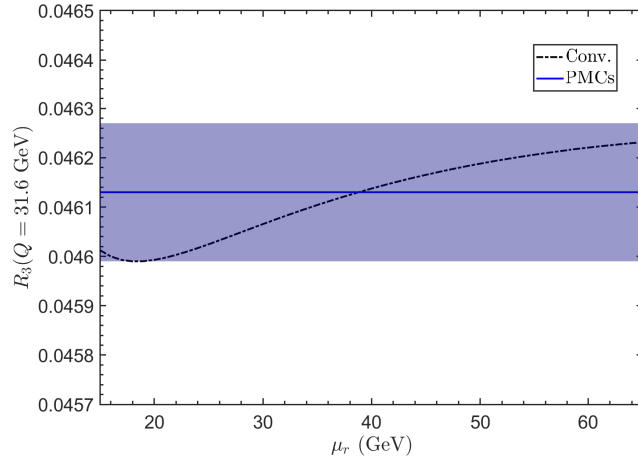


Figure 6.1: The renormalization scale dependence of the four-loop prediction $R_3(Q=31.6 \text{ GeV})$ using the conventional and PMCs scale-setting procedures (from Ref. [62]). The band represents a conservative estimate (6.21) of the *first kind of residual scale dependence* under the PMCs.

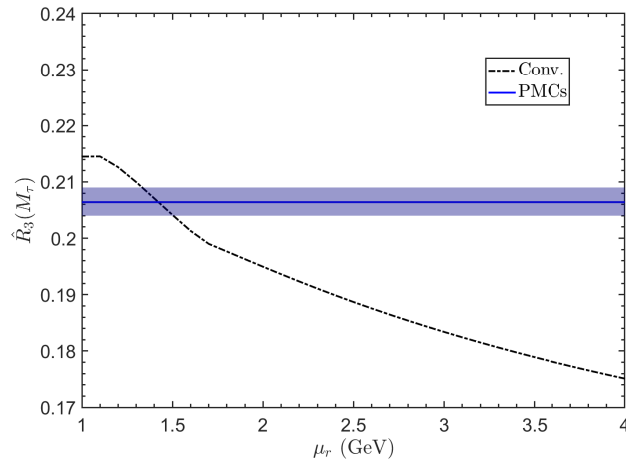


Figure 6.2: The renormalization scale dependence of the four-loop prediction $\hat{R}_3(M_\tau)$ using the conventional and PMCs scale-setting procedures (from Ref. [62]). The band represents a conservative estimate (6.22) of the *first kind of residual scale dependence* under the PMCs.

⁹Since the N²LL accuracy in Q_*^2/Q^2 -series of these pQCD approximants already show good perturbative behavior, it is found that by using the PAA predicted N³LL term, e.g. $\pm |S_2^2/S_1 a_s^3(Q_*)|$, to perform the estimates, one can obtain smaller *first kind of residual scale dependence* than the ones listed in Eqs. (6.21), (6.22), (6.23), which are ± 0.00002 , $\left(\begin{smallmatrix} +0.0002 \\ -0.0003 \end{smallmatrix}\right)$ and $\left(\begin{smallmatrix} +0.0007 \\ -0.0009 \end{smallmatrix}\right)$, respectively.

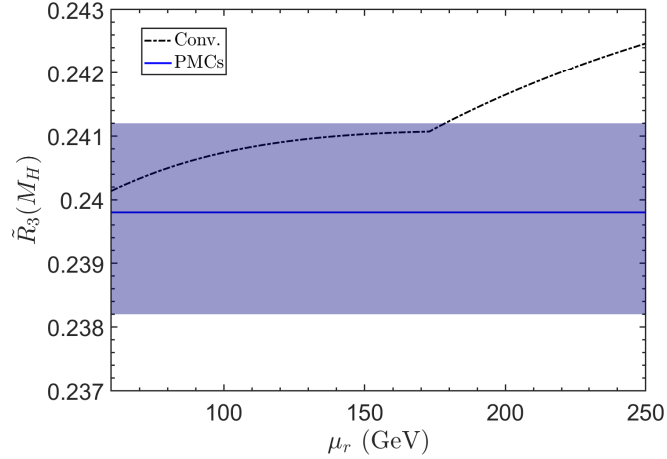


Figure 6.3: The renormalization scale dependence of the four-loop prediction $\tilde{R}_3(M_H)$ using the conventional and PMCs scale-setting procedures (from Ref. [62]). The band represents a conservative estimate (6.23) of the *first kind of residual scale dependence* under the PMCs.

The conformal PMCs series is scheme and scale independent; it thus provides a reliable basis for estimating the effect of unknown higher-order contributions. At present, there is no way to use a series with different effective $\alpha_s(Q_i)$ at different orders; and if there were any, its effectiveness would also be greatly affected by the possibly large residual scale dependence. Thus, we shall not use PMCm, PMC_∞ series to estimate the contribution of the unknown terms. As for the PMCs series, with an overall effective $\alpha_s(Q_*)$, we may directly use the PAA [219].

	$\hat{r}_{4,0}$	$\hat{r}_{5,0}$
$R(Q)$	[0/2]: -2541.35	[0/3]: -181893
$\hat{R}(M_\tau)$	[0/2]: 1245.3	[0/3]: 15088.6
$\tilde{R}(M_H)$	[0/2]: -185951	[0/3]: 3802450

Table 6.11: The preferable $[0/n-1]$ -type PAA predictions of the conformal coefficients $\hat{r}_{4,0}$ and $\hat{r}_{5,0}$ for $R_n(Q=31.6 \text{ GeV})$, $\hat{R}_n(M_\tau)$ and $\tilde{R}_n(M_H)$, respectively.

	N ³ LO	N ⁴ LO
$R_3 _{\text{PMCs}}$	[0/2]: -0.00003	[0/3]: -0.000003
$\hat{R}_3 _{\text{PMCs}}$	[0/2]: +0.0022	[0/3]: +0.0010
$\tilde{R}_3 _{\text{PMCs}}$	[0/2]: -0.0019	[0/3]: +0.0004

Table 6.12: The preferable $[0/n-1]$ -type PAA predictions of the N³LO and N⁴LO terms of $R_3(Q=31.6 \text{ GeV})$, $\hat{R}_3(M_\tau)$ and $\tilde{R}_3(M_H)$ using the PMCs scale-setting approach.

We present the preferable $[0/n-1]$ -type PAA predictions for the PMCs series of $R_3(Q=31.6 \text{ GeV})$, $\hat{R}_3(M_\tau)$ and $\tilde{R}_3(M_H)$ in Table 6.11 and 6.12. Table 6.11 shows the predicted N³LO and N⁴LO conformal coefficients $\hat{r}_{4,0}$ and $\hat{r}_{5,0}$. Note that the predicted $\hat{r}_{4,0}$ values are close to the exact values shown in Table 6.5 and those known conformal coefficients do not change when more loop terms are known. To obtain the final numerical result, we need to combine the coefficients $\hat{r}_{4,0}$ and $\hat{r}_{5,0}$ with the effective $\alpha_s(Q_*)$ at corresponding orders. Table 6.12 displays the numerical results, these values will be

very slightly changed for a more accurate Q_* , since the N²LL accuracy Q_* is already changed from that at NLL by less than $\sim 5\%$.

6.5. Properties using the PMC_∞ approach

Given the unique form of intrinsic conformality iCF, any other attempt (such as PMCa [107]) to write the perturbative expansion in a scale-invariant form would lead to the iCF (as shown in Ref. [62]).

Following the standard PMC_∞ procedures, we calculate $R_n(Q=31.6 \text{ GeV})$, $\hat{R}_n(M_\tau)$ and $\tilde{R}_n(M_H)$ up to four-loop QCD corrections. The perturbative coefficients ($\mathcal{C}_{i=(1,\dots,4),\text{IC}}$) are exactly the same as those of the PMCm and PMCs conformal coefficients ($\hat{r}_{i=(1,\dots,4),0}$). As shown by Eqs. (4.12), (4.14), (4.15), the PMC_∞ scales are definite and have no perturbative nature, they are free of renormalization scale ambiguities and do not have the *first kind of residual scale dependence*. Using the four-loop QCD corrections, we can determine their first three scales, i.e.

$$\{\mu_{\text{I}}, \mu_{\text{II}}, \mu_{\text{III}}\}|_{e^+e^-} = \{35.36, 71.11, 0.003\} \text{ GeV}, \quad (6.24)$$

$$\{\mu_{\text{I}}, \mu_{\text{II}}, \mu_{\text{III}}\}|_{\tau} = \{0.90, 1.16, 1.82\} \text{ GeV}, \quad (6.25)$$

$$\{\mu_{\text{I}}, \mu_{\text{II}}, \mu_{\text{III}}\}|_{H \rightarrow b\bar{b}} = \{60.94, 41.24, 46.44\} \text{ GeV}. \quad (6.26)$$

For the case $R_3(Q=31.6 \text{ GeV})$, its third scale $\mu_{\text{III}} = 0.003 \text{ GeV}$ is quite small and we adopt the above-mentioned MPT model to estimate its contribution, which gives $\alpha_s|_{\text{MPT}}(0.003) = 0.606$. As mentioned in Sec. 4, the fourth scale μ_{IV} is fixed to the initial scale μ_r , i.e. the kinematic scale of the process, and varied in the range $\mu_{\text{IV}} \in [\mu_r/2, 2\mu_r]$ to ascertain the level of conformality achieved by the series. In fact, the last PMC scale is entangled with the missing higher-order contributions. This is referred as *second kind of residual scale dependence*.

	$n = 1$	$n = 2$	$n = 3$	κ_1	κ_2	κ_3
$R_n _{\text{PMC}_\infty}$	0.04750	0.04652	0.03937	7.3%	2.1%	15.4%
$\hat{R}_n _{\text{PMC}_\infty}$	0.1805	0.2112	0.2199	102.6%	17.0%	4.1%
$\tilde{R}_n _{\text{PMC}_\infty}$	0.2438	0.2448	0.2405	19.9%	0.4%	1.8%

Table 6.13: Results for $R_n(Q=31.6 \text{ GeV})$, $\hat{R}_n(M_\tau)$, $\tilde{R}_n(M_H)$ up to four-loop QCD corrections using the PMC_∞ scale-setting approach. For each case, the undetermined PMC_∞ scale of the highest order terms is set as Q , M_τ and M_H , respectively.

	LO	NLO	N ² LO	N ³ LO	Total
$R_3 _{\text{PMC}_\infty}$	0.04383	0.00280	-0.00722	-0.00004 ^{+0.00001} _{-0.00004}	0.03937 ^{+0.00001} _{-0.00004}
$\hat{R}_3 _{\text{PMC}_\infty}$	0.1761	0.0396	0.0035	0.0007 ^{+0.0034} _{-0.0005}	0.2199 ^{+0.0034} _{-0.0005}
$\tilde{R}_3 _{\text{PMC}_\infty}$	0.2265	0.0246	-0.0099	-0.0007 ^{+0.0002} _{-0.0004}	0.2405 ^{+0.0002} _{-0.0004}

Table 6.14: The value of each loop term (LO, NLO, N²LO or N³LO) for the four-loop predictions $R_3(Q=31.6 \text{ GeV})$, $\hat{R}_3(M_\tau)$ and $\tilde{R}_3(M_H)$ using the PMC_∞ scale-setting approach. The errors, representing the *second kind of residual scale dependence*, are estimated by varying the undetermined PMC_∞ scale μ_{IV} within the range $[Q/2, 2Q]$ for $R_3(Q=31.6 \text{ GeV})$, $[1 \text{ GeV}, 2M_\tau]$ for $\hat{R}_3(M_\tau)$ and $[M_H/2, 2M_H]$ for $\tilde{R}_3(M_H)$.

We present the results of $R_n(Q=31.6 \text{ GeV})$, $\hat{R}_n(M_\tau)$ and $\tilde{R}_n(M_H)$ up to four-loop QCD corrections using the PMC_∞ scale-setting approach in Table 6.13. For the cases $R_n(Q=31.6 \text{ GeV})$ and $\tilde{R}_n(M_H)$, we have $\kappa_2 < \kappa_3$, indicating that the *second kind of residual scale dependence* is sizable for these two quantities, which largely affects the magnitude of the

lower-order series. When one has enough higher-order terms, the residual scale dependence is highly suppressed owing to the more convergent renormalon-free series. For example, we present the value of each loop term (LO, NLO, N²LO or N³LO) for the four-loop predictions $R_3(Q=31.6 \text{ GeV})$, $\hat{R}_3(M_\tau)$ and $\tilde{R}_3(M_H)$ in Table 6.14. At the four-loop level, the PMC_∞ series already exhibits convergent behavior. As shown in Table 6.14, the relative importance among the LO terms, the NLO terms, the N²LO terms and the N³LO terms for those approximants are

$$1 : +0.0639 : -0.1647 : -0.0009 \quad (\mu_r=Q), \quad (6.27)$$

$$1 : +0.2249 : +0.0199 : +0.0040 \quad (\mu_r=M_\tau), \quad (6.28)$$

$$1 : +0.1086 : -0.0437 : -0.0031 \quad (\mu_r=M_H). \quad (6.29)$$

This perturbative behavior is similar to the predictions of PMCm and PMCs, except for $R_3(Q=31.6 \text{ GeV})$, which due to a much smaller scale μ_{III} leads to quite large N²LO terms.

6.6. A comparison of the renormalization scale dependence of the various PMC approaches

We present the renormalization scale (μ_r) dependence of the four-loop predictions $R_3(Q=31.6 \text{ GeV})$, $\hat{R}_3(M_\tau)$ and $\tilde{R}_3(M_H)$ using the conventional, PMCm, PMCs and PMC_∞ scale-setting procedures in Figs. 6.4, 6.5 and 6.6, respectively. In these figures, we show the *second kind of residual scale dependence* of $R_3(Q=31.6 \text{ GeV})$, $\hat{R}_3(M_\tau)$ under the PMCm and PMC_∞ scale-setting procedures with the shaded bands. The green/lighter bands are obtained by changing the undetermined Q_4 to $2Q_3$, $Q_3/2$, Q_1 , Q_2 and $(Q_1+Q_2+Q_3)/3$. And the red/darker bands are obtained by varying the undetermined PMC_∞ scale μ_{IV} within the range $[Q/2, 2Q]$ for $R_3(Q=31.6 \text{ GeV})$, $[1 \text{ GeV}, 2M_\tau]$ for $\hat{R}_3(M_\tau)$ and $[M_H/2, 2M_H]$ for $\tilde{R}_3(M_H)$.

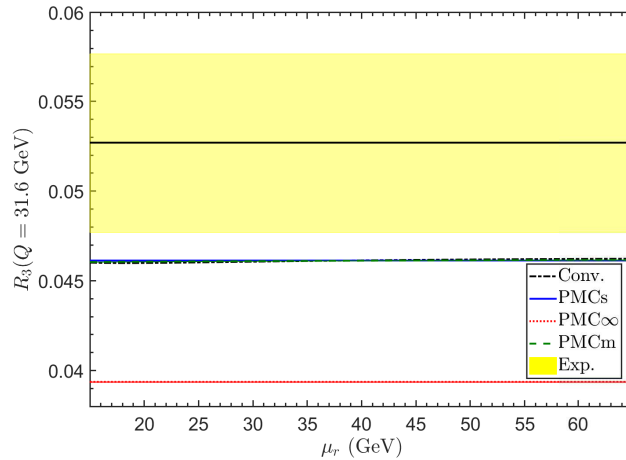


Figure 6.4: The renormalization scale dependence of the four-loop prediction $R_3(Q=31.6 \text{ GeV})$ using the conventional PMCm, PMCs and PMC_∞ scale-setting procedures (from Ref. [62]). The green/lighter band represents the *second kind of residual scale dependence* under the PMCm, which is obtained by changing the undetermined Q_4 to be $2Q_3$, $Q_3/2$, Q_1 , Q_2 and $(Q_1+Q_2+Q_3)/3$, respectively. The red/darker band represents the *second kind of residual scale dependence* under the PMC_∞, which is obtained by varying the undetermined PMC_∞ scale μ_{IV} within the range $[Q/2, 2Q]$. The experimental result $R^{\text{expt}}(Q=31.6 \text{ GeV}) = 0.0527 \pm 0.0050$ is extracted from $\frac{3}{11} R_{e^+e^-}^{\text{expt}} = 1.0527 \pm 0.0050$ [208].

Figure 6.4 shows that the theoretical predictions are smaller than the experimental result. This is reasonable since we have adopted the world average $\alpha_s(M_Z) = 0.1179$ [126] to set Λ_{QCD} for all these observables and, if we adopt a strong coupling $\alpha_s(M_Z)$ fixed by using the e^+e^- annihilation data alone, we obtain consistent predictions in agreement with the

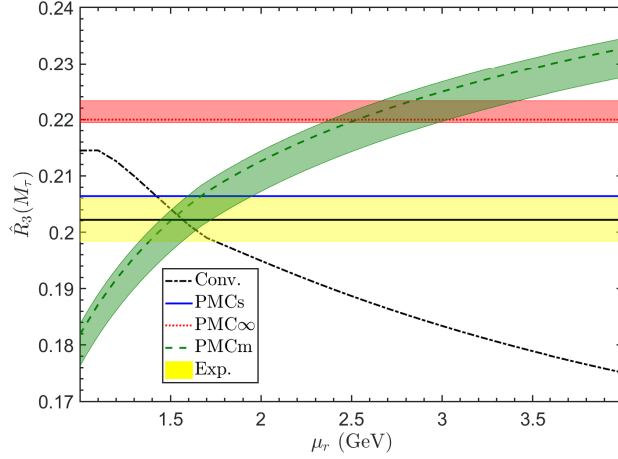


Figure 6.5: The renormalization scale dependence of the four-loop prediction $\hat{R}_3(M_\tau)$ using the conventional, PMCm, PMCs and PMC_∞ scale-setting procedures (from Ref. [62]). The green/lighter band represents the *second kind of residual scale dependence* under the PMCm, which is obtained by changing the undetermined Q_4 to be $2Q_3$, $Q_3/2$, Q_1 , Q_2 and $(Q_1 + Q_2 + Q_3)/3$, respectively. The red/darker band represents the *second kind of residual scale dependence* under the PMC_∞ , which is obtained by varying the undetermined PMC_∞ scale μ_{IV} within the region of $[1 \text{ GeV}, 2M_\tau]$. The experimental result $\hat{R}_3^{\text{expt}}(M_\tau) = 0.2022^{+0.0038}_{-0.0038}$ is extracted from $R_\tau^{\text{expt}}(M_\tau) = 3.475 \pm 0.011$ [220].

data. For example, using $\alpha_s(M_Z) = 0.1224$ [199], fixed by using the hadronic event shapes in e^+e^- annihilation to set Λ_{QCD} , we obtain a larger $R_3(Q=31.6 \text{ GeV})$, e.g. $R_3(Q=31.6 \text{ GeV}) = 0.04826$ for the PMCs approach, which is consistent with $R^{\text{expt}}(Q=31.6 \text{ GeV}) = 0.0527 \pm 0.0050$ within errors. It has been noticed that the *second kind of residual scale dependence* of $R_3(Q=31.6 \text{ GeV})$ under the PMCm and PMC_∞ scale-setting procedure are both very small, since the order α_s^4 correction is highly suppressed in $R_3(Q=31.6 \text{ GeV})$. These figures show that by including enough higher-order terms, the following hold.

- The renormalization scale dependence of the conventional prediction depends strongly on the convergence of the perturbative series and the cancellation of scale dependence among different orders. For a numerically strongly convergent series, such as $R_3(Q=31.6 \text{ GeV})$ and $\tilde{R}_3(M_H)$, the net scale dependence is only parts per thousand for a wide range of scale choices. For a less convergent series, such as $\hat{R}_3(M_\tau)$, the net renormalization scale uncertainty is sizable, which is up to $\sim 18\%$ for $\mu_r \in [1 \text{ GeV}, 2M_\tau]$, $\sim 24\%$ for $\mu_r \in [1 \text{ GeV}, 3M_\tau]$ and $\sim 28\%$ for $\mu_r \in [1 \text{ GeV}, 5M_\tau]$;
- The PMCm predictions have two kinds of residual scale dependence due to unknown terms. The second residual scale dependence can be greatly suppressed by the extra requirement of conformal invariance; the first property then dominates the net residual scale dependence. For numerically convergent series, such as $R_3(Q=31.6 \text{ GeV})$ and $\tilde{R}_3(M_H)$, the residual scale dependences are small, i.e. less than four parts per thousand.¹⁰ For a less convergent series, such as $\hat{R}_3(M_\tau)$, due to the large residual scale dependence of the NLO terms, its net residual scale dependence is sizable, it is $\sim 23\%$ for $\mu_r \in [1 \text{ GeV}, 2M_\tau]$, $\sim 28\%$ for $\mu_r \in [1 \text{ GeV}, 3M_\tau]$ and $\sim 32\%$ for $\mu_r \in [1 \text{ GeV}, 5M_\tau]$. Although in some special cases, such as $\hat{R}_3(M_\tau)$, the residual scale dependence may be comparable to the conventional prediction, the PMCm series has no renormalon divergence and it generally has a better pQCD convergence. For the case of $R_3(Q=31.6 \text{ GeV})$ and $\tilde{R}_3(M_H)$, the PMCm predictions show weaker dependence on μ_r and its prediction

¹⁰As a comparison, the conventional scale dependence of $\tilde{R}_3(M_H)$ is about nine parts per thousand for $\mu_r \in [M_H/2, 2M_H]$

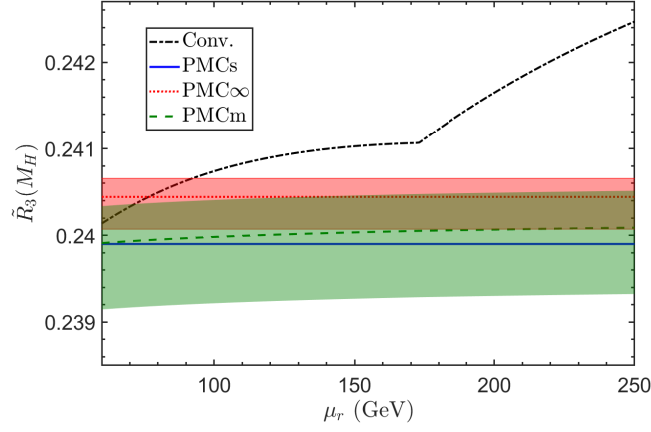


Figure 6.6: The renormalization scale dependence of the four-loop prediction $\tilde{R}_3(M_H)$ using the conventional, PMCm, PMCs and PMC_∞ scale-setting procedures (from Ref. [62]). The green/lighter band represents the *second kind of residual scale dependence* under the PMCm, which is obtained by changing the undetermined Q_4 to be $2Q_3$, $Q_3/2$, Q_1 , Q_2 and $(Q_1 + Q_2 + Q_3)/3$, respectively. The red/darker band represents the *second kind of residual scale dependence* under the PMC_∞ , which is obtained by varying the undetermined PMC_∞ scale μ_{IV} within the region of $[M_H/2, 2M_H]$.

can be more accurate than conventional pQCD predictions;

- The PMC_∞ predictions only have the *second kind of residual scale dependence*, which are suppressed for the present four-loop predictions. The magnitude of the residual scale dependence depends on the convergence of the resultant series and for the present processes, the *second kind of residual scale dependence* are only about parts per thousand to a few percent. Due to the application of “intrinsic conformality” or equivalently the requirement of scale invariance at each order, the PMC_∞ scales determined are not of a perturbative nature, but they can be very small in certain cases. For the case $R_3(Q=31.6 \text{ GeV})$, we obtain a much smaller scale $\mu_{\text{III}} = 0.003 \text{ GeV}$, which is unreasonable and indicates that the PMC_∞ approach may not be applicable for this process. To obtain a numerical estimate, we have adopted the MPT model to calculate the magnitude of α_s at such a small scale; Fig. 6.4 shows that the MPT prediction deviates from other approaches by about 15%. By including the uncertainty from the MPT model parameter $\xi = 10 \pm 2$, the PMC_∞ prediction still deviates from other approaches by about 11%;
- The PMCs predictions for the dependence of observables on the renormalization scale are flat lines. The *first kind of residual scale dependence* of the PMCs predictions only affects the precision of the magnitude of effective α_s and the PMCs predictions are exactly independent of the choice of μ_r , at any fixed order.

7. Summary

The Principle of Maximum Conformality (PMC) provides a rigorous first-principles method to eliminate conventional renormalization scheme and scale ambiguities for high-momentum-transfer processes. Its predictions have a solid theoretical foundation, satisfying renormalization group invariance and all other self-consistency conditions derived from the renormalization group. The PMC has now been successfully applied to many high-energy processes.

In this review, we have presented a new scale-setting procedure, namely PMC_∞ , which stems from the general PMC and preserves a particular property that we have defined as *intrinsic conformality* (iCF). The iCF is a particular parametrization of the perturbative series that exactly preserves the scale invariance of an observable perturbatively. We point out that this is a unique property of the perturbative expansion, any other attempt (such as PMCa [107]) to write the perturbative expansion in a scale-invariant form would lead to the iCF (as shown in Ref. [62]).

The PMC_∞ solves the conventional renormalization scale ambiguity in QCD, it preserves not only the iCF but also all the features of the PMC approach and leads to a final conformal series at any order of the perturbative calculation. In fact, the final series is given by perturbative conformal coefficients with the couplings determined at conformal renormalization scales. The PMC_∞ scale setting agrees with the Gell-Man–Low scheme and can be considered the non-Abelian analog of Serber–Uehling [221, 222] scale setting, which is essential in precision tests of QED and atomic physics.

Given the iCF form, a new “How-To” method for identifying conformal coefficients and scale has been developed and can be applied to either numerical or analytical calculations. The PMC_∞ has been applied to the NNLO thrust and C -parameter distributions and the results show perfect agreement with the experimental data.

The evaluation of theoretical errors using standard criteria demonstrate that the PMC_∞ significantly improves the theoretical predictions over the entire spectra of the shape variables order-by-order and both the IR conformal and QED limits of thrust respect the theoretical consistency requirements. Moreover, the position of the thrust peak is in perfect agreement with experiment and is preserved on varying N_f . Hence, even though for the thrust distribution the peak stems directly from resummation (or partial resummation) of the large logarithms in the low-momentum region, its correct position is fixed by the PMC scale and can be considered a “conformal” property, given its independence from the N_f or β_i terms.

Unlike the previous BLM/PMC approaches, the PMC_∞ scales are not perturbatively calculated but are conformal functions of the physical scale(s) of the process and any other unintegrated momentum or variable, e.g. the event-shape variable $(1 - T)$ or C . The PMC_∞ is totally independent of the initial scale μ_0 used for renormalization in perturbative calculations and it preserves the scale invariance at all stages of calculation, independently of the kinematic boundary conditions, of the starting order of the observable or of the order of the truncated expansion. Moreover, this property leads to the possibility of determining the entire coupling from a single experiment at a single center-of-mass energy (this new method is in progress and will soon appear.)

The iCF improves the general BLM/PMC procedure and point “3” of Section 3. In the same section, we suggested that an improvement and simplification of the perturbatively calculated BLM/PMC scales, would be achieved by setting the renormalization scale μ_r directly to the physical scale Q of the process, before applying the BLM/PMC procedure. This would remove the initial scale μ_0 dependence from the perturbatively calculated BLM/PMC scales.

We stress that, in contrast with the other PMCM and PMCs approaches, the PMC_∞ preserves the iCF; scales are thus set straightforwardly in kinematic regions where constraints cancel the effects of the lower-order conformal coefficients. These effects are particularly visible in the case of event-shape variables in the multi-jet region. For this case we have

shown only fixed-order calculation results and other effects due to factorization, such as large logarithms coming from soft and collinear configurations, have not been included. The iCF effects in these kinematic regions are neglected by the PMCm and PMCs approach, unless an *ad hoc* prescription is introduced.

Another application of the PMC_∞ is presented in Ref. [72] and shows an improvement of the results on $\Gamma(H \rightarrow gg)$ with respect to the CSS also in this process. From the detailed comparison shown in Sec. 6, it follows that, though the application of the PMC_∞ improves the theoretical predictions also for the $R_{e^+e^-}$, R_τ , $\Gamma(H \rightarrow b\bar{b})$ with respect to the CSS, the PMCs leads to more stable results for these quantities.

In general:

- The PMCs approach determines an overall effective α_s by eliminating all the RG-dependent nonconformal $\{\beta_i\}$ -terms; this results in a single effective scale which effectively replaces the individual PMC scales of PMCm approach in the sense of a mean-value theorem. The PMCs prediction is renormalization scale-and-scheme independent up to any fixed order. The *first kind of residual scale dependence* is highly suppressed, since the PMC scale at all known orders is determined at the same highest-order accuracy. There is no *second kind of residual scale dependence*. The PMCs prediction also avoids the small-scale problem, which sometimes emerges in multi-scale approaches.
- The PMC_∞ approach fixes the PMC scales at each order by using the property of intrinsic conformality, which ensures scale invariance of the pQCD series at each order. The resulting PMC scales have no ambiguities, are not of a perturbative nature and thus avoid the *first kind of residual scale dependence*. Since the last effective scale of the highest-order perturbative term is set to the kinematic scale or physical scale of the process, the PMC_∞ prediction still has a reduced *second kind of residual scale dependence*. However, when more loop terms are included and scales are not in the nonperturbative regime, all PMC's lead to similar results.

The PMCs approach is close to the PMCm approach in achieving the goals of the PMC by inheriting most of the features of the PMCm approach. It works remarkably well with fully integrated quantities, but has some difficulties in application to differential distributions, besides the fact that this approach may have an effect of averaging the differences of the PMC_∞ scales arising at each order, which might be significant to achieve a given precision at a certain level of accuracy. However, given the small differences that we have found in the first two consecutive PMC_∞ scales for thrust and C -parameter, i.e. μ_I, μ_{II} , in the LO allowed kinematic region, i.e. $0 < (1 - T) < 1/3$ and in $0 < C < 0.75$, we may argue that in the same accessible kinematic domain two consecutive PMC_∞ scales have such small differences that a single-scale approach, such as the PMCs, would be justified, leading to analogously precise predictions.

We recall that only the n_f terms related to the UV-divergent diagrams (i.e. the N_f terms) must be reabsorbed into the PMC_∞ scales. Thus, PMC_∞ perfectly agrees with the PMCm when an observable has a manifestly iCF form. We remark that the iCF underlies scale invariance perturbatively, i.e. the ordered scale invariance. We also remark that PMC_∞ agrees with the single-scale approach PMCs in the case of an observable with a particular iCF form with all scales equal, i.e. $\mu_I = \mu_{II} = \mu_{III} = \dots = \mu_N$. In this sense, the PMCm and PMCs may be considered more as “optimization procedures” that follow the purpose of the maximal conformal series by transforming the original perturbative series into an iCF-like final series by using the PMC scales. In contrast, the PMC_∞ does not indicate any particular value of the renormalization scale to be used, but indicates the final limit obtained by each conformal subset and then by the perturbative expansion, once all the terms related to each conformal subset are resummed.

The PMC_∞ is RG invariant at each order of accuracy, which means we may perform a change of scale at any stage and reobtain the initial perturbative quantity. In this sense PMC_∞ is not to be understood as an “optimization procedure”,

but as an explicit RG-invariant form to parametrize a perturbative quantity that leads to the conformal limit faster. By setting the renormalization scale of each subset to the corresponding PMC_∞ scale, one simply cancels the infinite series of β terms, leading to the same conformal result as the original series. Given that both scales and coefficients are conformal in the PMC_∞ , the scheme and scale dependence is also completely removed in the perturbative series up to infinity.

It was pointed out in Sec. 6 that the PMC_∞ scale might become quite small at a certain order for the case of fully integrated quantities, whose calculations were carried out using the analyticity property of the Adler function (this seems not to occur in direct multi-loop calculations, e.g. for the shape variables); and that the PMC_∞ retains the second kind of scale dependence. We stress that the last scale in the PMC_∞ controls the level of convergence and the conformality of the perturbative series and is thus entangled with the theoretical error of a given prediction. According to the PMC_∞ procedure the last scale must be set to the invariant physical scale of the process, given by \sqrt{s}, M_H, \dots . In this review we have shown that the usual PMC practice of setting the last scale equal to the last unknown scale is also consistent for the PMC_∞ and leads to precise and stable results. Improvements to these points are currently under investigation.

We finally remark that the evaluation of the theoretical errors using standard criteria shows that the PMC_∞ significantly improves the precision of pQCD calculations and eliminates the scheme and scale ambiguities. An improved and more reliable analysis of theoretical errors might be obtained by using a statistical approach for evaluating the contributions of the uncalculated higher-order terms, as suggested in Refs. [214–216] and recently applied with the PMCs in Refs. [81, 217]. This implementation would lead to a more rigorous method to evaluate errors, also giving indications on the possible range of values for the last unknown PMC_∞ scale.

Acknowledgements

We thank Francesco Sannino, André Hoang for useful discussions. XGW is supported in part by the Natural Science Foundation of China under Grant No.12175025 and No.12147102. SQW is supported in part by the Natural Science Foundation of China under Grant No.12265011. SJB is supported in part by the Department of Energy Contract No. DE-AC02-76SF00515. SLAC-PUB-17737.

References

- [1] E. C. G. Stueckelberg de Breidenbach, A. Petermann, Normalization of constants in the quanta theory, *Helv. Phys. Acta* 26 (1953) 499–520. [doi:10.5169/seals-112426](https://doi.org/10.5169/seals-112426).
- [2] M. Gell-Mann, F. E. Low, Quantum electrodynamics at small distances, *Phys. Rev.* 95 (1954) 1300–1312. [doi:10.1103/PhysRev.95.1300](https://doi.org/10.1103/PhysRev.95.1300).
- [3] A. Peterman, Renormalization Group and the Deep Structure of the Proton, *Phys. Rept.* 53 (1979) 157. [doi:10.1016/0370-1573\(79\)90014-0](https://doi.org/10.1016/0370-1573(79)90014-0).
- [4] C. G. Callan, Jr., Broken scale invariance in scalar field theory, *Phys. Rev. D* 2 (1970) 1541–1547. [doi:10.1103/PhysRevD.2.1541](https://doi.org/10.1103/PhysRevD.2.1541).
- [5] K. Symanzik, Small distance behavior analysis and Wilson expansion, *Commun. Math. Phys.* 23 (1971) 49–86. [doi:10.1007/BF01877596](https://doi.org/10.1007/BF01877596).

- [6] W. Celmaster, R. J. Gonsalves, The Renormalization Prescription Dependence of the QCD Coupling Constant, *Phys. Rev. D* 20 (1979) 1420. doi:[10.1103/PhysRevD.20.1420](https://doi.org/10.1103/PhysRevD.20.1420).
- [7] A. J. Buras, Asymptotic Freedom in Deep Inelastic Processes in the Leading Order and Beyond, *Rev. Mod. Phys.* 52 (1980) 199. doi:[10.1103/RevModPhys.52.199](https://doi.org/10.1103/RevModPhys.52.199).
- [8] P. M. Stevenson, Resolution of the Renormalization Scheme Ambiguity in Perturbative QCD, *Phys. Lett. B* 100 (1981) 61–64. doi:[10.1016/0370-2693\(81\)90287-2](https://doi.org/10.1016/0370-2693(81)90287-2).
- [9] P. M. Stevenson, Optimized Perturbation Theory, *Phys. Rev. D* 23 (1981) 2916. doi:[10.1103/PhysRevD.23.2916](https://doi.org/10.1103/PhysRevD.23.2916).
- [10] P. M. Stevenson, Optimization and the Ultimate Convergence of QCD Perturbation Theory, *Nucl. Phys. B* 231 (1984) 65–90. doi:[10.1016/0550-3213\(84\)90307-9](https://doi.org/10.1016/0550-3213(84)90307-9).
- [11] P. Stevenson, Sense and Nonsense in the Renormalization Scheme Dependence Problem, *Nucl. Phys. B* 203 (1982) 472–492. doi:[10.1016/0550-3213\(82\)90325-X](https://doi.org/10.1016/0550-3213(82)90325-X).
- [12] G. Grunberg, Renormalization Group Improved Perturbative QCD, *Phys. Lett. B* 95 (1980) 70, [Erratum: *Phys.Lett.B* 110, 501 (1982)]. doi:[10.1016/0370-2693\(80\)90402-5](https://doi.org/10.1016/0370-2693(80)90402-5).
- [13] G. Grunberg, Renormalization Scheme Independent QCD and QED: The Method of Effective Charges, *Phys. Rev. D* 29 (1984) 2315–2338. doi:[10.1103/PhysRevD.29.2315](https://doi.org/10.1103/PhysRevD.29.2315).
- [14] G. Grunberg, On Some Ambiguities in the Method of Effective Charges, *Phys. Rev. D* 40 (1989) 680. doi:[10.1103/PhysRevD.40.680](https://doi.org/10.1103/PhysRevD.40.680).
- [15] S. J. Brodsky, G. P. Lepage, P. B. Mackenzie, On the Elimination of Scale Ambiguities in Perturbative Quantum Chromodynamics, *Phys. Rev. D* 28 (1983) 228. doi:[10.1103/PhysRevD.28.228](https://doi.org/10.1103/PhysRevD.28.228).
- [16] F. Chishtie, D. G. C. McKeon, T. N. Sherry, Renormalization Scheme Dependence in a QCD Cross Section, *Phys. Rev. D* 94 (5) (2016) 054031. arXiv:[1512.08173](https://arxiv.org/abs/1512.08173), doi:[10.1103/PhysRevD.94.054031](https://doi.org/10.1103/PhysRevD.94.054031).
- [17] F. A. Chishtie, D. G. C. McKeon, Renormalization Scheme Dependence and the Renormalization Group Beta Function, *Phys. Rev. D* 95 (11) (2017) 116013. arXiv:[1612.01455](https://arxiv.org/abs/1612.01455), doi:[10.1103/PhysRevD.95.116013](https://doi.org/10.1103/PhysRevD.95.116013).
- [18] L. F. Abbott, Choosing an Expansion Parameter for QCD, *Phys. Rev. Lett.* 44 (1980) 1569. doi:[10.1103/PhysRevLett.44.1569](https://doi.org/10.1103/PhysRevLett.44.1569).
- [19] C. Anastasiou, C. Duhr, F. Dulat, E. Furlan, T. Gehrmann, F. Herzog, A. Lazopoulos, B. Mistlberger, High precision determination of the gluon fusion Higgs boson cross-section at the LHC, *JHEP* 05 (2016) 058. arXiv:[1602.00695](https://arxiv.org/abs/1602.00695), doi:[10.1007/JHEP05\(2016\)058](https://doi.org/10.1007/JHEP05(2016)058).
- [20] S. Catani, S. Devoto, M. Grazzini, S. Kallweit, J. Mazzitelli, Bottom-quark production at hadron colliders: fully differential predictions in NNLO QCD, *JHEP* 03 (2021) 029. arXiv:[2010.11906](https://arxiv.org/abs/2010.11906), doi:[10.1007/JHEP03\(2021\)029](https://doi.org/10.1007/JHEP03(2021)029).
- [21] D. J. Gross, A. Neveu, Dynamical Symmetry Breaking in Asymptotically Free Field Theories, *Phys. Rev. D* 10 (1974) 3235. doi:[10.1103/PhysRevD.10.3235](https://doi.org/10.1103/PhysRevD.10.3235).

- [22] B. E. Lautrup, On High Order Estimates in QED, Phys. Lett. B 69 (1977) 109–111. [doi:10.1016/0370-2693\(77\)90145-9](https://doi.org/10.1016/0370-2693(77)90145-9).
- [23] M. Beneke, Renormalons, Phys. Rept. 317 (1999) 1–142. [arXiv:hep-ph/9807443](https://arxiv.org/abs/hep-ph/9807443), [doi:10.1016/S0370-1573\(98\)00130-6](https://doi.org/10.1016/S0370-1573(98)00130-6).
- [24] C. F. Berger, Z. Bern, L. J. Dixon, F. Febres Cordero, D. Forde, T. Gleisberg, H. Ita, D. A. Kosower, D. Maitre, Next-to-Leading Order QCD Predictions for W+3-Jet Distributions at Hadron Colliders, Phys. Rev. D 80 (2009) 074036. [arXiv:0907.1984](https://arxiv.org/abs/0907.1984), [doi:10.1103/PhysRevD.80.074036](https://doi.org/10.1103/PhysRevD.80.074036).
- [25] S. Catani, G. Turnock, B. R. Webber, L. Trentadue, Thrust distribution in $e^+ e^-$ annihilation, Phys. Lett. B 263 (1991) 491–497. [doi:10.1016/0370-2693\(91\)90494-B](https://doi.org/10.1016/0370-2693(91)90494-B).
- [26] S. Catani, L. Trentadue, G. Turnock, B. R. Webber, Resummation of large logarithms in $e^+ e^-$ event shape distributions, Nucl. Phys. B 407 (1993) 3–42. [doi:10.1016/0550-3213\(93\)90271-P](https://doi.org/10.1016/0550-3213(93)90271-P).
- [27] S. Catani, M. L. Mangano, P. Nason, L. Trentadue, The Resummation of soft gluons in hadronic collisions, Nucl. Phys. B 478 (1996) 273–310. [arXiv:hep-ph/9604351](https://arxiv.org/abs/hep-ph/9604351), [doi:10.1016/0550-3213\(96\)00399-9](https://doi.org/10.1016/0550-3213(96)00399-9).
- [28] U. Aglietti, L. Di Giustino, G. Ferrera, L. Trentadue, Resummed Mass Distribution for Jets Initiated by Massive Quarks, Phys. Lett. B 651 (2007) 275–292. [arXiv:hep-ph/0612073](https://arxiv.org/abs/hep-ph/0612073), [doi:10.1016/j.physletb.2007.06.034](https://doi.org/10.1016/j.physletb.2007.06.034).
- [29] L. Di Giustino, G. Ricciardi, L. Trentadue, Minimal prescription corrected spectra in heavy quark decays, Phys. Rev. D 84 (2011) 034017. [arXiv:1102.0331](https://arxiv.org/abs/1102.0331), [doi:10.1103/PhysRevD.84.034017](https://doi.org/10.1103/PhysRevD.84.034017).
- [30] A. Banfi, H. McAslan, P. F. Monni, G. Zanderighi, A general method for the resummation of event-shape distributions in $e^+ e^-$ annihilation, JHEP 05 (2015) 102. [arXiv:1412.2126](https://arxiv.org/abs/1412.2126), [doi:10.1007/JHEP05\(2015\)102](https://doi.org/10.1007/JHEP05(2015)102).
- [31] R. Abbate, M. Fickinger, A. H. Hoang, V. Mateu, I. W. Stewart, Thrust at N^3LL with Power Corrections and a Precision Global Fit for $\alpha_s(m_Z)$, Phys. Rev. D 83 (2011) 074021. [arXiv:1006.3080](https://arxiv.org/abs/1006.3080), [doi:10.1103/PhysRevD.83.074021](https://doi.org/10.1103/PhysRevD.83.074021).
- [32] S. J. Brodsky, P. Huet, Aspects of $SU(N(c))$ gauge theories in the limit of small number of colors, Phys. Lett. B 417 (1998) 145–153. [arXiv:hep-ph/9707543](https://arxiv.org/abs/hep-ph/9707543), [doi:10.1016/S0370-2693\(97\)01209-4](https://doi.org/10.1016/S0370-2693(97)01209-4).
- [33] A. L. Kataev, Riemann $\zeta(3)$ - terms in perturbative QED series, conformal symmetry and the analogies with structures of multiloop effects in $N=4$ supersymmetric Yang-Mills theory, Phys. Lett. B 691 (2010) 82–86. [arXiv:1005.2058](https://arxiv.org/abs/1005.2058), [doi:10.1016/j.physletb.2010.06.005](https://doi.org/10.1016/j.physletb.2010.06.005).
- [34] A. De Rújula, H. Georgi, H. David Politzer, Demythification of electroproduction local duality and precocious scaling, Annals of Physics 103 (2) (1977) 315–353. [doi:https://doi.org/10.1016/S0003-4916\(97\)90003-8](https://doi.org/10.1016/S0003-4916(97)90003-8).
URL <https://www.sciencedirect.com/science/article/pii/S0003491697900038>
- [35] W. A. Bardeen, A. J. Buras, D. W. Duke, T. Muta, Deep Inelastic Scattering Beyond the Leading Order in Asymptotically Free Gauge Theories, Phys. Rev. D 18 (1978) 3998. [doi:10.1103/PhysRevD.18.3998](https://doi.org/10.1103/PhysRevD.18.3998).
- [36] W. Celmaster, R. J. Gonsalves, QCD Perturbation Expansions in a Coupling Constant Renormalized by Momentum Space Subtraction, Phys. Rev. Lett. 42 (1979) 1435. [doi:10.1103/PhysRevLett.42.1435](https://doi.org/10.1103/PhysRevLett.42.1435).

- [37] G. 't Hooft, M. J. G. Veltman, Regularization and Renormalization of Gauge Fields, Nucl. Phys. B 44 (1972) 189–213. [doi:10.1016/0550-3213\(72\)90279-9](https://doi.org/10.1016/0550-3213(72)90279-9).
- [38] J. Zeng, X.-G. Wu, X.-C. Zheng, J.-M. Shen, Gauge dependence of the perturbative QCD predictions under the momentum space subtraction scheme, Chin. Phys. C 44 (11) (2020) 113102. [arXiv:2004.12068](https://arxiv.org/abs/2004.12068), [doi:10.1088/1674-1137/abae4e](https://doi.org/10.1088/1674-1137/abae4e).
- [39] S. J. Brodsky, X.-G. Wu, Self-Consistency Requirements of the Renormalization Group for Setting the Renormalization Scale, Phys. Rev. D 86 (2012) 054018. [arXiv:1208.0700](https://arxiv.org/abs/1208.0700), [doi:10.1103/PhysRevD.86.054018](https://doi.org/10.1103/PhysRevD.86.054018).
- [40] X.-G. Wu, S. J. Brodsky, M. Mojaza, The Renormalization Scale-Setting Problem in QCD, Prog. Part. Nucl. Phys. 72 (2013) 44–98. [arXiv:1302.0599](https://arxiv.org/abs/1302.0599), [doi:10.1016/j.pnpnp.2013.06.001](https://doi.org/10.1016/j.pnpnp.2013.06.001).
- [41] A. Dhar, V. Gupta, A New Perturbative Approach to Renormalizable Field Theories, Phys. Rev. D 29 (1984) 2822. [doi:10.1103/PhysRevD.29.2822](https://doi.org/10.1103/PhysRevD.29.2822).
- [42] V. Gupta, D. V. Shirkov, O. V. Tarasov, New perturbative approach to general renormalizable quantum field theories, Int. J. Mod. Phys. A 6 (1991) 3381–3397. [doi:10.1142/S0217751X91001647](https://doi.org/10.1142/S0217751X91001647).
- [43] A. Deur, S. J. Brodsky, G. F. de Teramond, The QCD Running Coupling, Nucl. Phys. 90 (2016) 1. [arXiv:1604.08082](https://arxiv.org/abs/1604.08082), [doi:10.1016/j.pnpnp.2016.04.003](https://doi.org/10.1016/j.pnpnp.2016.04.003).
- [44] G. Kramer, B. Lampe, Jet production rates at LEP and the scale of alpha-s, Z. Phys. A 339 (1991) 189–193. [doi:10.1007/BF01282948](https://doi.org/10.1007/BF01282948).
- [45] S. J. Brodsky, L. Di Giustino, Setting the Renormalization Scale in QCD: The Principle of Maximum Conformality, Phys. Rev. D 86 (2012) 085026. [arXiv:1107.0338](https://arxiv.org/abs/1107.0338), [doi:10.1103/PhysRevD.86.085026](https://doi.org/10.1103/PhysRevD.86.085026).
- [46] S. J. Brodsky, X.-G. Wu, Scale Setting Using the Extended Renormalization Group and the Principle of Maximum Conformality: the QCD Coupling Constant at Four Loops, Phys. Rev. D 85 (2012) 034038, [Erratum: Phys.Rev.D 86, 079903 (2012)]. [arXiv:1111.6175](https://arxiv.org/abs/1111.6175), [doi:10.1103/PhysRevD.85.034038](https://doi.org/10.1103/PhysRevD.85.034038).
- [47] S. J. Brodsky, X.-G. Wu, Eliminating the Renormalization Scale Ambiguity for Top-Pair Production Using the Principle of Maximum Conformality, Phys. Rev. Lett. 109 (2012) 042002. [arXiv:1203.5312](https://arxiv.org/abs/1203.5312), [doi:10.1103/PhysRevLett.109.042002](https://doi.org/10.1103/PhysRevLett.109.042002).
- [48] L. Di Giustino, The Renormalization Scale Setting Problem in QCD [Ph.D. Thesis], Ph.D. thesis, Insubria U., Como (2022). [arXiv:2205.03689](https://arxiv.org/abs/2205.03689).
- [49] M. Mojaza, S. J. Brodsky, X.-G. Wu, Systematic All-Orders Method to Eliminate Renormalization-Scale and Scheme Ambiguities in Perturbative QCD, Phys. Rev. Lett. 110 (2013) 192001. [arXiv:1212.0049](https://arxiv.org/abs/1212.0049), [doi:10.1103/PhysRevLett.110.192001](https://doi.org/10.1103/PhysRevLett.110.192001).
- [50] S. J. Brodsky, M. Mojaza, X.-G. Wu, Systematic Scale-Setting to All Orders: The Principle of Maximum Conformality and Commensurate Scale Relations, Phys. Rev. D 89 (2014) 014027. [arXiv:1304.4631](https://arxiv.org/abs/1304.4631), [doi:10.1103/PhysRevD.89.014027](https://doi.org/10.1103/PhysRevD.89.014027).

- [51] X.-G. Wu, Y. Ma, S.-Q. Wang, H.-B. Fu, H.-H. Ma, S. J. Brodsky, M. Mojaza, Renormalization Group Invariance and Optimal QCD Renormalization Scale-Setting, Rept. Prog. Phys. 78 (2015) 126201. [arXiv:1405.3196](#), [doi:10.1088/0034-4885/78/12/126201](#).
- [52] X.-G. Wu, J.-M. Shen, B.-L. Du, X.-D. Huang, S.-Q. Wang, S. J. Brodsky, The QCD renormalization group equation and the elimination of fixed-order scheme-and-scale ambiguities using the principle of maximum conformality, Prog. Part. Nucl. Phys. 108 (2019) 103706. [arXiv:1903.12177](#), [doi:10.1016/j.pnpnp.2019.05.003](#).
- [53] R. Shrock, Study of Scheme Transformations to Remove Higher-Loop Terms in the β Function of a Gauge Theory, Phys. Rev. D 88 (2013) 036003. [arXiv:1305.6524](#), [doi:10.1103/PhysRevD.88.036003](#).
- [54] R. Shrock, Generalized Scheme Transformations for the Elimination of Higher-Loop Terms in the Beta Function of a Gauge Theory, Phys. Rev. D 90 (2014) 045011. [arXiv:1405.6244](#), [doi:10.1103/PhysRevD.90.045011](#).
- [55] T. A. Ryttov, R. Shrock, Scheme Transformations in the Vicinity of an Infrared Fixed Point, Phys. Rev. D 86 (2012) 065032. [arXiv:1206.2366](#), [doi:10.1103/PhysRevD.86.065032](#).
- [56] T. A. Ryttov, R. Shrock, An Analysis of Scheme Transformations in the Vicinity of an Infrared Fixed Point, Phys. Rev. D 86 (2012) 085005. [arXiv:1206.6895](#), [doi:10.1103/PhysRevD.86.085005](#).
- [57] P. M. Stevenson, ‘Maximal conformality’ is nonsense (8 2023). [arXiv:2308.05072](#).
- [58] X.-G. Wu, J.-M. Shen, B.-L. Du, S. J. Brodsky, Novel demonstration of the renormalization group invariance of the fixed-order predictions using the principle of maximum conformality and the C -scheme coupling, Phys. Rev. D 97 (9) (2018) 094030. [arXiv:1802.09154](#), [doi:10.1103/PhysRevD.97.094030](#).
- [59] Y. Ma, X.-G. Wu, H.-H. Ma, H.-Y. Han, General Properties on Applying the Principle of Minimum Sensitivity to High-order Perturbative QCD Predictions, Phys. Rev. D 91 (3) (2015) 034006. [arXiv:1412.8514](#), [doi:10.1103/PhysRevD.91.034006](#).
- [60] Y. Ma, X.-G. Wu, Renormalization scheme dependence of high-order perturbative QCD predictions, Phys. Rev. D 97 (3) (2018) 036024. [arXiv:1707.09886](#), [doi:10.1103/PhysRevD.97.036024](#).
- [61] L. Di Giustino, S. J. Brodsky, P. G. Ratcliffe, X.-G. Wu, S.-Q. Wang, High precision tests of QCD without scale or scheme ambiguities (7 2023). [arXiv:2307.03951](#).
- [62] X.-D. Huang, J. Yan, H.-H. Ma, L. Di Giustino, J.-M. Shen, X.-G. Wu, S. J. Brodsky, Detailed comparison of renormalization scale-setting procedures based on the principle of maximum conformality, Nucl. Phys. B 989 (2023) 116150. [arXiv:2109.12356](#), [doi:10.1016/j.nuclphysb.2023.116150](#).
- [63] S.-Q. Wang, S. J. Brodsky, X.-G. Wu, L. Di Giustino, J.-M. Shen, Renormalization scale setting for heavy quark pair production in e^+e^- annihilation near the threshold region, Phys. Rev. D 102 (1) (2020) 014005. [arXiv:2002.10993](#), [doi:10.1103/PhysRevD.102.014005](#).
- [64] A. Deur, S. J. Brodsky, C. D. Roberts, QCD Running Couplings and Effective Charges (3 2023). [arXiv:2303.00723](#).

- [65] A. Deur, J.-M. Shen, X.-G. Wu, S. J. Brodsky, G. F. de Teramond, Implications of the Principle of Maximum Conformality for the QCD Strong Coupling, *Phys. Lett. B* 773 (2017) 98. [arXiv:1705.02384](#), [doi:10.1016/j.physletb.2017.07.024](#).
- [66] S.-Q. Wang, X.-G. Wu, S. J. Brodsky, M. Mojaza, Application of the Principle of Maximum Conformality to the Hadroproduction of the Higgs Boson at the LHC, *Phys. Rev. D* 94 (5) (2016) 053003. [arXiv:1605.02572](#), [doi:10.1103/PhysRevD.94.053003](#).
- [67] S.-Q. Wang, X.-G. Wu, X.-C. Zheng, G. Chen, J.-M. Shen, An analysis of $H \rightarrow \gamma\gamma$ up to three-loop QCD corrections, *J. Phys. G* 41 (2014) 075010. [arXiv:1311.5106](#), [doi:10.1088/0954-3899/41/7/075010](#).
- [68] Q. Yu, X.-G. Wu, S.-Q. Wang, X.-D. Huang, J.-M. Shen, J. Zeng, Properties of the decay $H \rightarrow \gamma\gamma$ using the approximate α_s^4 corrections and the principle of maximum conformality, *Chin. Phys. C* 43 (9) (2019) 093102. [arXiv:1811.09179](#), [doi:10.1088/1674-1137/43/9/093102](#).
- [69] S.-Q. Wang, X.-G. Wu, X.-C. Zheng, J.-M. Shen, Q.-L. Zhang, The Higgs boson inclusive decay channels $H \rightarrow b\bar{b}$ and $H \rightarrow gg$ up to four-loop level, *Eur. Phys. J. C* 74 (4) (2014) 2825. [arXiv:1308.6364](#), [doi:10.1140/epjc/s10052-014-2825-3](#).
- [70] D.-M. Zeng, S.-Q. Wang, X.-G. Wu, J.-M. Shen, The Higgs-boson decay $H \rightarrow gg$ up to α_s^5 -order under the minimal momentum space subtraction scheme, *J. Phys. G* 43 (7) (2016) 075001. [arXiv:1507.03222](#), [doi:10.1088/0954-3899/43/7/075001](#).
- [71] J. Zeng, X.-G. Wu, S. Bu, J.-M. Shen, S.-Q. Wang, Reanalysis of the Higgs-boson decay $H \rightarrow gg$ up to α_s^6 -order level using the principle of maximum conformality, *J. Phys. G* 45 (8) (2018) 085004. [arXiv:1801.01414](#), [doi:10.1088/1361-6471/aace6f](#).
- [72] C.-T. Gao, X.-G. Wu, X.-D. Huang, J. Zeng, Total decay width of using the infinite-order scale-setting approach based on intrinsic conformality*, *Chin. Phys. C* 46 (12) (2022) 123109. [arXiv:2109.11754](#), [doi:10.1088/1674-1137/ac92da](#).
- [73] J. Yan, Z.-F. Wu, J.-M. Shen, X.-G. Wu, Precise perturbative predictions from fixed-order calculations, *J. Phys. G* 50 (4) (2023) 045001. [arXiv:2209.13364](#), [doi:10.1088/1361-6471/acb281](#).
- [74] S. J. Brodsky, X.-G. Wu, Application of the Principle of Maximum Conformality to Top-Pair Production, *Phys. Rev. D* 86 (2012) 014021, [Erratum: *Phys.Rev.D* 87, 099902 (2013)]. [arXiv:1204.1405](#), [doi:10.1103/PhysRevD.86.014021](#).
- [75] S. J. Brodsky, X.-G. Wu, Application of the Principle of Maximum Conformality to the Top-Quark Forward-Backward Asymmetry at the Tevatron, *Phys. Rev. D* 85 (2012) 114040. [arXiv:1205.1232](#), [doi:10.1103/PhysRevD.85.114040](#).
- [76] S.-Q. Wang, X.-G. Wu, Z.-G. Si, S. J. Brodsky, Application of the Principle of Maximum Conformality to the Top-Quark Charge Asymmetry at the LHC, *Phys. Rev. D* 90 (11) (2014) 114034. [arXiv:1410.1607](#), [doi:10.1103/PhysRevD.90.114034](#).

- [77] S.-Q. Wang, X.-G. Wu, Z.-G. Si, S. J. Brodsky, Predictions for the Top-Quark Forward-Backward Asymmetry at High Invariant Pair Mass Using the Principle of Maximum Conformality, *Phys. Rev. D* 93 (1) (2016) 014004. [arXiv:1508.03739](#), [doi:10.1103/PhysRevD.93.014004](#).
- [78] S.-Q. Wang, X.-G. Wu, Z.-G. Si, S. J. Brodsky, A precise determination of the top-quark pole mass, *Eur. Phys. J. C* 78 (3) (2018) 237. [arXiv:1703.03583](#), [doi:10.1140/epjc/s10052-018-5688-1](#).
- [79] S.-Q. Wang, X.-G. Wu, J.-M. Shen, S. J. Brodsky, Reanalysis of the top-quark pair hadroproduction and a precise determination of the top-quark pole mass at the LHC, *Chin. Phys. C* 45 (11) (2021) 113102. [arXiv:2011.00535](#), [doi:10.1088/1674-1137/ac1bfd](#).
- [80] R.-Q. Meng, S.-Q. Wang, T. Sun, C.-Q. Luo, J.-M. Shen, X.-G. Wu, QCD improved top-quark decay at next-to-next-to-leading order, *Eur. Phys. J. C* 83 (1) (2023) 59. [arXiv:2202.09978](#), [doi:10.1140/epjc/s10052-023-11224-4](#).
- [81] S.-Q. Wang, S. J. Brodsky, X.-G. Wu, J.-M. Shen, L. Di Giustino, Elimination of QCD Renormalization Scale and Scheme Ambiguities, *Universe* 9 (4) (2023) 193. [arXiv:2302.08153](#), [doi:10.3390/universe9040193](#).
- [82] M. Hentschinski, A. Sabio Vera, C. Salas, Hard to Soft Pomeron Transition in Small-x Deep Inelastic Scattering Data Using Optimal Renormalization, *Phys. Rev. Lett.* 110 (4) (2013) 041601. [arXiv:1209.1353](#), [doi:10.1103/PhysRevLett.110.041601](#).
- [83] X.-C. Zheng, X.-G. Wu, S.-Q. Wang, J.-M. Shen, Q.-L. Zhang, Reanalysis of the BFKL Pomeron at the next-to-leading logarithmic accuracy, *JHEP* 10 (2013) 117. [arXiv:1308.2381](#), [doi:10.1007/JHEP10\(2013\)117](#).
- [84] F. Caporale, D. Y. Ivanov, B. Murdaca, A. Papa, Brodsky-Lepage-Mackenzie optimal renormalization scale setting for semihard processes, *Phys. Rev. D* 91 (11) (2015) 114009. [arXiv:1504.06471](#), [doi:10.1103/PhysRevD.91.114009](#).
- [85] S.-Q. Wang, X.-G. Wu, S. J. Brodsky, Reanalysis of the Higher Order Perturbative QCD corrections to Hadronic Z Decays using the Principle of Maximum Conformality, *Phys. Rev. D* 90 (3) (2014) 037503. [arXiv:1406.1852](#), [doi:10.1103/PhysRevD.90.037503](#).
- [86] X.-D. Huang, X.-G. Wu, X.-C. Zheng, Q. Yu, S.-Q. Wang, J.-M. Shen, Z -boson hadronic decay width up to $\mathcal{O}(\alpha_s^4)$ -order QCD corrections using the single-scale approach of the principle of maximum conformality, *Eur. Phys. J. C* 81 (4) (2021) 291. [arXiv:2008.07362](#), [doi:10.1140/epjc/s10052-021-09092-x](#).
- [87] S.-Q. Wang, S. J. Brodsky, X.-G. Wu, L. Di Giustino, Thrust Distribution in Electron-Positron Annihilation using the Principle of Maximum Conformality, *Phys. Rev. D* 99 (11) (2019) 114020. [arXiv:1902.01984](#), [doi:10.1103/PhysRevD.99.114020](#).
- [88] S.-Q. Wang, S. J. Brodsky, X.-G. Wu, J.-M. Shen, L. Di Giustino, Novel method for the precise determination of the QCD running coupling from event shape distributions in electron-positron annihilation, *Phys. Rev. D* 100 (9) (2019) 094010. [arXiv:1908.00060](#), [doi:10.1103/PhysRevD.100.094010](#).
- [89] L. Di Giustino, S. J. Brodsky, S.-Q. Wang, X.-G. Wu, Infinite-order scale-setting using the principle of maximum conformality: A remarkably efficient method for eliminating renormalization scale ambiguities for perturbative QCD, *Phys. Rev. D* 102 (1) (2020) 014015. [arXiv:2002.01789](#), [doi:10.1103/PhysRevD.102.014015](#).

- [90] L. Di Giustino, F. Sannino, S.-Q. Wang, X.-G. Wu, Thrust distribution for 3-jet production from $e+e-$ annihilation within the QCD conformal window and in QED, Phys. Lett. B 823 (2021) 136728. [arXiv:2104.12132](#), [doi:10.1016/j.physletb.2021.136728](#).
- [91] S.-Q. Wang, C.-Q. Luo, X.-G. Wu, J.-M. Shen, L. Di Giustino, New analyses of event shape observables in electron-positron annihilation and the determination of α_s running behavior in perturbative domain, JHEP 09 (2022) 137. [arXiv:2112.06212](#), [doi:10.1007/JHEP09\(2022\)137](#).
- [92] S.-Q. Wang, X.-G. Wu, J.-M. Shen, H.-Y. Han, Y. Ma, QCD improved electroweak parameter ρ , Phys. Rev. D 89 (11) (2014) 116001. [arXiv:1402.0975](#), [doi:10.1103/PhysRevD.89.116001](#).
- [93] Q. Yu, H. Zhou, J. Yan, X.-D. Huang, X.-G. Wu, A new analysis of the pQCD contributions to the electroweak parameter ρ using the single-scale approach of principle of maximum conformality, Phys. Lett. B 820 (2021) 136574. [arXiv:2105.07230](#), [doi:10.1016/j.physletb.2021.136574](#).
- [94] J.-M. Shen, X.-G. Wu, H.-H. Ma, H.-Y. Bi, S.-Q. Wang, Renormalization group improved pQCD prediction for $\Upsilon(1S)$ leptonic decay, JHEP 06 (2015) 169. [arXiv:1501.04688](#), [doi:10.1007/JHEP06\(2015\)169](#).
- [95] X.-D. Huang, X.-G. Wu, J. Zeng, Q. Yu, J.-M. Shen, The $\Upsilon(1S)$ leptonic decay using the principle of maximum conformality, Eur. Phys. J. C 79 (8) (2019) 650. [arXiv:1904.04517](#), [doi:10.1140/epjc/s10052-019-7158-9](#).
- [96] S.-Q. Wang, X.-G. Wu, X.-C. Zheng, J.-M. Shen, Q.-L. Zhang, $J/\psi + \chi_{cJ}$ Production at the B Factories under the Principle of Maximum Conformality, Nucl. Phys. B 876 (2013) 731–746. [arXiv:1301.2992](#), [doi:10.1016/j.nuclphysb.2013.09.003](#).
- [97] Z. Sun, X.-G. Wu, Y. Ma, S. J. Brodsky, Exclusive production of $J/\psi + \eta_c$ at the B factories Belle and Babar using the principle of maximum conformality, Phys. Rev. D 98 (9) (2018) 094001. [arXiv:1807.04503](#), [doi:10.1103/PhysRevD.98.094001](#).
- [98] H.-M. Yu, W.-L. Sang, X.-D. Huang, J. Zeng, X.-G. Wu, S. J. Brodsky, Scale-fixed predictions for $\gamma + \eta_c$ production in electron-positron collisions at NNLO in perturbative QCD, JHEP 01 (2021) 131. [arXiv:2007.14553](#), [doi:10.1007/JHEP01\(2021\)131](#).
- [99] Q.-L. Zhang, X.-G. Wu, X.-C. Zheng, S.-Q. Wang, H.-B. Fu, Z.-Y. Fang, Hadronic decays of the spin-singlet heavy quarkonium under the principle of maximum conformality, Chin. Phys. Lett. 31 (2014) 051202. [arXiv:1401.4268](#), [doi:10.1088/0256-307X/31/5/051202](#).
- [100] B.-L. Du, X.-G. Wu, J. Zeng, S. Bu, J.-M. Shen, The η_c decays into light hadrons using the principle of maximum conformality, Eur. Phys. J. C 78 (1) (2018) 61. [arXiv:1709.08072](#), [doi:10.1140/epjc/s10052-018-5560-3](#).
- [101] Q. Yu, X.-G. Wu, J. Zeng, X.-D. Huang, H.-M. Yu, The heavy quarkonium inclusive decays using the principle of maximum conformality, Eur. Phys. J. C 80 (5) (2020) 362. [arXiv:1911.05342](#), [doi:10.1140/epjc/s10052-020-7967-x](#).
- [102] H. Zhou, Q. Yu, X.-D. Huang, X.-C. Zheng, X.-G. Wu, The P-wave charmonium annihilation into two photons $\chi_{c0,c2} \rightarrow \gamma\gamma$ with high-order QCD corrections, Eur. Phys. J. C 81 (7) (2021) 614. [arXiv:2105.13210](#), [doi:10.1140/epjc/s10052-021-09424-x](#).

- [103] Q. Yu, H. Zhou, X.-D. Huang, J.-M. Shen, X.-G. Wu, Novel and Self-Consistency Analysis of the QCD Running Coupling $\alpha_s(Q)$ in Both the Perturbative and Nonperturbative Domains, *Chin. Phys. Lett.* 39 (7) (2022) 071201. [arXiv:2112.01200](#), [doi:10.1088/0256-307X/39/7/071201](#).
- [104] C.-F. Qiao, R.-L. Zhu, X.-G. Wu, S. J. Brodsky, A possible solution to the $B \rightarrow \pi\pi$ puzzle using the principle of maximum conformality, *Phys. Lett. B* 748 (2015) 422–427. [arXiv:1408.1158](#), [doi:10.1016/j.physletb.2015.07.044](#).
- [105] S.-Q. Wang, X.-G. Wu, W.-L. Sang, S. J. Brodsky, Solution to the $\gamma\gamma^* \rightarrow \eta_c$ puzzle using the principle of maximum conformality, *Phys. Rev. D* 97 (9) (2018) 094034. [arXiv:1804.06106](#), [doi:10.1103/PhysRevD.97.094034](#).
- [106] P. A. Zyla, et al., Review of Particle Physics, *PTEP* 2020 (8) (2020) 083C01. [doi:10.1093/ptep/ptaa104](#).
- [107] H. A. Chawdhry, A. Mitov, Ambiguities of the principle of maximum conformality procedure for hadron collider processes, *Phys. Rev. D* 100 (7) (2019) 074013. [arXiv:1907.06610](#), [doi:10.1103/PhysRevD.100.074013](#).
- [108] T. Kinoshita, Mass singularities of Feynman amplitudes, *J. Math. Phys.* 3 (1962) 650–677. [doi:10.1063/1.1724268](#).
- [109] T. D. Lee, M. Nauenberg, Degenerate Systems and Mass Singularities, *Phys. Rev.* 133 (1964) B1549–B1562. [doi:10.1103/PhysRev.133.B1549](#).
- [110] G. M. Cicuta, E. Montaldi, Analytic renormalization via continuous space dimension, *Lett. Nuovo Cim.* 4 (1972) 329–332. [doi:10.1007/BF02756527](#).
- [111] C. G. Bollini, J. J. Giambiagi, Dimensional Renormalization: The Number of Dimensions as a Regularizing Parameter, *Nuovo Cim. B* 12 (1972) 20–26. [doi:10.1007/BF02895558](#).
- [112] G. 't Hooft, Dimensional regularization and the renormalization group, *Nucl. Phys. B* 61 (1973) 455–468. [doi:10.1016/0550-3213\(73\)90376-3](#).
- [113] S. Weinberg, New approach to the renormalization group, *Phys. Rev. D* 8 (1973) 3497–3509. [doi:10.1103/PhysRevD.8.3497](#).
- [114] K. G. Chetyrkin, Four-loop renormalization of QCD: Full set of renormalization constants and anomalous dimensions, *Nucl. Phys. B* 710 (2005) 499–510. [arXiv:hep-ph/0405193](#), [doi:10.1016/j.nuclphysb.2005.01.011](#).
- [115] S. R. Coleman, D. J. Gross, Price of asymptotic freedom, *Phys. Rev. Lett.* 31 (1973) 851–854. [doi:10.1103/PhysRevLett.31.851](#).
- [116] D. J. Gross, F. Wilczek, Ultraviolet Behavior of Nonabelian Gauge Theories, *Phys. Rev. Lett.* 30 (1973) 1343–1346. [doi:10.1103/PhysRevLett.30.1343](#).
- [117] H. D. Politzer, Reliable Perturbative Results for Strong Interactions?, *Phys. Rev. Lett.* 30 (1973) 1346–1349. [doi:10.1103/PhysRevLett.30.1346](#).
- [118] W. E. Caswell, Asymptotic Behavior of Nonabelian Gauge Theories to Two Loop Order, *Phys. Rev. Lett.* 33 (1974) 244. [doi:10.1103/PhysRevLett.33.244](#).
- [119] D. R. T. Jones, Two Loop Diagrams in Yang-Mills Theory, *Nucl. Phys. B* 75 (1974) 531. [doi:10.1016/0550-3213\(74\)90093-5](#).

- [120] E. Egorian, O. V. Tarasov, Two Loop Renormalization of the QCD in an Arbitrary Gauge, *Teor. Mat. Fiz.* 41 (1979) 26–32.
- [121] M. Mojaza, C. Pica, F. Sannino, Hot Conformal Gauge Theories, *Phys. Rev. D* 82 (2010) 116009. [arXiv:1010.4798](#), [doi:10.1103/PhysRevD.82.116009](#).
- [122] S. A. Larin, J. A. M. Vermaseren, The Three loop QCD Beta function and anomalous dimensions, *Phys. Lett. B* 303 (1993) 334–336. [arXiv:hep-ph/9302208](#), [doi:10.1016/0370-2693\(93\)91441-0](#).
- [123] T. van Ritbergen, J. A. M. Vermaseren, S. A. Larin, The Four loop beta function in quantum chromodynamics, *Phys. Lett. B* 400 (1997) 379–384. [arXiv:hep-ph/9701390](#), [doi:10.1016/S0370-2693\(97\)00370-5](#).
- [124] P. A. Baikov, K. G. Chetyrkin, J. H. Kühn, Five-Loop Running of the QCD coupling constant, *Phys. Rev. Lett.* 118 (8) (2017) 082002. [arXiv:1606.08659](#), [doi:10.1103/PhysRevLett.118.082002](#).
- [125] O. Antipin, F. Sannino, Conformal Window 2.0: The large N_f safe story, *Phys. Rev. D* 97 (11) (2018) 116007. [arXiv:1709.02354](#), [doi:10.1103/PhysRevD.97.116007](#).
- [126] R. L. Workman, et al., Review of Particle Physics, *PTEP* 2022 (2022) 083C01. [doi:10.1093/ptep/ptac097](#).
- [127] T. Banks, A. Zaks, On the Phase Structure of Vector-Like Gauge Theories with Massless Fermions, *Nucl. Phys. B* 196 (1982) 189–204. [doi:10.1016/0550-3213\(82\)90035-9](#).
- [128] E. Gardi, G. Grunberg, M. Karliner, Can the QCD running coupling have a causal analyticity structure?, *JHEP* 07 (1998) 007. [arXiv:hep-ph/9806462](#), [doi:10.1088/1126-6708/1998/07/007](#).
- [129] T. A. Ryttov, R. Shrock, Scheme-independent calculations of physical quantities in an $N = 1$ supersymmetric gauge theory, *Phys. Rev. D* 96 (10) (2017) 105018. [arXiv:1706.06422](#), [doi:10.1103/PhysRevD.96.105018](#).
- [130] J. L. Basdevant, The Pade approximation and its physical applications, *Fortsch. Phys.* 20 (1972) 283–331. [doi:10.1002/prop.19720200502](#).
- [131] M. A. Samuel, G. Li, E. Steinfelds, Estimating perturbative coefficients in quantum field theory using Pade approximants. 2., *Phys. Lett. B* 323 (1994) 188. [doi:10.1016/0370-2693\(94\)90290-9](#).
- [132] M. A. Samuel, J. R. Ellis, M. Karliner, Comparison of the Pade approximation method to perturbative QCD calculations, *Phys. Rev. Lett.* 74 (1995) 4380–4383. [arXiv:hep-ph/9503411](#), [doi:10.1103/PhysRevLett.74.4380](#).
- [133] E. Gardi, Why Pade approximants reduce the renormalization scale dependence in QFT?, *Phys. Rev. D* 56 (1997) 68–79. [arXiv:hep-ph/9611453](#), [doi:10.1103/PhysRevD.56.68](#).
- [134] B. A. Kniehl, A. V. Kotikov, A. I. Onishchenko, O. L. Veretin, Strong-coupling constant with flavor thresholds at five loops in the anti-MS scheme, *Phys. Rev. Lett.* 97 (2006) 042001. [arXiv:hep-ph/0607202](#), [doi:10.1103/PhysRevLett.97.042001](#).
- [135] G. 't Hooft, The Whys of Subnuclear Physics, in: *Proc. Intern. School of Subnuclear Physics (Erice, 1977)*, ed. A. Zichichi (Plenum, New York, 1979), p. 943.

- [136] P. Boucaud, F. de Soto, J. P. Leroy, A. Le Yaouanc, J. Micheli, H. Moutarde, O. Pene, J. Rodriguez-Quintero, Artefacts and $\langle A^{**2} \rangle$ power corrections: Revisiting the MOM Z psi (p^{**2}) and Z(V), Phys. Rev. D 74 (2006) 034505. [arXiv:hep-lat/0504017](https://arxiv.org/abs/hep-lat/0504017), [doi:10.1103/PhysRevD.74.034505](https://doi.org/10.1103/PhysRevD.74.034505).
- [137] K. G. Chetyrkin, A. Retey, Three loop three linear vertices and four loop similar to MOM beta functions in massless QCD (7 2000). [arXiv:hep-ph/0007088](https://arxiv.org/abs/hep-ph/0007088).
- [138] T. Appelquist, M. Dine, I. J. Muzinich, The Static Potential in Quantum Chromodynamics, Phys. Lett. B 69 (1977) 231–236. [doi:10.1016/0370-2693\(77\)90651-7](https://doi.org/10.1016/0370-2693(77)90651-7).
- [139] W. Fischler, Quark - anti-Quark Potential in QCD, Nucl. Phys. B 129 (1977) 157–174. [doi:10.1016/0550-3213\(77\)90026-8](https://doi.org/10.1016/0550-3213(77)90026-8).
- [140] M. Peter, The Static quark - anti-quark potential in QCD to three loops, Phys. Rev. Lett. 78 (1997) 602–605. [arXiv:hep-ph/9610209](https://arxiv.org/abs/hep-ph/9610209), [doi:10.1103/PhysRevLett.78.602](https://doi.org/10.1103/PhysRevLett.78.602).
- [141] Y. Schroder, The Static potential in QCD to two loops, Phys. Lett. B 447 (1999) 321–326. [arXiv:hep-ph/9812205](https://arxiv.org/abs/hep-ph/9812205), [doi:10.1016/S0370-2693\(99\)00010-6](https://doi.org/10.1016/S0370-2693(99)00010-6).
- [142] A. V. Smirnov, V. A. Smirnov, M. Steinhauser, Fermionic contributions to the three-loop static potential, Phys. Lett. B 668 (2008) 293–298. [arXiv:0809.1927](https://arxiv.org/abs/0809.1927), [doi:10.1016/j.physletb.2008.08.070](https://doi.org/10.1016/j.physletb.2008.08.070).
- [143] A. V. Smirnov, V. A. Smirnov, M. Steinhauser, Three-loop static potential, Phys. Rev. Lett. 104 (2010) 112002. [arXiv:0911.4742](https://arxiv.org/abs/0911.4742), [doi:10.1103/PhysRevLett.104.112002](https://doi.org/10.1103/PhysRevLett.104.112002).
- [144] C. Anzai, Y. Kiyo, Y. Sumino, Static QCD potential at three-loop order, Phys. Rev. Lett. 104 (2010) 112003. [arXiv:0911.4335](https://arxiv.org/abs/0911.4335), [doi:10.1103/PhysRevLett.104.112003](https://doi.org/10.1103/PhysRevLett.104.112003).
- [145] A. L. Kataev, V. S. Molokoedov, Fourth-order QCD renormalization group quantities in the V scheme and the relation of the β function to the Gell-Mann–Low function in QED, Phys. Rev. D 92 (5) (2015) 054008. [arXiv:1507.03547](https://arxiv.org/abs/1507.03547), [doi:10.1103/PhysRevD.92.054008](https://doi.org/10.1103/PhysRevD.92.054008).
- [146] M. Gockeler, R. Horsley, V. Linke, P. E. L. Rakow, G. Schierholz, H. Stuben, Is there a Landau pole problem in QED?, Phys. Rev. Lett. 80 (1998) 4119–4122. [arXiv:hep-th/9712244](https://arxiv.org/abs/hep-th/9712244), [doi:10.1103/PhysRevLett.80.4119](https://doi.org/10.1103/PhysRevLett.80.4119).
- [147] S. A. Larin, T. van Ritbergen, J. A. M. Vermaseren, The Large quark mass expansion of Gamma ($Z_0 \rightarrow$ hadrons) and Gamma ($\tau \rightarrow$ tau-neutrino + hadrons) in the order α_s^{**3} , Nucl. Phys. B 438 (1995) 278–306. [arXiv:hep-ph/9411260](https://arxiv.org/abs/hep-ph/9411260), [doi:10.1016/0550-3213\(94\)00574-X](https://doi.org/10.1016/0550-3213(94)00574-X).
- [148] K. G. Chetyrkin, B. A. Kniehl, M. Steinhauser, Strong coupling constant with flavor thresholds at four loops in the MS scheme, Phys. Rev. Lett. 79 (1997) 2184–2187. [arXiv:hep-ph/9706430](https://arxiv.org/abs/hep-ph/9706430), [doi:10.1103/PhysRevLett.79.2184](https://doi.org/10.1103/PhysRevLett.79.2184).
- [149] S. J. Brodsky, G. F. de Teramond, H. G. Dosch, J. Erlich, Light-Front Holographic QCD and Emerging Confinement, Phys. Rept. 584 (2015) 1–105. [arXiv:1407.8131](https://arxiv.org/abs/1407.8131), [doi:10.1016/j.physrep.2015.05.001](https://doi.org/10.1016/j.physrep.2015.05.001).
- [150] H.-J. Lu, S. J. Brodsky, Relating physical observables in QCD without scale - scheme ambiguity, Phys. Rev. D 48 (1993) 3310–3318. [arXiv:hep-ph/9211254](https://arxiv.org/abs/hep-ph/9211254), [doi:10.1103/PhysRevD.48.3310](https://doi.org/10.1103/PhysRevD.48.3310).

- [151] G. M. Prosperi, M. Raciti, C. Simolo, On the running coupling constant in QCD, *Prog. Part. Nucl. Phys.* 58 (2007) 387–438. [arXiv:hep-ph/0607209](#), [doi:10.1016/j.pnpnp.2006.09.001](#).
- [152] G. Altarelli, The QCD Running Coupling and its Measurement, *PoS Corfu2012* (2013) 002. [arXiv:1303.6065](#), [doi:10.22323/1.177.0002](#).
- [153] G. Grunberg, A. L. Kataev, On Some possible extensions of the Brodsky-Lepage-MacKenzie approach beyond the next-to-leading order, *Phys. Lett. B* 279 (1992) 352–358. [doi:10.1016/0370-2693\(92\)90404-R](#).
- [154] G. Grunberg, Method of effective charges and BLM criterion, *Phys. Rev. D* 46 (1992) 2228–2239. [doi:10.1103/PhysRevD.46.2228](#).
- [155] S. J. Brodsky, M. S. Gill, M. Melles, J. Rathsman, An Analytic extension of the $\overline{\text{MS}}$ renormalization scheme, *Phys. Rev. D* 58 (1998) 116006. [arXiv:hep-ph/9801330](#), [doi:10.1103/PhysRevD.58.116006](#).
- [156] H. J. Lu, C. A. R. Sa de Melo, Dressed skeleton expansion and the coupling scale ambiguity problem, *Phys. Lett. B* 273 (1991) 260–267, [Erratum: *Phys.Lett.B* 285, 399 (1992)]. [doi:10.1016/0370-2693\(91\)91681-K](#).
- [157] H. J. Lu, Dressed skeleton expansion in (1+1)-dimensional field theory models, *Phys. Rev. D* 45 (1992) 1217–1232. [doi:10.1103/PhysRevD.45.1217](#).
- [158] S. J. Brodsky, A. H. Hoang, J. H. Kuhn, T. Teubner, Angular distributions of massive quarks and leptons close to threshold, *Phys. Lett. B* 359 (1995) 355–361. [arXiv:hep-ph/9508274](#), [doi:10.1016/0370-2693\(95\)01070-7](#).
- [159] S. J. Brodsky, H. J. Lu, Commensurate scale relations in quantum chromodynamics, *Phys. Rev. D* 51 (1995) 3652–3668. [arXiv:hep-ph/9405218](#), [doi:10.1103/PhysRevD.51.3652](#).
- [160] R. J. Crewther, Nonperturbative evaluation of the anomalies in low-energy theorems, *Phys. Rev. Lett.* 28 (1972) 1421. [doi:10.1103/PhysRevLett.28.1421](#).
- [161] D. J. Broadhurst, A. L. Kataev, Connections between deep inelastic and annihilation processes at next to next-to-leading order and beyond, *Phys. Lett. B* 315 (1993) 179–187. [arXiv:hep-ph/9308274](#), [doi:10.1016/0370-2693\(93\)90177-J](#).
- [162] P. A. Baikov, K. G. Chetyrkin, J. H. Kuhn, Adler Function, Bjorken Sum Rule, and the Crewther Relation to Order α_s^4 in a General Gauge Theory, *Phys. Rev. Lett.* 104 (2010) 132004. [arXiv:1001.3606](#), [doi:10.1103/PhysRevLett.104.132004](#).
- [163] S. J. Brodsky, G. T. Gabadadze, A. L. Kataev, H. J. Lu, The Generalized Crewther relation in QCD and its experimental consequences, *Phys. Lett. B* 372 (1996) 133–140. [arXiv:hep-ph/9512367](#), [doi:10.1016/0370-2693\(96\)00057-3](#).
- [164] M. Beneke, V. M. Braun, Naive nonAbelianization and resummation of fermion bubble chains, *Phys. Lett. B* 348 (1995) 513–520. [arXiv:hep-ph/9411229](#), [doi:10.1016/0370-2693\(95\)00184-M](#).
- [165] P. Ball, M. Beneke, V. M. Braun, Resummation of $(\beta_0 \alpha_s)^n$ corrections in QCD: Techniques and applications to the tau hadronic width and the heavy quark pole mass, *Nucl. Phys. B* 452 (1995) 563–625. [arXiv:hep-ph/9502300](#), [doi:10.1016/0550-3213\(95\)00392-6](#).

- [166] M. Neubert, Scale setting in QCD and the momentum flow in Feynman diagrams, *Phys. Rev. D* 51 (1995) 5924–5941. [arXiv:hep-ph/9412265](#), [doi:10.1103/PhysRevD.51.5924](#).
- [167] S. V. Mikhailov, Generalization of BLM procedure and its scales in any order of pQCD: A Practical approach, *JHEP* 06 (2007) 009. [arXiv:hep-ph/0411397](#), [doi:10.1088/1126-6708/2007/06/009](#).
- [168] A. L. Kataev, S. V. Mikhailov, Generalization of the Brodsky-Lepage-Mackenzie optimization within the β -expansion and the principle of maximal conformality, *Phys. Rev. D* 91 (1) (2015) 014007. [arXiv:1408.0122](#), [doi:10.1103/PhysRevD.91.014007](#).
- [169] H.-Y. Bi, X.-G. Wu, Y. Ma, H.-H. Ma, S. J. Brodsky, M. Mojaza, Degeneracy Relations in QCD and the Equivalence of Two Systematic All-Orders Methods for Setting the Renormalization Scale, *Phys. Lett. B* 748 (2015) 13–18. [arXiv:1505.04958](#), [doi:10.1016/j.physletb.2015.06.056](#).
- [170] X.-D. Huang, X.-G. Wu, Q. Yu, X.-C. Zheng, J. Zeng, J.-M. Shen, Generalized Crewther relation and a novel demonstration of the scheme independence of commensurate scale relations up to all orders, *Chin. Phys. C* 45 (10) (2021) 103104. [arXiv:2010.08910](#), [doi:10.1088/1674-1137/ac1934](#).
- [171] X.-G. Wu, S.-Q. Wang, S. J. Brodsky, Importance of proper renormalization scale-setting for QCD testing at colliders, *Front. Phys. (Beijing)* 11 (1) (2016) 111201. [arXiv:1508.02332](#), [doi:10.1007/s11467-015-0518-5](#).
- [172] J.-M. Shen, X.-G. Wu, B.-L. Du, S. J. Brodsky, Novel All-Orders Single-Scale Approach to QCD Renormalization Scale-Setting, *Phys. Rev. D* 95 (9) (2017) 094006. [arXiv:1701.08245](#), [doi:10.1103/PhysRevD.95.094006](#).
- [173] S. Weinzierl, NNLO corrections to 3-jet observables in electron-positron annihilation, *Phys. Rev. Lett.* 101 (2008) 162001. [arXiv:0807.3241](#), [doi:10.1103/PhysRevLett.101.162001](#).
- [174] S. Weinzierl, Event shapes and jet rates in electron-positron annihilation at NNLO, *JHEP* 06 (2009) 041. [arXiv:0904.1077](#), [doi:10.1088/1126-6708/2009/06/041](#).
- [175] M. Binger, S. J. Brodsky, The Form-factors of the gauge-invariant three-gluon vertex, *Phys. Rev. D* 74 (2006) 054016. [arXiv:hep-ph/0602199](#), [doi:10.1103/PhysRevD.74.054016](#).
- [176] S. Kluth, Tests of Quantum Chromo Dynamics at e^+e^- Colliders, *Rept. Prog. Phys.* 69 (2006) 1771–1846. [arXiv:hep-ex/0603011](#), [doi:10.1088/0034-4885/69/6/R04](#).
- [177] A. Heister, et al., Studies of QCD at e^+e^- centre-of-mass energies between 91-GeV and 209-GeV, *Eur. Phys. J. C* 35 (2004) 457–486. [doi:10.1140/epjc/s2004-01891-4](#).
- [178] J. Abdallah, et al., A Study of the energy evolution of event shape distributions and their means with the DELPHI detector at LEP, *Eur. Phys. J. C* 29 (2003) 285–312. [arXiv:hep-ex/0307048](#), [doi:10.1140/epjc/s2003-01198-0](#).
- [179] G. Abbiendi, et al., Measurement of event shape distributions and moments in $e^+e^- \rightarrow$ hadrons at 91-GeV - 209-GeV and a determination of $\alpha(s)$, *Eur. Phys. J. C* 40 (2005) 287–316. [arXiv:hep-ex/0503051](#), [doi:10.1140/epjc/s2005-02120-6](#).
- [180] P. Achard, et al., Studies of hadronic event structure in e^+e^- annihilation from 30-GeV to 209-GeV with the L3 detector, *Phys. Rept.* 399 (2004) 71–174. [arXiv:hep-ex/0406049](#), [doi:10.1016/j.physrep.2004.07.002](#).

- [181] K. Abe, et al., Measurement of $\alpha_s(M(Z)^{**2})$ from hadronic event observables at the Z^0 resonance, Phys. Rev. D 51 (1995) 962–984. [arXiv:hep-ex/9501003](#), [doi:10.1103/PhysRevD.51.962](#).
- [182] R. K. Ellis, D. A. Ross, A. E. Terrano, The Perturbative Calculation of Jet Structure in $e^+ e^-$ Annihilation, Nucl. Phys. B 178 (1981) 421–456. [doi:10.1016/0550-3213\(81\)90165-6](#).
- [183] Z. Kunszt, Comment on the $O(\alpha_s^{**2-S})$ Corrections to Jet Production in $e^+ e^-$ Annihilation, Phys. Lett. B 99 (1981) 429–432. [doi:10.1016/0370-2693\(81\)90563-3](#).
- [184] J. A. M. Vermaseren, K. J. F. Gaemers, S. J. Oldham, Perturbative QCD Calculation of Jet Cross-Sections in $e^+ e^-$ Annihilation, Nucl. Phys. B 187 (1981) 301–320. [doi:10.1016/0550-3213\(81\)90276-5](#).
- [185] K. Fabricius, I. Schmitt, G. Kramer, G. Schierholz, Higher Order Perturbative QCD Calculation of Jet Cross-Sections in $e^+ e^-$ Annihilation, Z. Phys. C 11 (1981) 315. [doi:10.1007/BF01578281](#).
- [186] W. T. Giele, E. W. N. Glover, Higher order corrections to jet cross-sections in $e^+ e^-$ annihilation, Phys. Rev. D 46 (1992) 1980–2010. [doi:10.1103/PhysRevD.46.1980](#).
- [187] S. Catani, M. H. Seymour, The Dipole formalism for the calculation of QCD jet cross-sections at next-to-leading order, Phys. Lett. B 378 (1996) 287–301. [arXiv:hep-ph/9602277](#), [doi:10.1016/0370-2693\(96\)00425-X](#).
- [188] A. Gehrmann-De Ridder, T. Gehrmann, E. W. N. Glover, G. Heinrich, EERAD3: Event shapes and jet rates in electron-positron annihilation at order α_s^3 , Comput. Phys. Commun. 185 (2014) 3331. [arXiv:1402.4140](#), [doi:10.1016/j.cpc.2014.07.024](#).
- [189] A. Gehrmann-De Ridder, T. Gehrmann, E. W. N. Glover, G. Heinrich, Second-order QCD corrections to the thrust distribution, Phys. Rev. Lett. 99 (2007) 132002. [arXiv:0707.1285](#), [doi:10.1103/PhysRevLett.99.132002](#).
- [190] A. Gehrmann-De Ridder, T. Gehrmann, E. W. N. Glover, G. Heinrich, NNLO corrections to event shapes in $e^+ e^-$ annihilation, JHEP 12 (2007) 094. [arXiv:0711.4711](#), [doi:10.1088/1126-6708/2007/12/094](#).
- [191] V. Del Duca, C. Duhr, A. Kardos, G. Somogyi, Z. Szőr, Z. Trócsányi, Z. Tulipánt, Jet production in the CoLoRfulNNLO method: event shapes in electron-positron collisions, Phys. Rev. D 94 (7) (2016) 074019. [arXiv:1606.03453](#), [doi:10.1103/PhysRevD.94.074019](#).
- [192] V. Del Duca, C. Duhr, A. Kardos, G. Somogyi, Z. Trócsányi, Three-Jet Production in Electron-Positron Collisions at Next-to-Next-to-Leading Order Accuracy, Phys. Rev. Lett. 117 (15) (2016) 152004. [arXiv:1603.08927](#), [doi:10.1103/PhysRevLett.117.152004](#).
- [193] K. G. Chetyrkin, J. H. Kuhn, M. Steinhauser, RunDec: A Mathematica package for running and decoupling of the strong coupling and quark masses, Comput. Phys. Commun. 133 (2000) 43–65. [arXiv:hep-ph/0004189](#), [doi:10.1016/S0010-4655\(00\)00155-7](#).
- [194] T. Gehrmann, N. Häfliger, P. F. Monni, BLM Scale Fixing in Event Shape Distributions, Eur. Phys. J. C 74 (6) (2014) 2896. [arXiv:1401.6809](#), [doi:10.1140/epjc/s10052-014-2896-1](#).
- [195] D. D. Dietrich, F. Sannino, Conformal window of $SU(N)$ gauge theories with fermions in higher dimensional representations, Phys. Rev. D 75 (2007) 085018. [arXiv:hep-ph/0611341](#), [doi:10.1103/PhysRevD.75.085018](#).

- [196] G. Cacciapaglia, C. Pica, F. Sannino, Fundamental Composite Dynamics: A Review, *Phys. Rept.* 877 (2020) 1–70. [arXiv:2002.04914](#), [doi:10.1016/j.physrep.2020.07.002](#).
- [197] T. A. Ryttov, R. Shrock, Scheme-independent calculation of $\gamma_{\bar{\psi}\psi,IR}$ for an SU(3) gauge theory, *Phys. Rev. D* 94 (10) (2016) 105014. [arXiv:1608.00068](#), [doi:10.1103/PhysRevD.94.105014](#).
- [198] T. A. Ryttov, R. Shrock, Scheme-Independent Series Expansions at an Infrared Zero of the Beta Function in Asymptotically Free Gauge Theories, *Phys. Rev. D* 94 (12) (2016) 125005. [arXiv:1610.00387](#), [doi:10.1103/PhysRevD.94.125005](#).
- [199] G. Dissertori, A. Gehrmann-De Ridder, T. Gehrmann, E. W. N. Glover, G. Heinrich, G. Luisoni, H. Stenzel, Determination of the strong coupling constant using matched NNLO+NLLA predictions for hadronic event shapes in e^+e^- annihilations, *JHEP* 08 (2009) 036. [arXiv:0906.3436](#), [doi:10.1088/1126-6708/2009/08/036](#).
- [200] A. H. Hoang, D. W. Kolodrubetz, V. Mateu, I. W. Stewart, Precise determination of α_s from the C -parameter distribution, *Phys. Rev. D* 91 (9) (2015) 094018. [arXiv:1501.04111](#), [doi:10.1103/PhysRevD.91.094018](#).
- [201] M. Dasgupta, G. P. Salam, Event shapes in e^+e^- annihilation and deep inelastic scattering, *J. Phys. G* 30 (2004) R143. [arXiv:hep-ph/0312283](#), [doi:10.1088/0954-3899/30/5/R01](#).
- [202] M. Tanabashi, et al., Review of Particle Physics, *Phys. Rev. D* 98 (3) (2018) 030001. [doi:10.1103/PhysRevD.98.030001](#).
- [203] A. H. Hoang, D. W. Kolodrubetz, V. Mateu, I. W. Stewart, C -parameter distribution at N^3LL' including power corrections, *Phys. Rev. D* 91 (9) (2015) 094017. [arXiv:1411.6633](#), [doi:10.1103/PhysRevD.91.094017](#).
- [204] G. Abbiendi, et al., Measurement of the running of the QED coupling in small-angle Bhabha scattering at LEP, *Eur. Phys. J. C* 45 (2006) 1–21. [arXiv:hep-ex/0505072](#), [doi:10.1140/epjc/s2005-02389-3](#).
- [205] P. A. Baikov, K. G. Chetyrkin, J. H. Kuhn, Order α_s^4 QCD Corrections to Z and tau Decays, *Phys. Rev. Lett.* 101 (2008) 012002. [arXiv:0801.1821](#), [doi:10.1103/PhysRevLett.101.012002](#).
- [206] P. A. Baikov, K. G. Chetyrkin, J. H. Kuhn, J. Rittinger, Vector Correlator in Massless QCD at Order $\mathcal{O}(\alpha_s^4)$ and the QED beta-function at Five Loop, *JHEP* 07 (2012) 017. [arXiv:1206.1284](#), [doi:10.1007/JHEP07\(2012\)017](#).
- [207] P. A. Baikov, K. G. Chetyrkin, J. H. Kuhn, J. Rittinger, Adler Function, Sum Rules and Crewther Relation of Order $\mathcal{O}(\alpha_s^4)$: the Singlet Case, *Phys. Lett. B* 714 (2012) 62–65. [arXiv:1206.1288](#), [doi:10.1016/j.physletb.2012.06.052](#).
- [208] R. Marshall, A Determination of the Strong Coupling Constant α_s From e^+e^- Total Cross-section Data, *Z. Phys. C* 43 (1989) 595. [doi:10.1007/BF01550938](#).
- [209] B. Ananthanarayan, D. Das, M. S. A. Alam Khan, Renormalization group improved m_s and $|V_{us}|$ determination from hadronic τ decays, *Phys. Rev. D* 106 (11) (2022) 114036. [arXiv:2207.00754](#), [doi:10.1103/PhysRevD.106.114036](#).
- [210] M. Davier, A. Hocker, Z. Zhang, The Physics of Hadronic Tau Decays, *Rev. Mod. Phys.* 78 (2006) 1043–1109. [arXiv:hep-ph/0507078](#), [doi:10.1103/RevModPhys.78.1043](#).

- [211] S. Schael, et al., Branching ratios and spectral functions of tau decays: Final ALEPH measurements and physics implications, Phys. Rept. 421 (2005) 191–284. [arXiv:hep-ex/0506072](#), [doi:10.1016/j.physrep.2005.06.007](#).
- [212] C. S. Lam, T.-M. Yan, Decays of Heavy Lepton and Intermediate Weak Boson in Quantum Chromodynamics, Phys. Rev. D 16 (1977) 703. [doi:10.1103/PhysRevD.16.703](#).
- [213] P. A. Baikov, K. G. Chetyrkin, J. H. Kuhn, Scalar correlator at $O(\alpha(s)^{**4})$, Higgs decay into b-quarks and bounds on the light quark masses, Phys. Rev. Lett. 96 (2006) 012003. [arXiv:hep-ph/0511063](#), [doi:10.1103/PhysRevLett.96.012003](#).
- [214] M. Cacciari, N. Houdeau, Meaningful characterisation of perturbative theoretical uncertainties, JHEP 09 (2011) 039. [arXiv:1105.5152](#), [doi:10.1007/JHEP09\(2011\)039](#).
- [215] M. Bonvini, Probabilistic definition of the perturbative theoretical uncertainty from missing higher orders, Eur. Phys. J. C 80 (10) (2020) 989. [arXiv:2006.16293](#), [doi:10.1140/epjc/s10052-020-08545-z](#).
- [216] C. Duhr, A. Huss, A. Mazeliauskas, R. Szafron, An analysis of Bayesian estimates for missing higher orders in perturbative calculations, JHEP 09 (2021) 122. [arXiv:2106.04585](#), [doi:10.1007/JHEP09\(2021\)122](#).
- [217] J.-M. Shen, Z.-J. Zhou, S.-Q. Wang, J. Yan, Z.-F. Wu, X.-G. Wu, S. J. Brodsky, Extending the predictive power of perturbative QCD using the principle of maximum conformality and the Bayesian analysis, Eur. Phys. J. C 83 (4) (2023) 326. [arXiv:2209.03546](#), [doi:10.1140/epjc/s10052-023-11531-w](#).
- [218] D. V. Shirkov, 'Massive' Perturbative QCD, regular in the IR limit, Phys. Part. Nucl. Lett. 10 (2013) 186–192. [arXiv:1208.2103](#), [doi:10.1134/S1547477113030138](#).
- [219] B.-L. Du, X.-G. Wu, J.-M. Shen, S. J. Brodsky, Extending the Predictive Power of Perturbative QCD, Eur. Phys. J. C 79 (3) (2019) 182. [arXiv:1807.11144](#), [doi:10.1140/epjc/s10052-019-6704-9](#).
- [220] M. Davier, A. Höcker, B. Malaescu, C.-Z. Yuan, Z. Zhang, Update of the ALEPH non-strange spectral functions from hadronic τ decays, Eur. Phys. J. C 74 (3) (2014) 2803. [arXiv:1312.1501](#), [doi:10.1140/epjc/s10052-014-2803-9](#).
- [221] R. Serber, Linear modifications in the Maxwell field equations, Phys. Rev. 48 (1935) 49. [doi:10.1103/PhysRev.48.49](#).
- [222] E. A. Uehling, Polarization effects in the positron theory, Phys. Rev. 48 (1935) 55–63. [doi:10.1103/PhysRev.48.55](#).